UCLA
UCLA Electronic Theses and Dissertations

Title
Defining the role of oxygen tension in cell fate decision making of human neural progenitors

Permalink
https://escholarship.org/uc/item/4jd62857

Author
Xie, Yuan

Publication Date
2015

Peer reviewed|Thesis/dissertation

eScholarship.org Powered by the California Digital Library
University of California

UNIVERSITY OF CALIFORNIA

Los Angeles

Defining the Role of Oxygen Tension in Cell Fate Decision Making of Human Neural Progenitors

A dissertation submitted in partial satisfaction of the

requirements for the degree Doctor of Philosophy

in Molecular, Cell and Developmental Biology

by

Yuan Xie

2016

© Copyright by

Yuan Xie

2016

ABSTRACT OF THE DISSERTATION

Defining the Role of

Oxygen Tension in Cell Fate Decision Making of

Human Neural Progenitors

by

Yuan Xie

Doctor of Philosophy in Molecular, Cell and Developmental Biology

University of California, Los Angeles, 2016

Professor William E. Lowry, Chair

Human pluripotent stem cells (hPSCs) have opened up numerous avenues, including regenerative medicine and modeling development and disease. However, when compared to the fetal tissue-derived counterparts, *in vitro* derived hPSC progenies reflect very early human development (<6 weeks). Therefore, it is vital to understand the mechanisms of early human development to facilitate maturation of hPSCs *in vitro*. Low oxygen tension is important for maintaining the pluripotency of *in vitro* cultured human embryonic stem cells. However, the influence of oxygen tension on fidelity of PSC differentiation had not been studied extensively until now. In fact, embryogenesis before 10 weeks of gestation occurs under low oxygen (<2.5% O_2). We hypothesized that manipulating oxygen tension to a physiological level *in vitro* would facilitate the transcriptional and functional maturity of hPSC derivatives by more faithfully mimicking *in vivo* conditions. We discovered that physiological oxygen tension promotes

astrogliogenesis upon NPC differentiation and determined that hypoxia inducible factors (HIFs) are key transcription factors involved in this process. Activating HIF with small molecules facilitated astrogliogenesis, whereas silencing HIF delayed this process. Even transient changes in oxygen concentration affected cell fate through HIF by regulating the activity of MYC, a regulator of LIN28/*let-7* that is critical for fate decisions in neural progenitors. Taking advantage of RNA-seq, metabolomics, and ChIP-seq techniques, we uncovered evidence of an early coherent response of neural progenitors to physiological oxygen at the transcriptional, metabolic and epigenetic levels. This response correlates with a persistent cell fate change, namely, the neuroepithelial cell (NEC) to radial glial cell (RGC) transition, which may contribute to astrogliogenesis upon differentiation. Taken together, physiological oxygen and HIF signaling play a key role in regulating cell fate decision in human neural progenitors. Furthermore, small molecules that activate HIF signaling can be simple tools to quickly and efficiently promote the development of mature cell types.

The dissertation of Yuan Xie is approved.

Stephen T. Smale

Jau-Nian Chen

Alvaro Sagasti

William E. Lowry, Committee Chair

University of California, Los Angeles

2016

This dissertation is dedicated to my parents Jianghe Gu and Hongyan Xie

For their endless love, support and encouragement

TABLE OF CONTENTS

ABSTRACT ii

DEDICATIONS v

TABLE OF CONTENTS vi

LIST OF FIGURES viii

LIST OF TABLES x

ACKNOWLEDGEMENTS xi

VITA xiv

Chapter 1: Introduction 1

Embryonic stem cells 2

Human induced pluripotent stem cells 2

Induced pluripotent stem cell as a biological tool 3

Neural stem and progenitor cells 5

Developmental stages in vertebrate embryogenesis 6

Developmental stages of human central nervous system 7

The molecular basis of vertebrate neocortical neurogenesis 8

Oxygen tension in embryo and adult brain 9

HIF regulation under normal and hypoxic conditions 11

HIF in embryonic development 12

The LIN28 and *let-7* axis 13

The LIN28 and *let-7* axis in nervous system 15

Significance and specific aims of this dissertation 18

References 24

Chapter 2: Defining the role of oxygen tension in human neural progenitor fate.... 32

Abstract 33

Introduction 33

Results 37

Discussion 43

Materials and Methods 45

References 64

Chapter 3: Molecular traces of a low oxygen state in human neural progenitors.... 78

Abstract 79

Introduction 79

Results 82

Discussion 90

Materials and Methods 94

References 114

Chapter 4: Conclusions and Perspectives 118

The concept of physioxia 119

The role of physioxia in modeling development *in vitro* 119

Applications of physioxia in cell based therapy and regenerative medicine..... 124

References 127

LIST OF FIGURES

Figure 1-1. Personalized medicine in the advent of iPSC technology 20

Figure 1-2. Schematic overview of neurogenesis in the embryonic vertebrate central nervous system 21

Figure 1-3. Extracellular and intracellular factors affecting the balance between NPC proliferation versus differentiation 22

Figure 1-4. Cortical progenitor cells follow an intrinsic developmental sequence both *in vivo* and *in vitro* 23

Figure 2-1. Germ layer formation is regulated by the oxygen sensing pathway 51

Figure 2-2. Neurogenesis is affected by oxygen tension 53

Figure 2-3. The HIF pathway regulates neurogenesis 55

Figure 2-4. Small molecule driven HIF activation can drive gliogenesis 56

Figure 2-5. Identification of important target genes of the HIF pathway in neurogenesis 58

Figure 2-6. LIN28 is regulated jointly by HIF and MYC through a shared binding site 60

Figure 2-7. MYC inhibition mimics the effect of HIF activation to suppress immaturity markers and promote gliogenesis 62

Figure S2-1. Generation of hESC lines with diminished HIF signaling..... 69

Figure S2-2. The effect of oxygen tension on proliferation and apoptosis 71

Figure S2-3. HIF2α is induced by low oxygen tension and DFX treatment 73

Figure S2-4. The effect of DFX on gliogenesis is completely blocked by coordinated inhibition of *let-7* activity by antagomirs 74

Figure 3-1. Activation of HIF by low oxygen or small molecules at NPC stage promotes generation of astrocyte upon differentiation. 100

Figure 3-2. RNA-sequencing data on differentially expressed genes between control and HIF activation groups 102

Figure 3-3. Global metabolite analysis suggested increased glycolysis and decreased oxidative phosphorylation upon HIF activation 104

Figure 3-4. Histone mass spectrometry revealed a global change of H3K27Ac and H3K9Me2/3 upon HIF activation 106

Figure 3-5. ChIP-sequencing data suggested H3K27Ac is highly involved in regulating gene expression upon HIF activation in NPCs 108

Figure 3-6. H3K27Ac super-enhancer analysis suggested epigenetic regulation of glycolysis related genes upon HIF activation 111

Figure 3-7. There is no clear relationship between distribution of H3K9Me3 loci and HIF regulated transcription changes 112

Figure 4-1. A proposed model that NPC differentiation is affected by HIF and MYC through regulating LIN28-*let-7* axis 126

LIST OF TABLES

Table 1-1. Carnegie Stages Comparison Graph (Species/Days) 6

Table 1-2. Normal values of pO_2 in various human tissues..... 10

Table 1-3. Patients brain pO_2 level at different depth measured by catheter probe..... 10

Table 1-4. Regional rat brain tissue pO_2 measured by microelectrode 11

Table 1-5. Targets of *let-7* and their functions in neural development..... 17

Table S2-1. A complete list of TFs regulating HIF target genes predicted by GSEA..... 75

ACKNOWLEDGMENTS

First and foremost, I would like to acknowledge my thesis advisor and mentor, Dr. William Lowry, for his guidance and support during my entire graduate study. He has been supportive of my research and career decisions over the years, giving me freedom to pursue independent research, and teaching me how to become a successful scientist. I would like to thank my thesis committee members, Dr. Stephen Smale, Dr. Jaunian Chen, and Dr. Alvaro Sagasti for their encouragement, suggestions, and criticisms along the way.

I am grateful to all the past and present members of the Lowry lab for making it such a fun and friendly place to work at. I want thank my former undergraduate students, Ying Lin, Xiangzhi Meng and Eden Maloney, for their excellent support of my research over the years. I want to give my special thanks to Jessica Cinkornpumin, who was not only helpful during my research as a lab technician, but has also been so supportive in my life as my best friend at UCLA. I want to thank members in Lowry lab, especially Xavier Gaeta, Minori Ohashi, Kimberly Loo, Aimee Flores, Matilde Miranda, Soheila Azghadi, Dr. David Chan, Dr. Michaela Patterson, Dr. Andrew White, Dr. Igal Germanguz, Dr. Peiyee Lee, and Dr. Jim Rheinwald for the help during my graduate study and constructive suggestions in my research.

In addition, I would like to thank all my collaborators throughout the years for sharing ideas and broadening my scope of research, including Dr. Michael Teitell, Dr. Jin Zhang, Dr.Roberto Spreafico, Dr. Benjamin Garcia, and Dr. Miguel Edwards for their help in various experiments and data analysis. I want to give my sincere thanks to Dr. Kathrin Plath, Dr. Heather Christofk, Dr. Konstantinos Chronis, Dr. Bernadett Papp, Dr. Tonis Gro and Wen Gu for all the insightful suggestions on science and specific techniques. I would also like to acknowledge the

core facilities at UCLA including: BSCRC High Throughput Sequencing Core (Dr. Suhua Feng); UCLA Clinical Microarray Core (Dr. Xinmin Li and Jian Zhou); UCLA Metabolomics Center (Dr. Daniel Braas), UCLA Human Embryonic and Induced Pluripotent Stem Cell Core (Jinghua Tang); and the Computational Bioscience Collaboratory (Dr. Matteo Pellegrini and Weihong Yan). I want to thank California Institute of Regenerative Medicine for my predoctoral training grant.

I want to thank all my teachers back to college and high school for their mentorship, especially Zhiling Zhao, who brought me into the field of biology. I would like to give special thanks to Dr. Ren Sun, Dr. Yibin Wang, and Dr. Stephen Smale for making my first summer at UCLA a wonderful experience.

Finally, I would like to thank my family and friends. I would like to thank my parents for their love and support throughout my life. Thank you both for being wonderful parents and wonderful friends. I am grateful to all my family for the help and support during my graduate study at UCLA. Lastly, I would like to thank my husband Minglei Zhao. He is not only a great scientist, with whom I could discuss research and share ideas, but also a wonderful person, to share all the memories in life.

Chapter 2 was originally published in *Stem Cell Reports*: Xie, Y., Zhang, J., Lin, Y., Gaeta, X., Meng, X., Wisidagama, D. R. R., Cinkornpumin, J., Koehler, C. M., Malone, C. S., Teitell, M. A., and Lowry, W. E. (2014). Defining the Role of Oxygen Tension in Human Neural Progenitor Fate. *Stem Cell Reports*, *3*(5), 743–757. It is reprinted here with permission from Cell Press and all co-authors. This work was supported by CIRM grants RB3- 05207, RS1-00313, RB1-01397, TB1-01183; and NIH grants P01GM99134, P01GM081621, R01GM073981,

R01CA185189, R01CA156674, and R01CA90571. Yuan Xie was supported by scholarship from China Scholarship Council and a Predoctoral Training Grant from CIRM (TG2-01169).

Chapter 3 is unpublished work performed by Yuan Xie, Roberto Spreafico, Ying Lin, and William Lowry. It is published here with permission from all-coauthors.

VITA

2010	Bachelor of Medicine, Basic Medicine Peking University, Beijing, P. R. China
2012	Advanced to Candidacy in Philosophy in Molecular, Cell and Developmental Biology University of California, Los Angeles Los Angeles, California

AWARDS AND HONORS

2013-2015	Predoctoral Training Grant, California Institute for Regenerative Medicine
2010-2013	Predoctoral Scholarship, Chinese Scholarship Council
2009	Fellowship for excellent medical student, Peking University
2004	Silver Medal, National Biology Olympic Competition (National level), China
2003	First Prize, National Biology Competition (Provincial level), Shanxi, China
2003	Second Prize, National Chemistry Competition (Provincial level), Shanxi, China

PUBLICATIONS

Xie, Y., Zhang, J., Lin, Y., Gaeta, X., Meng, X., Wisidagama, D. R. R., Cinkornpumin, J., Koehler, C. M., Malone, C. S., Teitell, M. A., and Lowry, W. E. (2014). Defining the Role of Oxygen Tension in Human Neural Progenitor Fate. *Stem Cell Reports*, *3*(5), 743–757

Patterson, M., Gaeta, X., Loo, K., Edwards, M., Smale, S., Cinkornpumin, J., Xie, Y., Listgarten, J., Azghadi, S., Douglass, S. M., Pellegrini, M., and Lowry, W. E. (2014). *let-7* miRNAs Can Act through Notch to Regulate Human Gliogenesis. *Stem Cell Reports*, *3*(5), 758–773.

Gaeta, X., Xie, Y., and Lowry, W. E. (2013). Sequential addition of reprogramming factors improves efficiency. *Nature cell biology*, *15*(7), 725-727.

Tian, L., Qi, H., Xie, Y., Zhang, Y., Zhang, W., Sun, X., Wang, Y., and Ma, D. (2010). Rat CC chemokine receptor 4 is the functional homologue of human CC chemokine receptor 4 and can interact with human CCL17 and CCL22. *Chinese Science Bulletin*, *55*(14), 1388-1395.

PRESENTATIONS

Xie, Y. and Chih, B. (August 2015) “Facilitating the differentiation of human neural progenitors into neurons.” Poster presentation. Genentech 2015 Intern Poster Day. South San Francisco, CA, United States.

Xie, Y., Lin, Y., Cinkornpumin, J., Lowry, W. E. (March 2015) “Defining the role of oxygen

tension in human neural progenitor fate." Poster presentation. Keystone Symposia: Transcriptional and Epigenetic Influences on Stem Cell States. Steamboat springs, CO, United States.

Xie, Y., Lin, Y., Cinkornpumin, J., and Lowry, W. E. (June 2014) "The role of oxygen tension in neural progenitor cell differentiation." Poster presentation. Gordon Research Conferences on Molecular & Cellular Neurobiology: Mechanisms of Neural Development, Circuit Assembly, Synaptic Plasticity and Neuropsychiatric Disorders. Hong Kong, China.

Xie, Y., Lin, Y., and Lowry, W. E. (March 2014) "The role of oxygen tension in neural differentiation." Poster presentation. 5th NIGMS Workshop on Pluripotent Stem Cell Research: Recent Progress and Future Directions of NIGMS Grantees. National Institute of Health, Washington, D.C., United States.

Xie, Y., Azghadi, S. F., Maloney, E., Zhang, J., Teitell, M. A., and Lowry, W. E. (June 2013) "The role of oxygen tension in neural maturation." Poster presentation, New Avenues for Brain Repair: Programming and Reprogramming the Central Nervous System. Harvard University, Cambridge, MA, United States.

CHAPTER 1

Introduction

Embryonic Stem Cells (ESCs)

By definition, all pluripotent stem cells have the capacity for 1) self-renewal for an unlimited number of cell divisions, and 2) multipotency, the ability to give rise to all the cells of the body.

Embryonic Stem cells (ESCs) are pluripotent stem cells with the potential to give rise to every type of tissue and organ in the body. ESCs are originated from the inner cell mass (ICM) of a pre-implantation blastocyst. Murine ESC lines were first isolated in 1981 from mouse embryos. The mouse ESCs can grow and expand on a fibroblast-feeder layer, and maintain the ability to develop into a chimeric mouse (Evans and andKaufman, 1981; Martin, 1981). The first human blastocyst-derived pluripotent stem cell line was established in 1998 (Thomson et al., 1998). Most human embryonic stem cell (hESC) lines are generated from cleavage stage human embryos produced by *in vitro* fertilization (IVF) for clinical purposes. Although hESCs have huge potential in the field of developmental biology and regenerative medicine, the traditional method of generating hESC lines using human embryos is under scrutiny because of ethical issues.

Human induced Pluripotent Stem Cells (hiPSCs)

In 1962, John Gurdon showed that by transplanting nucleus from a mature cell into a denucleated egg cell, this egg would develop into an embryo and eventually become a living frog (Gurdon et al., 1958). This technique is called somatic cell nuclear transfer (SCNT), and it demonstrated that the nucleus of mature cells contains all genetic information necessary to form every cell type in an organism. Because of the low efficiency of SCNT in mammalian systems, it took another 30 years to generate the first SCNT mammal, Dolly the Sheep (Campbell et al., 1996).

Over decades, scientists attempted to define the molecular foundation of pluripotency. By knocking out pluripotency-related genes in mouse ESCs, dozens of genes that related to self-renew capacity or pluripotency were identified, such as Oct4, Nanog, Sox2, Klf4, c-Myc, and Sox15 [see review (Hotta and Yamanaka, 2015)]. Building upon this knowledge, in 2006, Shinya Yamanaka opened a completely new avenue in stem cell research, induced pluripotent stem cell (iPSC) technology. By forced expression of only four transcription factors Oct4, Sox2, Klf4, and c-Myc (OSKM), mouse fibroblast cells were converted into ESC-like cells (Takahashi and Yamanaka, 2006). Because of their groundbreaking work in reprogramming somatic cells into a pluripotent state, Gurdon and Yamanaka won the Nobel Prize in Physiology or Medicine in 2012.

Induced pluripotent stem cell as a biological tool

hiPSC technology has many advantages over hESCs as a tool in biological research, drug discovery and regenerative medicine.

First, generation of hiPSC does not require destruction of human embryos, therefore it avoids the ethical issues involved in using hESCs.

Moreover, disease-specific iPSCs are great tools to unravel the developmental, molecular and cellular mechanisms underlying disease onset and progression. For example, many neurological diseases are difficult to study using animal models, because of following reasons: 1) neurodegenerative diseases arise so late in human life that short-lived rodent models can not

adequately recapitulate disease progression; 2) Neuropsychiatric and neurodevelopmental disorders, such as autism and schizophrenia are difficult to model using animals because the diagnostic symptoms are human-specific behaviors; 3) Some other diseases selectively impact certain subpopulations of neurons that may differ between species. To date, iPSCs have been generated from many neurological disorders, including amyotrophic lateral sclerosis (Dimos et al., 2008), spinal muscular atrophy (Corti et al., 2012; Ebert et al., 2009), Parkinson disease (Danés, 2012; Soldner et al., 2011), Alzheimer disease (Israel et al., 2012), and Rett syndrome (Velasco et al., 2014), and provided a novel platform to explore underlying mechanisms of diseases.

Another beneficial use for iPSC is in drug discovery and toxicity testing. Currently, drug discovery is hampered by inadequate tools and cell sources for cell-based assays. More relevant cell types generated from normal or disease-specific iPSCs can be used for efficacy and toxicity studies (Figure 1-1).

In terms of clinical applications, organ transplantation is an established medical treatment, however, a shortage of donor tissue and transplant rejection are big issues in transplantation therapy. To date, clinical trials using hESC-derived products have been allogeneic, therefore current applications require significant and sometimes toxic immunosuppression. Organ transplantation, especially the bone marrow transplantation, requires stringent HLA matching, therefore matching donors are very difficult to find. The first iPSC-based human clinical trail to treat dry age-related macular degeneration was initiated in Japan in 2014 (Hotta and Yamanaka, 2015). Because iPSCs can be generated patient specifically, autologous transplantation is ideal to

minimize immune rejection. With the advancement of genome editing technology, especially the clustered regularly interspaced short palindromic repeat (CRISPER)/Cas9 system (Jiang et al., 2013; Jinek et al., 2012), iPSC technology can be an unlimited personalized source for transplantation. Therefore, it is vital that *in vitro* differentiation methods are developed to produce mature, functional tissue and organs from hESCs and hiPSC to fully exploit their potential for clinical applications [see review (Hotta and Yamanaka, 2015)].

Neural stem and progenitor cells

During development, neural stem cells (NSCs) give rise to almost all cell types in the mammalian central nervous system (CNS). Usually, two criteria are applied to define a cell as a stem cell: 1) self-renewal, for an unlimited number of cell divisions, and 2) multipotency, the ability to give rise to numerous types of differentiated cell. However, it is not clear to what extent multipotent stem cells exist during the development of the CNS (Götz and Huttner, 2005). Thus, we use the term neural progenitor cells (NPCs) to describe the neural cells that are 1) capable of dividing a finite number of times, and 2) multipotent to differentiate into restricted cell types, such as neuronal and glial cells (Götz and Huttner, 2005).

Neuroepithelial cells (NECs)

During early development of the vertebrate embryo, the nervous system originates as the neural tube, which is induced in the ectoderm by the underlying notochord. The neural tube wall constitutes a pseudo-stratified epithelium, which is made up of cells called neuroepithelial cells (NECs). NECs undergo symmetric divisions to maintain and expand the neural progenitor pool.

Radial glial cells (RGCs)

At the onset of neurogenesis, NECs switch their identity and turn into RGCs. RGCs will then

directly or indirectly generate each type of neurons and glial cells in the nervous system.

Morphologically, NPCs, such as NECs and RGCs, are highly polarized, with their apical membrane exposed to the ventricle surface (bottom, also called apical surface) and their basal process contacting the pial basal membrane (top, also called basal lamina) (Figure 1-2). Adherens junctions are located basal to the apical plasma membrane of NPCs to mediate cell-cell adhesion. These junctions consist of catenins and cadherins that connect to the intracellular actin network. Together with polarity proteins, such as Par3 and Par6 (Costa et al., 2008), adherens junctions are important for NPCs to maintain apical polarity, which is essential for NPC proliferation and normal function (Paridaen and Huttner, 2014).

Developmental stages in vertebrate embryogenesis

Because most of the developmental studies in the central nervous system were performed in mouse or rat, it is important to normalize developmental stages of these model organisms to study human embryogenesis. To better understand the developmental timing of the *in vitro* derived NPCs from human ESC or iPSC progenies, Carnegie staging is used to compare the developmental stage of human and other species based on specific developmental features shared by vertebrate embryos (Butler and Juurlink, 1987) (Table 1-1).

Table 1-1. Carnegie Stages Comparison Graph (Species/Days)

	Stages	9	10	11	12	13	14	15	16	17	18	19	20	21	22	23
Human	Days	20	22	24	28	30	33	36	40	42	44	48	52	54	55	58
Monkey	Days	21	22	25	28	29	30	32	34	36	37	3	41	43	45	47

Mouse	Days	9	9.5	10	10.5	11	11.5	12	12.5	13	13.5	14	14.5	15	15.5	16
Rat	Days	10.5	11	11.5	12	12.5	13	13.5	14	14.5	15	15.5	16	16.5	17	17.5

Adapted from Butler and Juurlink (Butler and Juurlink, 1987)

Developmental stage of human central nervous system

The neural tube is the first well-defined brain structure in the human embryo, which starts to form during the third week of gestation, between E20-27 (Carnegie stage 10-11). From the end of gastrulation through approximately E42 in humans, NPCs undergo symmetric cell division to produce two identical NPCs. Over multiple rounds of cell division between E25 to E42 (Carnegie stage 12-17), symmetrical cell division augments the neural progenitor pool size (Butler and Juurlink, 1987; Stiles and Jernigan, 2010). Beginning on E42, NPCs shift from symmetrical to asymmetrical cell division, producing one neural progenitor and one neuron (Wodarz and Huttner, 2003). This is called cortical neurogenesis phase, and is complete by approximately E108 (Clancy et al., 2001).

Neurogenesis precedes gliogenesis in vertebrate neocortical development. In mammalian system, the first divisions of NPCs are exclusively neurogenic, giving rise to neural-restricted intermediate progenitors or directly to daughter neurons (Sloan and Barres, 2014). After that, those existing NPCs switch their fate and begin to generate astrocytes and oligodendrocytes. For example, in rats, neurogenesis peaks at E14, astrogliogenesis peaks at P2, and oligodendrogenesis peaks at P14 (Sauvageot, 2002) (Figure 1-4). Similar to the rodent model, proliferation and migration of glial progenitors continues for an extended period after birth in human, and the differentiation and maturation of glial cells continue throughout childhood (Stiles

and Jernigan, 2010). Because of limited human postmortem material, the specific timing of gliogenesis in human is not well defined, especially the postnatal developmental processes. However, the phenomenon that neurogenesis proceeds gliogenesis in human embryonic development is also recapitulated in hESC and hiPSC models *in vitro* (Morrow et al., 2001; Patterson et al., 2011; Shaltouki et al., 2013).

The molecular basis of vertebrate neocortical neurogenesis

After the onset of neurogenesis, RGCs divide mainly asymmetrically, and give rise to one RGC daughter cell and one differentiating cell. The asymmetric division is tightly regulated by mitotic spindle orientation (Lancaster and Knoblich, 2012), apical and basal domain structure (Lancaster and Knoblich, 2012; Shitamukai and Matsuzaki, 2012; Shitamukai et al., 2011) and polarity proteins (Alexandre et al., 2010; Roper et al., 2004). Notch signaling components such as Notch ligand Delta-like 1 (DLL1), the regulator of Delta internalization, Mindbomb (MIB1), and the notch antagonist Numb are differentially segregated between daughter cells. In mouse, one daughter cell is maintained as an RGC that has higher Notch activity and contains higher Mindbomb and Numb, compared with the other daughter cell with neuronal or intermediate progenitor fate (Bultje et al., 2009). The balance between proliferation versus differentiation of neural progenitors is tightly regulated by many extracellular and intracellular factors as listed in Figure 1-3.

During neurogenesis, the newborn neurogenic daughter cells need to withdraw their apical endfoot, which is connected by adherens junctions. Proneural genes expressed in differentiating daughter cells down-regulate cadherins to enable the migration from ventricular surface to upper

layers of the cortical plate (Rousso et al., 2012). Since each newborn neuron migrates past the existing cortical layers to form the upper layer, it is called the "inside-out" pattern. During this process, the cell loses its apical polarity, which contributes to the subsequent cell-cycle exit and terminal differentiation (Paridaen and Huttner, 2014).

Once committed to a certain cell fate, RGCs undergo cell cycle arrest and terminal differentiation leading to the exhibition of cell-type-specific features. Neuronal differentiation is induced through the expression of region-specific proneural genes. For example, NPCs in the dorsal telencephalon express bHLH transcription factors *Neurog1/2*, and generate glutamatergic pyramidal neurons. The NPCs in the ventral telencephalon express Ascl1, *Nkx2.1* and *Gsh1/2* (*GSX1/2* in human), that instructs the generation of GABAergic interneurons.

Oxygen tension in embryo and adult brain

Oxygen (O_2) is vital for living cells to maintain normal metabolism. *In vitro* cultures are mostly performed in atmospheric oxygen, which is 95% air (79% N_2 and 21% O_2) supplemented by 5% of carbon dioxide. However, the oxygen level in human body is much lower than the atmospheric oxygen level. Furthermore, there is heterogeneity in oxygen levels within the human body: with14.5% O_2 in the alveoli, 12% O_2 in the arterial blood, 5.3% O_2 in venous blood, and ranging from 1% to 9.5% O_2 in various tissues (Carreau et al., 2011) (Table 1-2).

Two units to measure the oxygen partial pressure (pO_2) are widely used in clinical setting: millimeters of mercury (1 mmHg = 133.322 Pa), and percentage of oxygen (1% = 1013 Pa), with the conversion of 1 mmHg equals 0.132% O_2.

Table 1-2. Normal values of pO_2 in various human tissues

	pO_2 (mmHg)	**pO_2 (%)**
Air	160	21.1
Inspired air (in the tracheus)	150	19.7
Air in the alveoli	110	14.5
Arterial blood	100	13.2
Venous blood	40	5.3
Cell	9.9–19	1.3–2.5
Mitochondria	9.9	<1.3
Brain	33.8 ± 2.6	4.4 ± 0.3
Lung	42.8	5.6
Skin (sub-papillary plexus)	35.2 ± 8	4.6 ± 1.1
Skin (dermal papillae)	24 ± 6.4	3.2 ± 0.8
Skin (superficial region)	8 ± 3.2	1.1 ± 0.4
Intestinal tissue	57.6 ± 2.3	7.6 ± 0.3
Liver	40.6 ± 5.4	5.4 ± 0.7
Kidney	72 ± 20	9.5 ± 2.6
Muscle	29.2 ± 1.8	3.8 ± 0.2
Bone marrow	48.9 ± 4.5	6.4 ± 0.6

Adapted from Carreau et al. (Carreau et al., 2011)

Using probes, the first reported average pO_2 values in human brain was 33-36 mmHg by Assad et al (Assad et al., 1984).After that, several groups have reported pO_2 in patients brain ranging from 25-42 mmHg (Hoffman et al., 1996; Meixensberger et al., 1993). Dings et al. reported that the mean pO_2 level decreased with the brain depth, with 33.3 mmHg (4.4% O_2) at 7-12 mm below the dura and an average of 23.8 mmHg (3.1% O_2) at 22-27 mm below the dura (Dings et al., 1998) (Table 1-3).

Table 1-3. Patients brain pO_2 level at different depth measured by catheter probe

Subdural Depth (mm)	**pO_2 (mmHg)**	**pO_2 (%)**
22-27 (n=27)	23.8 ± 8.1	3.1 ± 1.1

17-22 (n=27)	25.7 ± 8.3	3.4 ± 1.1
12-17 (n=26)	33.0 ± 13.3	4.4 ± 1.8
7-12 (n=15)	33.3 ± 13.3	4.4 ± 1.8

Adapted with modification from Dings et al. (Dings et al., 1998)

Difference in oxygen level at different brain region was reported using rat brain, with highest pO_2 in cortex gray matter and lowest pO_2 in the pons (Table 1-4) (Silver and Erecińska, 1998).

Table 1-4. Regional rat brain tissue pO_2 measured by microelectrode

Brain area	**pO_2 (%)**
Cortex (gray)	2.5 –5.3
Cortex (white)	0.8 –2.1
Hypothalamus	1.4 –2.1
Hippocampus	2.6 –3.9
Pons, fornix	0.1 –0.4

Adapted from Silver, Ian, and Maria Erecińska. (Silver and Erecińska, 1998)

Low levels of oxygen occur naturally in developing embryos. Before the establishment of the utero–placental circulation in the second trimester, the oxygen level in the uterine surface is low (17.9mm Hg, ~2.36% O_2) (Genbacev et al., 1997). As a result, embryogenesis before 10 weeks of gestation occurs under low oxygen level (<2.5% O_2) (Simon and Keith, 2008).

Oxygen tension is important for mammalian nervous system development. Morriss et al reported that *in vitro* cultured rat E9.5 embryo underwent normal cranial neurulation at 5% O_2, however, culture at 20% or 40% O_2 resulted in abnormal morphogenesis of the cranial neural folds and failure of neural tube closure (Morriss and New, 1979).

HIF regulation under normal and hypoxic conditions

Hypoxia-inducible factors (HIFs) are key regulators of the cellular response to oxygen tension

(Denko, 2008; Lendahl et al., 2009; Simon and Keith, 2008). HIFs are a heterodimeric transcription factors composed of alpha-subunit (HIF1α, HIF2α, and HIF3α) and a beta-subunit (HIF1β, also called aryl hydrocarbon receptor nuclear translocator, or ARNT) (Ema et al., 1997; Gu et al., 1998; Tian et al., 1997; Wang et al., 1995). In mammals, HIF1β is constitutively expressed. HIF activity is regulated by alpha-subunit protein stability in an oxygen-dependent manner. When oxygen is abundant, HIFα subunit is hydroxylated by prolyl hydroxylase domain (PHD) proteins (in the presence of Fe^{2+}) and recognized by an E3 ubiquitin ligase, VHL (Von Hippel-Lindau), leading to its degradation in the proteasome (Ruas and Poellinger, 2005). In hypoxic conditions, decreased O_2 diminishes enzymatic activity of PHDs. As a result, HIF1α and HIF2α proteins are stabilized, translocate into nucleus, dimerize with HIF1β subunit, recruit the coactivators P300/CBP and bind to hypoxia response element (HRE) core sequence [A/G]CGTG to transactivate specific target genes (Ratcliffe, 2007; Ravenna et al., 2015; Webb et al., 2009).

Several small molecular compounds are widely used to mimic hypoxia by stabilizing HIF. Deferoxamine (DFX) is a FDA approved iron-chelating agent to treat acute iron poisoning. DFX stabilizes HIF through inhibition of prolyl hydroxylase by Fe^{2+} chelation of the catalytic core (Gleadle et al., 1995; Wang and Semenza, 1993). Metal ions (such as Co^{2+} and Cu^{2+}) also inhibit prolyl hydroxylase by substitution for Fe^{2+} of the catalytic core (Gleadle et al., 1995; Schofield and Ratcliffe, 2004). Dimethyloxallyl glycine (DMOG) is an analogue of oxoglutarate, the substrate of prolyl-4-hydroxylase. Thus, DMOG stabilize HIF by inhibition of prolyl-4-hydroxylase by competition with its substrate (Baader et al., 1994; Ivan et al., 2002).

HIF in embryonic development

In *Hif1α*, *Hif2α*, and *Hif1β* knockout mice, abrogation of HIF activity impaired vascularization of the placenta (Adelman et al., 2000; Cowden Dahl et al., 2005; Kozak et al., 1997), cardiovascular morphogenesis and angiogenesis (Maltepe et al., 1997), heart development (Krishnan et al., 2008; Licht et al., 2006; Ryan et al., 1998), and endochondral bone formation during early embryogenesis (Amarilio et al., 2007; Dunwoodie, 2009; Provot et al., 2007).

In terms of nervous system development, both *Hif1α* and *Hif1β* deficient mice had abnormalities including neural-fold closure defects and forebrain hypoplasia (Kozak et al., 1997; Lyer et al., 1998). HIFs are shown to be required for neural crest cell migration (Compernolle et al., 2003). Furthermore, neural-specific *Hif1a*-deficient mice driven by *Nestin-Cre* exhibit hydrocephalus accompanied by a reduction of neural cells and an impairment of spatial memory (Tomita et al., 2003). Those studies demonstrated the importance of HIF in embryonic brain development.

The LIN28 and *let-7* axis

The LIN28 and *let-7* axis is an evolutionarily conserved pathway that is involved in regulating early development, oncogenesis, stem cell differentiation and metabolism (Paranjpe, 2015; Shyh-Chang and Daley, 2013; Thornton and Gregory, 2012).

MicroRNAs (miRNAs) are a class of 22-nucleotide, non-coding RNAs that post-transcriptionally regulate target mRNAs. Upon base pairing of their seed sequence to the target mRNA, mature miRNAs recruit Argonaute to form RNA-induced-silencing-complex (RISC), which targets mRNAs to be either degraded or not translated (Ha and Kim, 2014). In a genome, the *let-7* miRNAs are often present in multiple copies. Different members are identified by divergent

stem-loop regions, but all have an identical seed sequence. One of the major function of *let-7* miRNAs is to promote differentiation or developmental timing (Roush and Slack, 2008). Their targets include many pluripotency genes and oncogenes (c-Myc, Ras, Hmga2, Igfbps), cell-cycle regulators (Cyclins), and components of insulin-PI3K-mTOR pathway (Igf1r, Insr, Irs2) (Shyh-Chang and Daley, 2013). It is worth mentioning that *let-7* binding sites are present in the 3' UTR of both Lin28A and Lin28B mRNAs. Thus *let-7* miRNAs negatively regulate Lin28 post-transcriptionally.

Lin28 was first identified in the nematode *C. elegans* as an important regulator of developmental timing (Ambros and Horvitz, 1984; Moss et al., 1997). Its mammalian homologs, LIN28A and LIN28B, are RNA-binding proteins that selectively repress the maturation of *let-7* family miRNAs by bind to the stem loops of pre-*let-7* GGAG motif, and subsequently leading to its degradation (Nam et al., 2011; Newman et al., 2008; Viswanathan et al., 2008). In terms of molecular mechanism, both Lin28a and Lin28b have been observed to shuttle between nucleus and cytoplasm, and act on both primary and precursor *let-7* miRNAs (Shyh-Chang and Daley, 2013). In the nucleus, they potentially work with heterogeneous nuclear ribonucleoproteins (hnRNPs) to regulate splicing or interact with Msi1 to block pri-*let-7* processing (Kawahara et al., 2011; Newman et al., 2008; Viswanathan et al., 2008). In the cytoplasm, Lin28a recruits Tut4 and Tut7 to oligouridylate pre-*let-7* and block the process into mature *let-7* mediated by Dicer (Heo et al., 2009). Thus, Lin28 suppress the maturation of *let-7* miRNAs in multiple steps during biogenesis.

As mentioned above, Lin28 blocks maturation of *let-7* miRNAs, and *let-7* suppresses Lin28

translation. This double negative feedback loop results in an opposing expression pattern between Lin28 and *let-7* miRNAs. Generally, Lin28 is highly expressed in stem and progenitor cells during the neonatal period, and then diminishes and disappears by adulthood. Neonatal overexpression of Lin28A delayed the onset of puberty in mice (Zhu et al., 2010). As progenitor cell differentiate, Lin28 expression decreases, which allows *let-7* processing and increased production of mature *let-7* miRNAs. *let-7* miRNAs levels gradually increase as an organism matures to allow the lineage commitment and terminal differentiation (Viswanathan and Daley, 2010).

Multiple regulatory mechanisms have been identified upstream of Lin28. In tumor models, c-MYC and NFκB have been shown to promote transformation and oncogenesis by transactivating Lin28b and a subsequent decrease of mature *let-7* miRNAs (Chang et al., 2009; Iliopoulos et al., 2009). In mammalian ESCs, pluripotency factors such as Oct4, Sox2, Nanog and Tcf3 have been shown to regulate *Lin28a* transcription (Marson et al., 2008). Sox2 binds to Lin28a directly in a nuclear protein-protein complex, suggesting a close relationship between them in regulating pluripotency (Cox et al., 2010). Indeed, LIN28 has been used to reprogram somatic cells to iPSCs (Yu et al., 2007). During reprogramming, repression of Dot1L H3K79 histone methyltransferase upregulates *Lin28a* indirectly through TGFβ signaling (Onder et al., 2012).

The LIN28 and *let-7* axis in nervous system

Lin28 and *let-7* play an important role in the nervous system development, specifically during neurogenesis. In the neuroepithelium, Lin28a is present throughout the neural tube until E15.5, and the expression drops thereafter (Yang and Moss, 2003). In human, LIN28A

and LIN28B are highly expressed in PSC-derived NPCs, and early-stage fetal spinal cord (week7) but not late-stage fetal spinal cord (13 week). Upon passaging, LIN28A and LIN28B levels drop whereas *let-7* miRNAs increase in the PSC-NPCs, representing a more mature stage in development (Patterson et al., 2011). The loss of Lin28a roughly coincides with the transition of NEC to RGC populations, which do not express Lin28a (Rehfeld et al., 2015). These expression patterns suggest that the Lin28 to *let-7* switch is an early event triggered at the onset of neurogenesis.

Let-7 miRNAs are highly expressed in post-mitotic neurons, making *let-7* family members the most abundant miRNAs in the brain (Rehfeld et al., 2015). The onset of *let-7* expression, together with miR-9 and miR-125, has been shown between E12 and P0 in mouse retina, when progenitors shift production from early to late cell types (La Torre et al., 2013). This observation is consistent with our study that later stage fetal-tissue derived gliogenic NPCs have higher mature *let-7* miRNAs than PSC-derived neurogenic NPCs. And using *let-7* miRNA mimic could convert the neurogenic NPC into a more mature, gliogenic stage (Patterson et al., 2014; 2011). Many oncogenes and pluripotent genes are targets of *let-7* miRNAs, such as *HMGA2*, *MYC*, *LIN28A/B* (see Table 1-5 for a summary of *let-7* target genes). Proper differentiation of neural progenitor cells requires silencing of those genes in terminal differentiated cells. Interestingly, *let-7* has been shown to down-regulate two neurogenic bHLH transcription factors Ascl1 and Neurogenin (Cimadamore et al., 2013; Ramachandran et al., 2010). This could imply that premature *let-7* expression is detrimental to early stages of neurogenesis (Cimadamore et al., 2013).

Table 1-5. Targets of *let-7* and their functions in neural development

***let-7* target**	**Function**	**References**
Ascl1	• Dedifferentiation of Müller glia cells into retinal progenitors	Ramachandran et al. 2010
	• Maintenance of neural progenitor proliferation and neurogenic potential	Cimadamore et al. 2013
Hmga2	• Adult stem cell plasticity in the SVZ	Nishino et al. 2008
	• Fetal versus adult stem cell identity	Yuan et al. 2012; Copley et al. 2013;
	• Oncogenesis	Mayr et al. 2007; Lee and Dutta 2007; F. Yu et al. 2007
Hspd1	• Dedifferentiation of Müller glia cells into retinal progenitors	Ramachandran et al. 2010
Igf1r, Insr, Irs2 Imp1	• Regulation of the mTOR pathway	Frost and Olson 2011; Shinoda et al. 2013
Lin28a	• Expansion of neural stem cells during cortical development	Nishino et al. 2013
	• Regulation of proliferation and neurogenesis in neural precursors	Cimadamore et al. 2013
	• Dedifferentiation of Müller glia cells into retinal progenitors	Ramachandran et al. 2010
	• Maintenance of stemness	Rybak et al. 2008
	• Reprogramming into iPS cells	Melton et al. 2010
Lin28b	• Maintenance of early progenitors in retinal neurogenesis	La Torre et al. 2013
Lin41	• Maintenance of stemness, inhibition of miRNA activity	Slack et al. 2000; Rybak et al. 2009
	• Axonal regeneration in larval vs adult neurons	Zou et al. 2013
c-Myc	• Dedifferentiation of Müller glia cells into retinal progenitors	Ramachandran et al. 2010
	• Pluripotency gene networks and oncogenesis	Koscianska et al. 2007; Kumar et al. 2007
n-Myc	• Development of neuroblastomas	Molenaar et al. 2012
	• Maintenance of stemness	Melton et al. 2010
Pax6	• Dedifferentiation of Müller glia cells into retinal progenitors	Ramachandran et al. 2010
Protogenin	• Maintenance of early progenitors in retinal neurogenesis	La Torre et al. 2013
Sal4	• Maintenance of stemness	Melton et al. 2010

Tlx	• Cell cycle progression of neural stem cells	Zhao et al. 2009

Adapted from Rehfeld et al. (Rehfeld et al., 2015)

Significance and specific aims of this dissertation

Previous studies in our lab compared *in vitro* cultured hESC and hiPSC derivatives with tissue-derived natural counterparts, and found that *in vitro* derived human pluripotent stem cell (PSC) progeny most closely reflect very early human development (<6 weeks) (Patterson et al., 2011). Therefore, it is vital to understand the mechanisms of early human development to facilitate maturation of hESC and hiPSCs *in vitro*. Low oxygen tension has been shown to be important for maintaining the pluripotency of *in vitro* cultured hESCs. However, the influence of oxygen tension on fidelity of PSC differentiation has not been studied extensively. As described previously, embryogenesis before 10 weeks of gestation occurs under low oxygen (<2.5% O2). Thus, the nervous system develops *in vivo* in lower oxygen tension than traditional *in vitro* culture conditions. We hypothesize that manipulating oxygen tension to a physiological level *in vitro* will facilitate the transcriptional and functional maturity of human pluripotent stem cell derivatives by more faithfully mimicking *in vivo* conditions.

In the next two chapters, I will talk about my own contributions to understand the molecular mechanisms of oxygen tension in regulating the differentiation of human neural progenitor cells.

In Chapter 2 of this dissertation, I present our work demonstrating the first three aims of this dissertation: 1) characterize the influence of low oxygen tension on NPC differentiation; 2) identify key transcription factors involved in this process; and 3) determine the molecular

mechanism of low oxygen mediated astrogliogenesis. This chapter was previously published in *Stem Cell Reports* (Xie et al., 2014) and is reprinted here with permission from Cell Press and all co-authors.

In the *Stem Cell Reports* paper, we also documented that a short-term (3-5 days) exposure to low oxygen could induce a "memory effect" in NPCs. This "memory effect" resulted in a cell fate specification after long-term differentiation (more than 3 weeks). In chapter 3, I will present our unpublished work on the fourth aim: identify the genetic and epigenetic mechanisms of HIF-mediated "memory effect" in NPC fate specification. Using next-generation RNA-sequencing, ChIP-sequencing, and metabolomics approaches, we identified a coherent response of the cell that leads to a persistent cell fate change in human neural progenitors. This work is published here with permission from all co-authors.

Our work suggests physiological oxygen, or small molecules that activate HIF, can be simple tools to promote developmental maturity of human neural progenitors *in vitro*. Because of the late onset of gliogenesis during embryonic development, differentiation of glial linages *in vitro* is extremely time-consuming. For example, direct differentiation of function astrocytes and oligodendrocytes from hPSCs takes three and four months, respectively (Krencik and Zhang, 2011; Wang et al., 2013). We identified key small molecules that drive neural progenitors through developmental stages to produce glia instead of neurons, and thus provide a simple tool to quickly and efficiently differentiate mature cell types to fully exploit the potential of hPSCs for drug discovery and regenerative medicine.

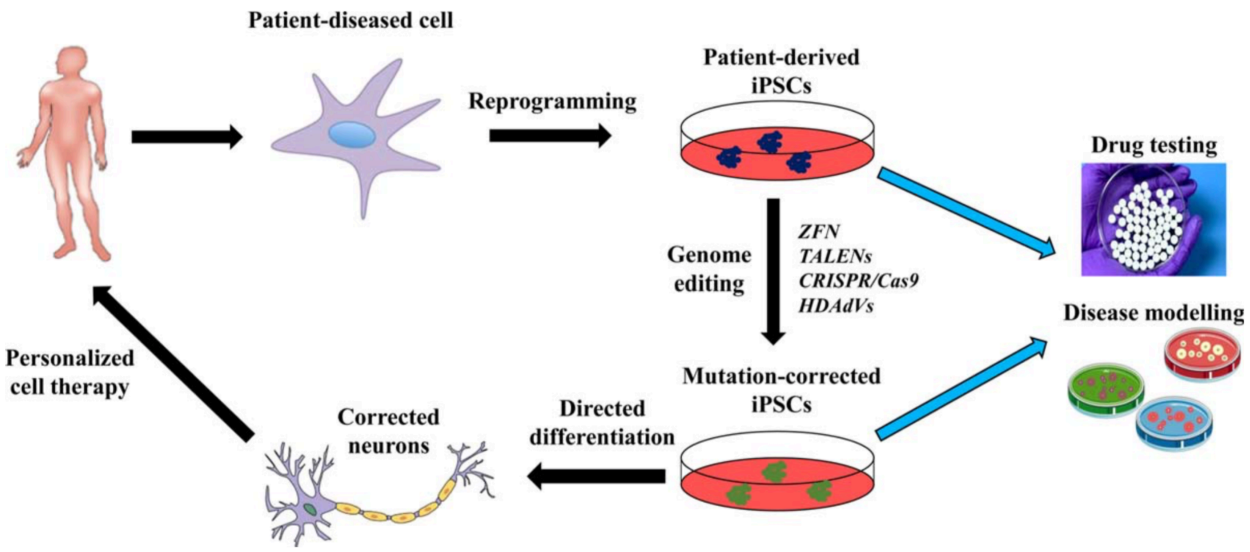


Figure 1-1. Personalized medicine in the advent of iPSC technology

Cartoon depicting the strategy for combining patient-specific hiPSCs and genome editing for *in vitro* generation of diseased and corrected lineage-specific derivatives for disease modeling, drug screening and personalized medicine. Abbreviations: CRISPR/CAS9, clustered regularly interspaced short palindromic repeat/CAS9 RNA-guided nucleases; HDAdV, helper-dependent adenoviral vectors; iPSCs, induced pluripotent stem cells; TALENs, transcription activator-like effector nucleases; ZFN, zinc finger nucleases. Adapted with permission from Velasco et al (Velasco et al., 2014) and John Wiley & Sons publications.

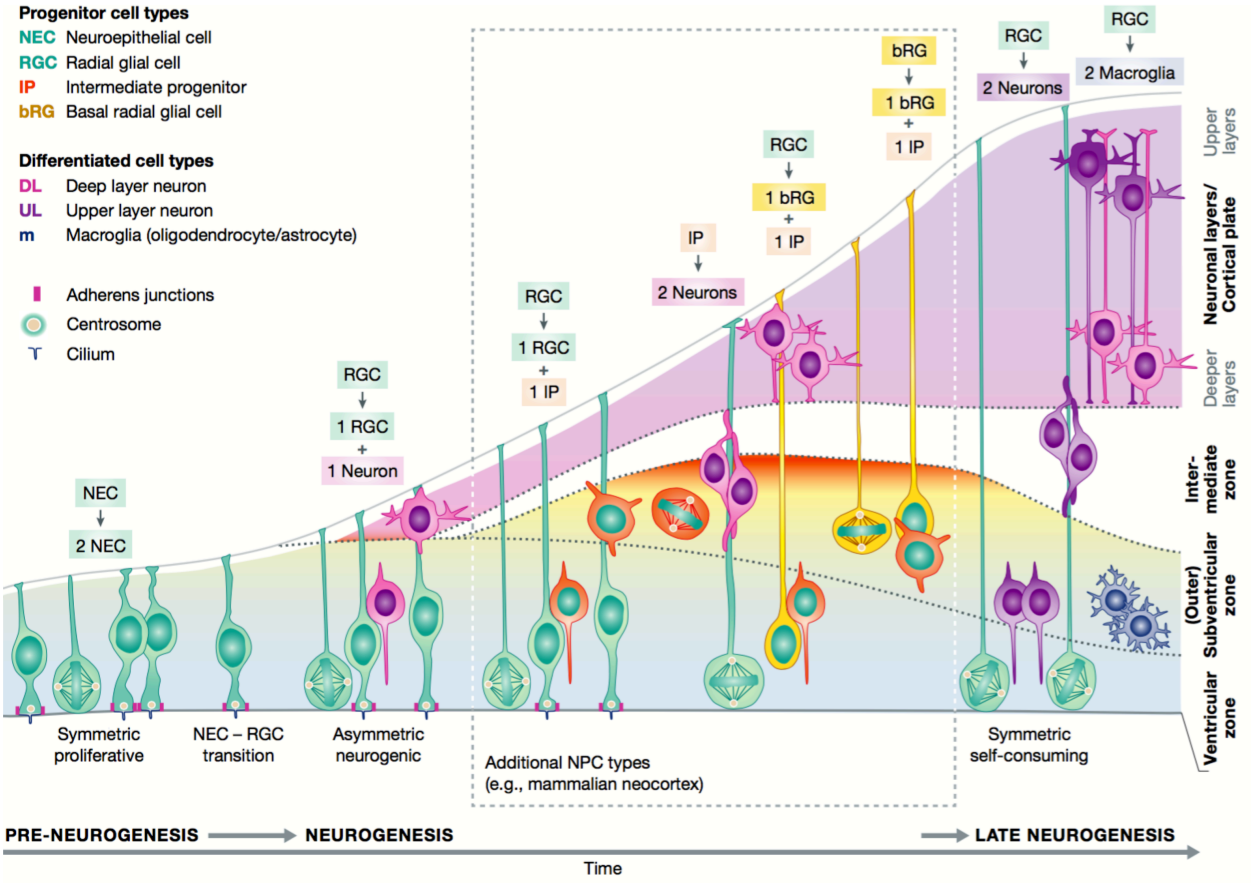


Figure 1-2. Schematic overview of neurogenesis in the embryonic vertebrate central nervous system

The principal types of NPCs with the progeny they produce are indicated by different colors. Additional NPC types that are typically found in mammalian neocortex are indicated in the box; note that only some of the possible daughter cell outcomes are depicted. Adapted from Paridaen and Huttner (Paridaen and Huttner, 2014) with permission from EMBO Press.

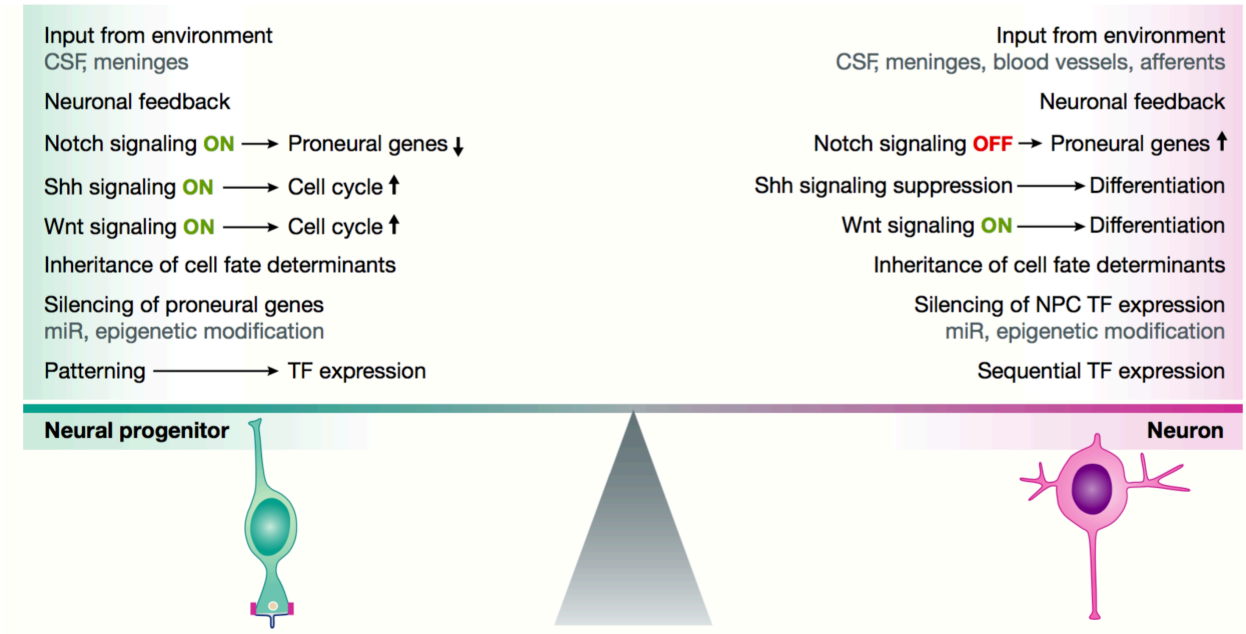


Figure 1-3. Extracellular and intracellular factors affecting the balance between NPC proliferation versus differentiation.

Adapted from Paridaen and Huttner (Paridaen and Huttner, 2014) with permission from EMBO Press.

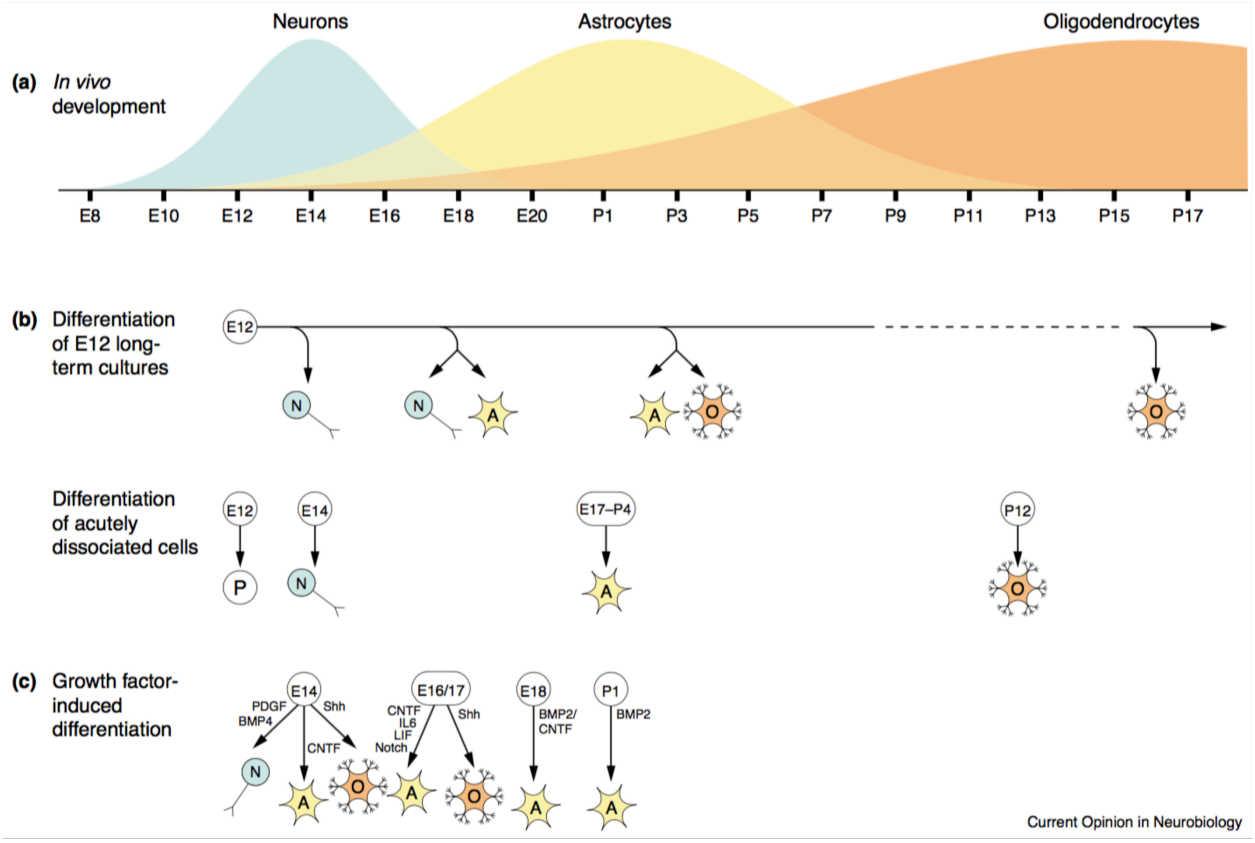


Figure 1-4. Cortical progenitor cells follow an intrinsic developmental sequence both *in vivo* and *in vitro*.

(a) The generation of the three cell types within the brain occurs in a temporally distinct yet overlapping pattern. In rats, neurogenesis peaks at E14, astrogliogenesis at P2, and oligodendrogenesis at P14.

(b) *In vitro* cultures mimic the NPC differentiation pattern *in vivo*. Long-term cultures of cells isolated at E12 will sequentially give rise to neurons, then astrocytes, and finally oligodendrocytes. Cells dissected at different developmental periods differentiate into progeny that reflect the developmental activity occurring at time of dissection.

(c) Growth factor stimulation of cells dissected from different developmental stages reveals that cortical progenitor cells become progressively more fate- restricted and respond differently to extracellular cues over time. Cells isolated at E14 have the potential to develop into all three cell types, whereas older cells preferentially adopt glial fates. PDGF drives neuronal differentiation. Cytokines and Notch proteins promote astrocytic fate determination. Oligodendrocyte formation is driven by Shh, and the BMPs promote either neuronal or astrocytic fates depending on the age of the cell. A, astrocyte; N, neuron; O, oligodendrocyte; P, progenitor cell.

Adapted form Sauvageot and Stiles (Sauvageot, 2002) with permission from Elsevier.

References

Adelman, D.M., Gertsenstein, M., Nagy, A., Simon, M.C., and Maltepe, E. (2000). Placental cell fates are regulated *in vivo* by HIF-mediated hypoxia responses. Genes & Development *14*, 3191–3203.

Alexandre, P., Reugels, A.M., Barker, D., Blanc, E., and Clarke, J.D.W. (2010). Neurons derive from the more apical daughter in asymmetric divisions in the zebrafish neural tube. Nat. Neurosci. *13*, 673–679.

Amarilio, R., Viukov, S.V., Sharir, A., Eshkar-Oren, I., Johnson, R.S., and Zelzer, E. (2007). HIF1α regulation of Sox9 is necessary to maintain differentiation of hypoxic prechondrogenic cells during early skeletogenesis. Development *134*, 3917–3928.

Ambros, V., and Horvitz, H.R. (1984). Heterochronic mutants of the nematode. Science.

Assad, F., Schultheiss, R., Leniger-Follert, E., and Wüllenweber, R. (1984). Measurement of Local Oxygen Partial Pressure (PO2) of the Brain Cortex in Cases of Brain Tumors. In CNS Metastases Neurosurgery in the Aged, (Berlin, Heidelberg: Springer Berlin Heidelberg), pp. 263–270.

Baader, E., Tschank, G., Baringhaus, K.H., Burghard, H., and Günzler, V. (1994). Inhibition of prolyl 4-hydroxylase by oxalyl amino acid derivatives *in vitro*, in isolated microsomes and in embryonic chicken tissues. Biochem. J. *300 (Pt 2)*, 525–530.

Bultje, R.S., Castaneda-Castellanos, D.R., Jan, L.Y., Jan, Y.-N., Kriegstein, A.R., and Shi, S.-H. (2009). Mammalian Par3 Regulates Progenitor Cell Asymmetric Division via Notch Signaling in the Developing Neocortex. Neuron *63*, 189–202.

Butler, H., and Juurlink, J.B.H. (1987). An atlas for staging mammalian and chick embryos.

Campbell, K.H.S., McWhir, J., Ritchie, W.A., and Wilmut, I. (1996). Sheep cloned by nuclear transfer from a cultured cell line. , Published Online: 07 March 1996; | Doi:10.1038/380064a0 *380*, 64–66.

Carreau, A., Hafny Rahbi, B.E., Matejuk, A., Grillon, C., and Kieda, C. (2011). Why is the partial oxygen pressure of human tissues a crucial parameter? Small molecules and hypoxia. Journal of Cellular and Molecular Medicine *15*, 1239–1253.

Chang, T.C., Zeitels, L.R., Hwang, H.W., Chivukula, R.R., Wentzel, E.A., Dews, M., Jung, J., Gao, P., Dang, C.V., Beer, M.A., et al. (2009). Lin-28B transactivation is necessary for Myc-mediated *let-7* repression and proliferation. Proceedings of the National Academy of Sciences *106*, 3384–3389.

Cimadamore, F., Amador-Arjona, A., Chen, C., Huang, C.-T., and Terskikh, A.V. (2013). SOX2-LIN28/*let-7* pathway regulates proliferation and neurogenesis in neural precursors. Proc. Natl. Acad. Sci. U.S.a. *110*, E3017–E3026.

Clancy, B., Darlington, R.B., and Finlay, B.L. (2001). Translating developmental time across mammalian species. Neuroscience *105*, 7–17.

Compernolle, V., Brusselmans, K., Franco, D., Moorman, A., Dewerchin, M., Collen, D., and Carmeliet, P. (2003). Cardia bifida, defective heart development and abnormal neural crest migration in embryos lacking hypoxia-inducible factor-1α. Cardiovascular Research *60*, 569–579.

Corti, S., Nizzardo, M., and Simone, C. (2012). Genetic correction of human induced pluripotent stem cells from patients with spinal muscular atrophy. Science Translational ….

Costa, M.R., Wen, G., Lepier, A., Schroeder, T., and Götz, M. (2008). Par-complex proteins promote proliferative progenitor divisions in the developing mouse cerebral cortex. Development *135*, 11–22.

Cowden Dahl, K.D., Fryer, B.H., Mack, F.A., Compernolle, V., Maltepe, E., Adelman, D.M., Carmeliet, P., and Simon, M.C. (2005). Hypoxia-inducible factors 1alpha and 2alpha regulate trophoblast differentiation. Molecular and Cellular Biology *25*, 10479–10491.

Cox, J.L., Mallanna, S.K., Luo, X., and Rizzino, A. (2010). Sox2 Uses Multiple Domains to Associate with Proteins Present in Sox2-Protein Complexes. PLoS ONE *5*, e15486.

Danés, A.S. (2012). Disease-specific phenotypes in dopamine neurons from human iPS-based models of genetic and sporadic Parkinson's disease. EMBO Molecular ….

Denko, N.C. (2008). Hypoxia, HIF1 and glucose metabolism in the solid tumour. Nature Reviews| Cancer *8*, 705–713.

Dimos, J.T., Rodolfa, K.T., Niakan, K.K., Weisenthal, L.M., Mitsumoto, H., Chung, W., Croft, G.F., Saphier, G., Leibel, R., Goland, R., et al. (2008). Induced pluripotent stem cells generated from patients with ALS can be differentiated into motor neurons. Science *321*, 1218–1221.

Dings, J., Meixensberger, J., Jäger, A., and Roosen, K. (1998). Clinical experience with 118 brain tissue oxygen partial pressure catheter probes. Neurosurgery *43*, 1082–1095.

Dunwoodie, S. (2009). The Role of Hypoxia in Development of the Mammalian Embryo. Developmental Cell.

Ebert, A.D., Yu, J., Rose, F.F., Mattis, V.B., Lorson, C.L., Thomson, J.A., and Svendsen, C.N. (2009). Induced pluripotent stem cells from a spinal muscular atrophy patient. Nature *457*, 277–280.

Ema, M., Taya, S., Yokotani, N., Sogawa, K., Matsuda, Y., and Fujii-Kuriyama, Y. (1997). A novel bHLH-PAS factor with close sequence similarity to hypoxia-inducible factor 1alpha regulates the VEGF expression and is potentially involved in lung and vascular development. Proceedings of the National Academy of Sciences *94*, 4273–4278.

Evans, M.J., and andKaufman, M.H. (1981). Establishmentin cultureofpluripotentialcellsfrom

mouseembryos (Nature).

Genbacev, O., Zhou, Y., Ludlow, J.W., and Fisher, S.J. (1997). Regulation of human placental development by oxygen tension. Science *277*, 1669–1672.

Gleadle, J.M., Ebert, B.L., Firth, J.D., and Ratcliffe, P.J. (1995). Regulation of angiogenic growth factor expression by hypoxia, transition metals, and chelating agents. Am. J. Physiol. *268*, C1362–C1368.

Götz, M., and Huttner, W.B. (2005). The cell biology of neurogenesis. Nat Rev Mol Cell Biol *6*, 777–788.

Gu, Y.Z., Moran, S.M., Hogenesch, J.B., Wartman, L., and Bradfield, C.A. (1998). Molecular characterization and chromosomal localization of a third alpha-class hypoxia inducible factor subunit, HIF3alpha. Gene Expr. *7*, 205–213.

Gurdon, J.B., Elsdale, T.R., and Fischberg, M. (1958). Sexually Mature Individuals of Xenopus laevis from the Transplantation of Single Somatic Nuclei. , Published Online: 05 July 1958; | Doi:10.1038/182064a0 *182*, 64–65.

Ha, M., and Kim, V.N. (2014). Regulation of microRNA biogenesis. Nat Rev Mol Cell Biol *15*, 509–524.

Heo, I., Joo, C., Kim, Y.-K., Ha, M., Yoon, M.-J., Cho, J., Yeom, K.-H., Han, J., and Kim, V.N. (2009). TUT4 in Concert with Lin28 Suppresses MicroRNA Biogenesis through Pre-MicroRNA Uridylation. Cell *138*, 696–708.

Hoffman, W.E., Charbel, F.T., and Edelman, G. (1996). Brain tissue oxygen, carbon dioxide, and pH in neurosurgical patients at risk for ischemia. Anesth. Analg. *82*, 582–586.

Hotta, A., and Yamanaka, S. (2015). From Genomics to Gene Therapy: Induced Pluripotent Stem Cells Meet Genome Editing. Http://Dx.Doi.org/10.1146/Annurev.Neuro.25.030702.130823 *49*, annurev–genet–112414–054926.

Iliopoulos, D., Hirsch, H.A., and Struhl, K. (2009). An Epigenetic Switch Involving NF-κB, Lin28, *Let-7* MicroRNA, and IL6 Links Inflammation to Cell Transformation. Cell *139*, 693–706.

Israel, M.A., Yuan, S.H., Bardy, C., Reyna, S.M., Mu, Y., Herrera, C., Hefferan, M.P., Van Gorp, S., Nazor, K.L., Boscolo, F.S., et al. (2012). Probing sporadic and familial Alzheimer/'s disease using induced pluripotent stem cells. Nature *482*, 216–220.

Ivan, M., Haberberger, T., Gervasi, D.C., Michelson, K.S., Gunzler, V., Kondo, K., Yang, H., Sorokina, I., Conaway, R.C., Conaway, J.W., et al. (2002). Biochemical purification and pharmacological inhibition of a mammalian prolyl hydroxylase acting on hypoxia-inducible factor. Proceedings of the National Academy of Sciences *99*, 13459–13464.

Jiang, W., Bikard, D., Cox, D., Zhang, F., and Marraffini, L.A. (2013). RNA-guided editing of

bacterial genomes using CRISPR-Cas systems. Nature Biotechnology *31*, 233–239.

Jinek, M., Chylinski, K., Fonfara, I., Hauer, M., Doudna, J.A., and Charpentier, E. (2012). A programmable dual-RNA-guided DNA endonuclease in adaptive bacterial immunity. Science *337*, 816–821.

Kawahara, H., Okada, Y., Imai, T., Iwanami, A., Mischel, P.S., and Okano, H. (2011). Musashi1 cooperates in abnormal cell lineage protein 28 (Lin28)-mediated *let-7* family microRNA biogenesis in early neural differentiation. Journal of Biological Chemistry *286*, 16121–16130.

Kozak, K.R., Abbott, B., and Hankinson, O. (1997). ARNT-deficient mice and placental differentiation. Dev. Biol. *191*, 297–305.

Krencik, R., and Zhang, S.-C. (2011). Directed differentiation of functional astroglial subtypes from human pluripotent stem cells. Nat Protoc *6*, 1710–1717.

Krishnan, J., Ahuja, P., Bodenmann, S., Knapik, D., Perriard, E., Krek, W., and Perriard, J.-C. (2008). Essential role of developmentally activated hypoxia-inducible factor 1alpha for cardiac morphogenesis and function. Circulation Research *103*, 1139–1146.

La Torre, A., Georgi, S., and Reh, T.A. (2013). Conserved microRNA pathway regulates developmental timing of retinal neurogenesis. Proc. Natl. Acad. Sci. U.S.a. *110*, E2362–E2370.

Lancaster, M.A., and Knoblich, J.A. (2012). Spindle orientation in mammalian cerebral cortical development. Current Opinion in Neurobiology *22*, 737–746.

Lendahl, U., Lee, K., Yang, H., and Poellinger, L. (2009). Generating specificity and diversity in the transcriptional response to hypoxia. Nature Reviews Genetics.

Licht, A.H., Müller-Holtkamp, F., Flamme, I., and Breier, G. (2006). Inhibition of hypoxia-inducible factor activity in endothelial cells disrupts embryonic cardiovascular development. Blood *107*, 584–590.

Lyer, N.V., Kotch, L.E., Agani, F., Leung, S.W., and Laughner, E. (1998). Cellular and developmental control of O2 homeostasis by hypoxia-inducible factor 1a (Genes Dev).

Maltepe, E., Schmidt, J.V., Baunoch, D., Bradfield, C.A., and Simon, M.C. (1997). Abnormal angiogenesis and responses to glucose and oxygen deprivation in mice lacking the protein ARNT. Nature *386*, 403–407.

Marson, A., Levine, S.S., Cole, M.F., Frampton, G.M., Brambrink, T., Johnstone, S., Guenther, M.G., Johnston, W.K., Wernig, M., Newman, J., et al. (2008). Connecting microRNA genes to the core transcriptional regulatory circuitry of embryonic stem cells. Cell *134*, 521–533.

Martin, G.R. (1981). Isolation of a pluripotent cell line from early mouse embryos cultured in medium conditioned by teratocarcinoma stem cells. Proceedings of the National Academy of Sciences *78*, 7634–7638.

Meixensberger, D.J., Dings, J., Kuhnigk, H., and Roosen, K. (1993). Studies of Tissue PO2 in Normal and Pathological Human Brain Cortex. In Monitoring of Cerebral Blood Flow and Metabolism in Intensive Care, (Vienna: Springer Vienna), pp. 58–63.

Morriss, G.M., and New, D.A.T. (1979). Effect of oxygen concentration on morphogenesis of cranial neural folds and neural crest in cultured rat embryos. Development *54*, 17–35.

Morrow, T., Song, M.R., and Ghosh, A. (2001). Sequential specification of neurons and glia by developmentally regulated extracellular factors. Development *128*, 3585–3594.

Moss, E.G., Lee, R.C., and Ambros, V. (1997). The Cold Shock Domain Protein LIN-28 Controls Developmental Timing in C. elegans and Is Regulated by the lin-4 RNA. Cell *88*, 637–646.

Nam, Y., Chen, C., Gregory, R.I., Chou, J.J., and Sliz, P. (2011). Molecular Basis for Interaction of *let-7* MicroRNAs with Lin28. Cell *147*, 1080–1091.

Newman, M.A., Thomson, J.M., and Hammond, S.M. (2008). Lin-28 interaction with the *Let-7* precursor loop mediates regulated microRNA processing. Rna *14*, 1539–1549.

Onder, T.T., Kara, N., Cherry, A., Sinha, A.U., Zhu, N., Bernt, K.M., Cahan, P., Mancarci, B.O., Unternaehrer, J., Gupta, P.B., et al. (2012). Chromatin-modifying enzymes as modulators of reprogramming. Nature *483*, 598–602.

Paranjpe, M. (2015). The Lin28/*Let-7* Axis: An Evolutionarily Conserved Superpathway.

Paridaen, J.T., and Huttner, W.B. (2014). Neurogenesis during development of the vertebrate central nervous system. EMBO Reports *15*, e201438447–364.

Patterson, M., Gaeta, X., Loo, K., Edwards, M., Smale, S., Cinkornpumin, J., Xie, Y., Listgarten, J., Azghadi, S., Douglass, S.M., et al. (2014). *let-7* miRNAs Can Act through Notch to Regulate Human Gliogenesis. Stem Cell Reports *3*, 758–773.

Patterson, M., Chan, D.N., Ha, I., Case, D., Cui, Y., Handel, B.V., Mikkola, H.K., and Lowry, W.E. (2011). Defining the nature of human pluripotent stem cell progeny. Cell Res *22*, 178–193.

Provot, S., Zinyk, D., Gunes, Y., Kathri, R., Le, Q., Kronenberg, H.M., Johnson, R.S., Longaker, M.T., Giaccia, A.J., and Schipani, E. (2007). Hif-1alpha regulates differentiation of limb bud mesenchyme and joint development. J Cell Biol *177*, 451–464.

Ramachandran, R., Fausett, B.V., and Goldman, D. (2010). Ascl1a regulates Muller glia dedifferentiation and retinal regeneration through a Lin-28-dependent, *let-7* microRNA signalling pathway. Nat Cell Biol *12*, 1101–1107.

Ratcliffe, P.J. (2007). HIF-1 and HIF-2: working alone or together in hypoxia? J. Clin. Invest. *117*, 862–865.

Ravenna, L., Salvatori, L., and Russo, M.A. (2015). HIF3α: the little we know. Febs J. n/a–n/a.

Rehfeld, F., Rohde, A.M., Nguyen, D.T.T., and Wulczyn, F.G. (2015). Lin28 and *let-7*: ancient milestones on the road from pluripotency to neurogenesis. Cell Tissue Res *359*, 145–160.

Roper, K., Kosodo, Y., Marzesco, A.M., and Haubensak, W. (2004). Asymmetric distribution of the apical plasma membrane during neurogenic divisions of mammalian neuroepithelial cells. The EMBO Journal 2314–2324.

Roush, S., and Slack, F.J. (2008). The *let-7* family of microRNAs. Trends in Cell Biology *18*, 505–516.

Rousso, D.L., Pearson, C.A., Gaber, Z.B., Miquelajauregui, A., Li, S., Portera-Cailliau, C., Morrisey, E.E., and Novitch, B.G. (2012). Foxp-mediated suppression of N-cadherin regulates neuroepithelial character and progenitor maintenance in the CNS. Neuron *74*, 314–330.

Ruas, J.L., and Poellinger, L. (2005). Hypoxia-dependent activation of HIF into a transcriptional regulator. Seminars in Cell & Developmental Biology *16*, 514–522.

Ryan, H.E., Lo, J., and Johnson, R.S. (1998). HIF-1α is required for solid tumor formation and embryonic vascularization. The EMBO Journal.

Sauvageot, C. (2002). Molecular mechanisms controlling cortical gliogenesis. Current Opinion in Neurobiology *12*, 244–249.

Schofield, C.J., and Ratcliffe, P.J. (2004). Oxygen sensing by HIF hydroxylases. Nat Rev Mol Cell Biol *5*, 343–354.

Shaltouki, A., Peng, J., Liu, Q., Rao, M.S., and Zeng, X. (2013). Efficient Generation of Astrocytes from Human Pluripotent Stem Cells in Defined Conditions. Stem Cells *31*, 941–952.

Shitamukai, A., and Matsuzaki, F. (2012). Control of asymmetric cell division of mammalian neural progenitors. Development, Growth & Differentiation *54*, 277–286.

Shitamukai, A., Konno, D., and Matsuzaki, F. (2011). Oblique radial glial divisions in the developing mouse neocortex induce self-renewing progenitors outside the germinal zone that resemble primate outer subventricular zone progenitors. J. Neurosci. *31*, 3683–3695.

Shyh-Chang, N., and Daley, G.Q. (2013). Lin28: primal regulator of growth and metabolism in stem cells. Cell Stem Cell *12*, 395–406.

Silver, I., and Erecińska, M. (1998). Oxygen and Ion Concentrations in Normoxic and Hypoxic Brain Cells. In Oxygen Transport to Tissue XX, (Boston, MA: Springer US), pp. 7–16.

Simon, M.C., and Keith, B. (2008). The role of oxygen availability in embryonic development and stem cell function. Nat Rev Mol Cell Biol *9*, 285–296.

Sloan, S.A., and Barres, B.A. (2014). Mechanisms of astrocyte development and their contributions to neurodevelopmental disorders. Current Opinion in Neurobiology *27*, 75–81.

Soldner, F., Laganière, J., Cheng, A.W., Hockemeyer, D., Gao, Q., Alagappan, R., Khurana, V., Golbe, L.I., Myers, R.H., Lindquist, S., et al. (2011). Generation of Isogenic Pluripotent Stem Cells Differing Exclusively at Two Early Onset Parkinson Point Mutations. Cell *146*, 318–331.

Stiles, J., and Jernigan, T.L. (2010). The Basics of Brain Development. Neuropsychol Rev *20*, 327–348.

Takahashi, K., and Yamanaka, S. (2006). Induction of Pluripotent Stem Cells from Mouse Embryonic and Adult Fibroblast Cultures by Defined Factors. Cell *126*, 663–676.

Thomson, J.A., Itskovitz-Eldor, J., Shapiro, S.S., Waknitz, M.A., Swiergiel, J.J., Marshall, V.S., and Jones, J.M. (1998). Embryonic stem cell lines derived from human blastocysts. Science *282*, 1145–1147.

Thornton, J.E., and Gregory, R.I. (2012). How does Lin28 *let-7* control development and disease? Trends in Cell Biology *22*, 474–482.

Tian, H., McKnight, S.L., and Russell, D.W. (1997). Endothelial PAS domain protein 1 (EPAS1), a transcription factor selectively expressed in endothelial cells. Genes & Development *11*, 72–82.

Tomita, S., Ueno, M., Sakamoto, M., Kitahama, Y., Ueki, M., Maekawa, N., Sakamoto, H., Gassmann, M., Kageyama, R., Ueda, N., et al. (2003). Defective brain development in mice lacking the Hif-1alpha gene in neural cells. Molecular and Cellular Biology *23*, 6739–6749.

Velasco, I., Salazar, P., Giorgetti, A., Ramos Mejía, V., Castaño, J., Romero Moya, D., and Menendez, P. (2014). Concise Review: Generation of Neurons From Somatic Cells of Healthy Individuals and Neurological Patients Through Induced Pluripotency or Direct Conversion. Stem Cells *32*, 2811–2817.

Viswanathan, S.R., Daley, G.Q., and Gregory, R.I. (2008). Selective Blockade of MicroRNA Processing by Lin28. Science *320*, 97–100.

Viswanathan, S.R., and Daley, G.Q. (2010). Lin28: A MicroRNA Regulator with a Macro Role. Cell *140*, 445–449.

Wang, G.L., and Semenza, G.L. (1993). Desferrioxamine induces erythropoietin gene expression and hypoxia-inducible factor 1 DNA-binding activity: implications for models of hypoxia signal transduction. Blood *82*, 3610–3615.

Wang, G.L., Jiang, B.H., Rue, E.A., and Semenza, G.L. (1995). Hypoxia-inducible factor 1 is a basic-helix-loop-helix-PAS heterodimer regulated by cellular O2 tension. Proceedings of the National Academy of Sciences *92*, 5510–5514.

Wang, S., Bates, J., Li, X., Schanz, S., Chandler-Militello, D., Levine, C., Maherali, N., Studer, L., Hochedlinger, K., Windrem, M., et al. (2013). Human iPSC-derived oligodendrocyte progenitor cells can myelinate and rescue a mouse model of congenital hypomyelination. Cell Stem Cell *12*, 252–264.

Webb, J.D., Coleman, M.L., and Pugh, C.W. (2009). Hypoxia, hypoxia-inducible factors (HIF), HIF hydroxylases and oxygen sensing. Cell. Mol. Life Sci. *66*, 3539–3554.

Wodarz, A., and Huttner, W.B. (2003). Asymmetric cell division during neurogenesis in Drosophila and vertebrates. Mechanisms of Development *120*, 1297–1309.

Xie, Y., Zhang, J., Lin, Y., Gaeta, X., Meng, X., Wisidagama, D.R.R., Cinkornpumin, J., Koehler, C.M., Malone, C.S., Teitell, M.A., et al. (2014). Defining the role of oxygen tension in human neural progenitor fate. Stem Cell Reports *3*, 743–757.

Yang, D.-H., and Moss, E.G. (2003). Temporally regulated expression of Lin-28 in diverse tissues of the developing mouse. Gene Expression Patterns *3*, 719–726.

Yu, J., Vodyanik, M.A., Smuga-Otto, K., Antosiewicz-Bourget, J., Frane, J.L., Tian, S., Nie, J., Jonsdottir, G.A., Ruotti, V., Stewart, R., et al. (2007). Induced pluripotent stem cell lines derived from human somatic cells. Science *318*, 1917–1920.

Zhu, H., Shah, S., Shyh-Chang, N., Shinoda, G., Einhorn, W.S., Viswanathan, S.R., Takeuchi, A., Grasemann, C., Rinn, J.L., Lopez, M.F., et al. (2010). Lin28a transgenic mice manifest size and puberty phenotypes identified in human genetic association studies. Nat Genet *42*, 626–630.

CHAPTER 2

Defining the role of oxygen tension in human neural progenitor fate

ABSTRACT

Hypoxia augments human embryonic stem cell self-renewal via hypoxia-inducible factor 2α activated *OCT4* transcription. Hypoxia also increases the efficiency of reprogramming differentiated cells to a pluripotent-like state. Combined, these findings suggest that low oxygen (O_2) tension would impair the purposeful differentiation of pluripotent stem cells. Here, we show that low O_2 tension and HIF activity instead promotes appropriate hESC differentiation. Through gain and loss of function studies, we implicate O_2 tension as a modifier of a key cell fate decision, namely whether neural progenitors differentiate towards neurons or glia. Furthermore, our data show that even transient changes in O_2 concentration can affect cell fate through HIF by regulating the activity of MYC, a regulator of LIN28/*let-7* that is critical for fate decisions in the neural lineage. We also identify key small molecules that can take advantage of this pathway to quickly and efficiently promote the development of mature cell types.

INTRODUCTION

Human embryonic stem cells (hESCs) originate from the blastocyst inner cell mass (Thomson et al., 1998), which is in a hypoxic microenvironment estimated at 1.5 – 5.3% O_2 in the mammalian reproductive tract (Dunwoodie, 2009; Mohyeldin et al., 2010; Simon and Keith, 2008). hESCs grown in physiological O_2 (~5% or less O_2) self-renew with reduced levels of spontaneous differentiation compared to hESCs grown in atmospheric O_2 (~21% O_2) (Ezashi et al., 2005; Westfall et al., 2008). hESCs isolated and passed exclusively in physiological O_2 contain two active X chromosomes (XaXa), marking a less differentiated state than that in atmospheric O2 which typically contains one inactive X chromosome (Lengner et al., 2010). Physiological O_2

also improves the efficiency of defined factor-induced cellular reprogramming to a pluripotent-like state (Yoshida et al., 2009). Combined, these studies show the importance of physiological O_2 in supporting stem cell self-renewal and in suppressing spontaneous, usually unwanted hESC differentiation.

Studies on the role of O_2 tension in promoting pluripotency have indicated hypoxia-inducible factor 2α (HIF2α) (also called endothelial PAS domain protein 1, EPAS1) and HIF3α in the transcriptional upregulation of *OCT4* in hESCs (Forristal et al., 2010). These findings are also consistent with the role of Hif2α in trans-activating *Oct4* expression in mouse ESCs (Covello et al., 2006). Since the activation of HIF pathway appears to favor self-renewal, it might be expected that HIF activity would also inhibit purposeful hESC differentiation. Four studies have examined the effects of hypoxia on early hESC differentiation, but none have specifically examined the role of HIF. In these studies, hESCs in physiological O_2 showed enhanced embryoid body (EB) formation or endothelial and cardiomyocyte differentiation (Ezashi et al., 2005; Lim et al., 2011; Ng et al., 2010; Prado-Lopez et al., 2010). However, physiological O_2 induces pleiotropic cellular and molecular effects and the underlying cause(s) for paradoxically enhanced EB or lineage formation in physiological O_2 is unclear. For example, O_2 concentration is known to affect 1) oxidative stress and hESC growth (Ezashi et al., 2005); 2) the activity of O_2-dependent enzymes, such as Jumonji domain-containing dioxygenases (Xia et al., 2009) which have broad roles in the epigenetic regulation of gene expression; 3) multiple O_2-sensing signal transduction pathways including the mTOR pathway (Wouters and Koritzinsky, 2008) and the unfolded protein response-activated endoplasmic reticulum stress pathway (Wouters and Koritzinsky, 2008); and 4) the HIF-controlled gene transcription network (Lendahl et al., 2009).

Therefore, it remains unclear whether the enhancement of EB or lineage specific differentiation in physiological O_2 occurs mainly through HIF transactivation or other molecular mechanisms.

HIFs are major regulators of the cellular response to O_2 tension (Denko, 2008; Lendahl et al., 2009; Majmundar et al., 2010). HIFs form a heterodimer composed of HIF-α and HIF-1β (also called aryl hydrocarbon receptor nuclear translocator, ARNT) to transactivate hypoxia-responsive genes. They are regulated at the level of α-subunit protein stability in an O_2-dependent manner. When oxygen is abundant, HIF-α subunits are hydroxylated by prolyl hydroxylase domain (PHDs) proteins (in the presence of Fe^{2+}) and recognized by an E3 ubiquitin ligase, VHL (Von Hippel-Lindau), leading to degradation in the proteasome. In hypoxic conditions, decreased O_2 diminished enzymatic activity of PHDs. As a result, HIF1α and HIF2α proteins are stabilized and dimerize with HIF1β in the nucleus to transactivate specific target genes. In *Hif1α*, *Hif2α*, and *Hif1β* knockout mice, deficient Hif activity impaired placental development (Adelman et al., 2000; Cowden Dahl et al., 2005; Kozak et al., 1997), heart development (Krishnan et al., 2008; Licht et al., 2006), and endochondrial bone formation during early embryogenesis (Amarilio et al., 2007; Dunwoodie, 2009; Provot et al., 2007). Furthermore, conditional knockout mice of *Hif1α* in central nervous system exhibit hydrocephalus accompanied by a reduction in neural cells and an impairment of spatial memory (Tomita et al., 2003). Those studies demonstrated the importance of *Hifs* in normal brain development. It is clear from the vast majority of studies on human pluripotent cell differentiation that typical protocols generate cells more akin to those found during the earliest stages of tissue formation, prior to significant tissue vascularization. What is less understood is whether methods to culture

cells that more accurately replicate *in vivo* conditions can affect the developmental potential of pluripotent progeny.

Previous studies describing antagonism between HIF and MYC were mostly in the context of cancer, and the roles of HIF1α and HIF2α were determined to be distinct. HIF1α induced cell cycle arrest by functionally counteracting MYC through $p21^{cip1}$ (Koshiji et al., 2004). HIF1α induced MXI1 expression to inhibit a subset of MYC target genes that are involved in mitochondrial biogenesis and oxygen consumption (Corn et al., 2005; Zhang et al., 2007). However, HIF2α promoted cell proliferation in various cell lines under hypoxic conditions by stimulating MYC binding to its target gene promoters (Gordan et al., 2007). Increased HIF2α and decreased p21 level in patients with VHL gene mutations could lead to increased hepatocyte proliferation, which explained the increased volumes of liver relative to their body mess. (Yoon et al., 2010). Most of the studies mentioned above were performed in disease models, and thus may not be applicable to normal human development.

To determine whether O_2 tension regulates differentiation from pluripotent stem cells and affects the developmental maturity of their progeny, we specifically evaluated HIF transactivation in both undirected and directed hESC differentiation using loss and gain-of-function approaches. We report that HIF activity is required for induction of appropriate germ layer specification. In addition, we identify LIN28 and *let-7* family microRNAs as key molecular nodes through which HIF activity promotes appropriate directed differentiation of neural progenitors towards either neurons or glia through MYC. Our study reveals that O_2 tension and HIF activity could be vital

to maintaining appropriate fate progression *in vitro* and identify simple methods to facilitate these transitions.

RESULTS

Oxygen tension regulates human germ layer formation

Using EB formation from human pluripotent stem cells as a model of germ layer formation, we assayed the role of O_2 tension by altering the concentration of O_2 in culture. As shown in Figure 2-1, reducing the O_2 tension to levels more close to physiological conditions (2% O_2) dramatically altered the acquisition of germ layer fates in EBs as measured by transcriptome profiling (Fig 2-1A) for hallmark genes. Gene Ontology (GO) analysis demonstrated that neural, vascular, and skeletal differentiation was altered by changes in O_2 concentration (Fig 2-1A). In particular, neural differentiation appeared to be significantly promoted in EBs generated in physiological O_2 at the expense of other lineages, with classic markers such as *SOX1*, *HES5*, *FOXG1,* and other neural lineage genes all induced (Fig 2-1B).

Since O_2 levels are monitored molecularly by the HIF pathway (Fig S2-1), we blocked HIF1α or HIF1β using small hairpin RNA (shRNA) (Fig S2-1). Generating EBs with stable knockdown of either HIF1α or β under physiological O_2 conditions disrupted gene expression significantly (Fig 2-1C), and altered the acquisition of neural, cardiac, and skeletal muscle lineages (Fig 2-1D). Many of the gene expression changes induced by altering the HIF sensing machinery were also validated in independent EB experiments by RT-PCR (Fig S2-1F). As anticipated, the genes changed by altering O_2 levels were highly similar to those affected by shHIF1β (Fig 2-1E),

demonstrating the critical role for HIF1β in O_2 sensing during EB formation. These data demonstrate that the HIF O_2 sensing pathway regulates appropriate early undirected differentiation and potentially germ layer acquisition. To determine whether the HIF pathway is also important for directed differentiation, pluripotent stem cells were subjected to culture conditions that promote the neural lineage.

Developmental maturity of the neural lineage is regulated by oxygen tension

Human pluripotent stem cells can be driven toward the neural lineage by simply changing the culture medium and generating rosette structures. Rosette derived neural progenitor cell (NPC) can generate both neurons and glia. Human pluripotent stem cell (PSC) derived NPCs typically differentiate into neurons with a small proportion of glia. Current consensus suggests that this neuronal bias is due to the developmental immaturity of pluripotent derivatives and the fact that neurogenesis precedes gliogenesis during development (Miyata et al., 2010). Most of the experiments that have generated this consensus have thus far been carried out in atmospheric O_2; therefore, we assayed the effect of lowering the O_2 tension in human NPC cultures. Remarkably, simply lowering the concentration of O_2 in NPC cultures completely shifted the bias away from neuronal towards glia differentiation (Fig 2-2A and Fig S2-2B), suggesting that O_2 tension can affect cell fate decisions in the neural lineage. Interestingly, even just a brief exposure of NPCs to a physiological O_2 concentration influenced cell fate in the neural lineage towards glial production (Fig 2-2B), suggesting that the O_2 sensing machinery induces a lasting effect on NPC differentiation potential. Cell cycle analysis suggested that the effect of low O_2 tension on differentiation was not related to cell cycle changes (Fig S2-2A). Furthermore, immunostaining of NPCs in 2% and 20% O_2 suggested that the glial induction was not due to changes of

apoptosis as the percentage of cells positive for cleaved Caspase-3 was less than 1.5% in all conditions tested (Fig S2-2C).

To delineate the role of the O_2 sensing pathway in neural fate decisions, the shHIF1α and shHIF1β hESC lines were used to make NPCs. Relative to control lines, NPCs with reduced HIF signaling displayed an almost complete block in producing astroglia in 2% O_2 (Fig 2-3A and B), consistent with our data showing that HIF stabilization in physiologic O_2 drives gliogenesis. Note that HIF1β knockdown had a more significant role in blocking gliogenesis than knocking down HIF1α. Because HIF1β forms heterodimer with either HIFα or HIF2α, we tested the role of HIF2α in this cell fate decision. Despite the fact that some reports argue for differential roles for HIF1α versus HIF2α we found that silencing HIF2α either by siRNA or by shRNA blocked the effect of low oxygen on gliogenesis in PSC-NPCs (Fig S2-3C and D). These results demonstrate that O_2 concentration is a key mediator of neurogenesis through the HIF signaling pathway.

Furthermore, several small molecules have been identified that induce the HIF pathway by blocking HIF degradation. Deferoxamine (DFX) stabilizes HIF by chelating Fe^{2+}, which is required for enzymatic activity of PHDs. NPCs grown in atmospheric O_2 and treated with DFX showed a translocation of HIF1α to the nucleus (Fig 2-4A) and a distinct increase in gliogenesis, as were shown for NPCs grown in physiological O_2 (Fig 2-4B and C). Importantly, key HIF target genes were induced by these manipulations, demonstrating *bona fide* HIF activation, such as *VEGFA, HK1, HK2, PGK1, PDK1* and *HIF2α* (Fig S2-3A and B). Because silencing HIF1β

and HIF2α each had significant effects on gliogenesis, we tested the effect of DFX when both of these key HIF transducers were silenced. In fact, gliogenesis was not affected in cells lacking these key mediators of the O_2 sensing pathway (Fig 2-4D), demonstrating that DFX indeed acts through the HIF pathway. Combined, these data show that HIF pathway signaling has an influence on cell fate decisions within the nervous system and also provides a rather simple method to create NPCs with a glial differentiation bias.

Molecular mechanism of neurogenesis by the HIF pathway

To understand how the HIF pathway can regulate NPC fate decisions, we probed for the gene expression changes induced by altering HIF activity with various methods. As shown above, HIF activity and neurogenesis was influenced by stabilizing HIF with DFX, or removal of HIF1β. We also overlaid differentially expressed genes between PSC-derived NPCs and human fetal brain derived NPCs, which are highly gliogenic and more developmental mature than PSC-NPCs (Patterson et al., 2012). Just a few gene expression changes were in common for all the manipulations performed including *LIN28A* (Fig 2-5A), a gene previously implicated in neurogenesis (Balzer et al., 2010; Cimadamore et al., 2013; Kawahara et al., 2011). To gain mechanistic insight into the function of HIF, we evaluated a broader profile of gene expression changes and attempted to identify common regulatory elements in those genes affected changes in HIF activity. Gene Set Enrichment Analysis (GSEA) identified a number of regulatory elements amongst the group of genes affected by changes in HIF activity (Table S2-1). At the top of the list was HIF and MYC, suggesting that a large number of genes affected by HIF activity are potentially MYC target genes (Fig 2-5B). Narrowing gene expression changes to those genes known to be directly regulated by HIF showed almost universal induction of HIF

target genes (Fig 2-5C). On the other hand, a similar analysis of MYC targets showed that roughly half of these genes were induced by physiological O_2, whereas the other half of these genes were suppressed (Fig 2-5D).

MYC stood out as an important regulator of HIF target genes because the binding sites for MYC and HIF can be highly overlapping (Fig 2-6A). One interesting gene that was affected by both HIF perturbation and known to be a MYC target gene is *LIN28*. The LIN28/*let-7* circuit can regulate developmental maturity in lower organisms, and the balance of activity of this circuit also correlates with neurogenic versus gliogenic potential in human NPCs (Patterson et al., 2012; Patterson et al., in press). The suppression of *LIN28* and gain of *let-7* miRNA expression is known to strongly correlate with the adoption of a gliogenic phenotype (La Torre et al., 2013; Patterson et al., 2012), as shown here by the induction of HIF activity. Based on these data, we explored the hypothesis that HIF regulates *LIN28* amongst a number of other target genes by competing for binding to specific gene promoters and displacing MYC.

To monitor transcriptional activity of the *LIN28* gene, we took advantage of an expression construct with defined MYC binding sites known to report transactivation of *LIN28B* (Chang et al., 2009). *LIN28B* reporter activity was induced with MYC overexpression (Fig 2-6A) and strongly suppressed by stabilization of HIF by DFX in a dose-dependent manner, consistent with HIF activity suppressing the *LIN28B* target genes (Fig 2-6B). Furthermore, when the MYC/HIF binding site within the *LIN28B* promoter was mutated, the reporter was no longer sensitive to DFX treatment (Fig 2-6B). In addition, both 2% O_2 and DFX drove a decrease in *LIN28A* and *LIN28B* expression levels in NPCs as measured by RT-PCR and immunostaining (Fig 2-6C and

D), and, as a result, mature *let-7* microRNA levels also increased (Fig 2-6E). Finally, using a reporter to detect *let-7* activity (Iwasaki et al., 2009), physiological O_2 significantly enhanced the activity of this family of miRNAs (Fig 2-6F). To explore the potential functional link between LIN28/*let-7* and O_2 tension in gliogenesis, DFX was combined with disruption of *let-7* levels. The ability of DFX to stimulate gliogenesis was completely abrogated by inhibition of *let-7* by antagomirs (Fig 2-6G and Fig S2-4).

These combined results predict that manipulation of MYC in NPCs would affect the balance of neurons and glia produced during NPC differentiation. Human pluripotent stem cell derived NPCs show a high level of expression for MYC family members, particularly N-MYC, whereas tissue derived progenitors isolated from mid-gestation brain are highly gliogenic and express negligible MYC (Patterson et al., in press). Therefore, *N-MYC* was silenced in NPCs by siRNA to determine whether it plays a functional role in developmental maturity in this context (Fig 2-7A). Silencing *N-MYC* in NPCs decreased the expression of *LIN28A*, *LIN28B*, and *HMGA2* (Fig 2-7A), which are the genes known to promote neurogenesis (Patterson et al., in press; Sanosaka et al., 2008).

Recently, it was shown that a small molecule inhibitor of BRD4 called JQ1 blocks transcription of *MYC* (Delmore et al., 2011; Mertz et al., 2011). To determine whether this inhibitor could also suppress *MYC* and *LIN28* expression, NPCs were treated with JQ1, which strongly suppressed *N-MYC* expression, but had little effect on *MYC* expression (Fig 2-7B). In addition, JQ1 treatment of NPCs led to decreased *LIN28A*, *LIN28B*, *HMGA2*, and *HES5* transcription (Fig 2-7B). This effect was quantifiable at the protein level as well for LIN28A and LIN28B (Fig 2-

7C and D). All of these transcripts have been implicated in neurogenesis (Patterson et al., in press; Sanosaka et al., 2008), and this pattern is consistent with a model in which JQ1 inhibits *N-MYC* expression, leading to lower *LIN28* expression, higher *let-7* activity, and lower expression of *let-7* target genes, such as *HMGA2*. Importantly, siRNA against *N-MYC* increased gliogenesis (Fig 2-7E). Furthermore, growth factor withdrawal to induce the differentiation of NPCs treated with JQ1 also shows a profound increase in gliogenesis (Fig 2-7F). Coupled with results using DFX, these data also provide relatively simple methods to improve the generation of glial cells *in vitro*.

DISCUSSION

The ability to culture human pluripotent stem cells *in vitro* has opened up significant avenues of biological exploration from development to cancer. As experimenters attempt to recapitulate tissue-like environments in *in vitro* systems, one important consideration is the concentration of cell permeable gasses such as O_2, nitric oxide, and CO_2. Almost all culture systems do not control for O_2 concentration and therefore use atmospheric O_2 levels. The physiological range of O_2 concentrations in brain tissues is much lower than atmospheric O_2 levels (Silver and Erecinska, 1998) and most studies of undirected or lineage specific differentiation *in vitro* have not considered O_2. Significant effort has delineated a role for O_2 tension in maintaining pluripotent stem cells, with the consensus that these cells "prefer" physiological O_2 concentrations as judged by their ability to self-renew and express pluripotency factors (Forristal et al., 2010; Lengner et al., 2010; Mohyeldin et al., 2010; Westfall et al., 2008; Yoshida et al., 2009). Less is understood about the role of O_2 tension during differentiation, with the early embryo thought to be in a particularly hypoxic environment due to low vascularity prior to

implantation. Even after implantation, there is heterogeneity in oxygen levels within the brain. Coupling this with the notion that pluripotent derivatives most accurately reflect cells found at the earliest stages of development, one could hypothesize that pluripotent differentiation should be performed under low oxygen conditions to more closely recapitulate the situation into which these cells are normally born.

Our data demonstrate that the concentration of oxygen has profound effects on both undirected and directed differentiation of human pluripotent stem cells. Portions of the pathway described here are consistent with the previous work describing neurogenesis in murine cells through Hif1, Lin28 and Myc (Balzer et al., 2010; Mutoh et al., 2012; Nagao et al., 2008). Here, we were able to piece together the entire pathway by which changes in oxygen concentration lead to altered cell fate decisions by NPCs, and have done so in a human model. The fact that this was done in the human systems is important because the relatively long time course typically required to generate glia in human PSC differentiation serves as a barrier to our understanding of non-neuronal cell types of the brain.

These findings provide a pathway by which neural progenitors can be driven through developmental stages to produce glia instead of neurons. At the most basic level, these data point towards relatively simple ways to guide developmental maturity of neural progenitors. More generally, these data could suggest that maintaining physiological oxygen concentrations could be important not only for more accurately recapitulating *in vivo* conditions, but also for

preserving developmental timing during *in vitro* differentiation to yield cell types that are not born until later time points in utero.

The results presented here suggest that HIF and MYC are antagonistic to each other in neurogenesis. While others have suggested this could be the case in other types of cells(Koshiji et al., 2004; Yoon et al., 2010), the mechanism proposed here is distinct. We found that a portion of MYC target sites in promoters also code for HIF binding. We propose a model whereby activation of HIF1α/β displaces MYC from targets such as LIN28, driving developmental progression. In our experiments, the use of low oxygen tension or hypoxia mimetics appeared to speed the process of development without dramatically altering the functional capacity of the cells generated.

An interesting aspect of these results is the fact that brief exposure to low oxygen or hypoxia mimetics was sufficient to induce the effect observed on developmental maturity. This suggests that low oxygen induces a lasting molecular change, perhaps in the epigenome of the cells. Significant efforts will be required to identify such a change, but this could lead to important insights into differences observed between NPCs born in tissue versus those born in culture in atmospheric oxygen (Patterson et al., in press).

MATERIALS AND METHODS

Cell culture

hESCs and human induced pluripotent stem cells (hiPSCs) were cultured as described previously

(Patterson et al., 2011) in accordance with UCLA Embryonic Stem Cell Research Oversight (ESCRO) committee. Experiments were performed on at least two independent hESC lines and one hiPSC line as indicated in the text. Feeder-free pluripotent stem cells were maintained with mTeSR1 (Stem Cell Technologies) and passaged mechanically using StemPro EZPassage Tool (Invitrogen). Neural rosette derivation, NPC purification, and further differentiation to neurons and glia were performed as described (Patterson et al., 2011). Briefly, rosettes were generated by growing pluripotent stem cells for at least 7 days in DMEM/F12 with N2 and B27 supplements (Invitrogen), 20 ng/mL basic fibroblast growth factor (FGF) (R&D systems), 1μM retinoic acid (RA) (Sigma), and 1μM Sonic Hedgehog Agonist (SAG) (Calbiochem). Once rosettes were picked, they were then cultured in NPC medium containing DMEM/F12, N2 and B27, 20 ng/ml basic FGF, and 50ng/ml epidermal growth factor (EGF) (Gibco). Deferoxamine (DFX) (Sigma) (100 to 200μM) and JQ1 (TOCRIS) (250 to 500nM) were added at the NPC stage for 4 to 6 days, and their concentrations were adjusted for each cell line individually. Neural differentiation (Growth Factor Withdrawal assay, GFWD) was induced by withdrawing growth factors (EGF and FGF) from NPC medium for 2-6 weeks. Physiological oxygen tension growth was established in 2% O_2, 5% CO_2, and 92% N_2. Atmospheric oxygen tension growth was established in 20% O_2, 5% CO_2, and 75% N_2.

Immunofluorescent Staining and Quantification

Immunofluorescent staining was performed as described (Patterson et al., 2011). Antibodies used include the following: rabbit anti-TUJ1 (Covance, RPB-435P-100), chicken anti-GFAP (Abcam, ab4674), mouse anti-MAP2 (Abcam, ab11267), mouse anti-NESTIN (Neuromics, MO15012), rabbit anti-HIF1α (Novus, NB100-479), rabbit anti-LIN28A (Cell Signaling, A177), rabbit anti-

LIN28B (Cell Signaling 4196S) and rabbit anti-cleaved Caspase-3 (Cell Signaling, 9661). For the GFWD assay, cells grown on coverslips were fixed at different time points with 4% (w/v) paraformaldehyde (Electron Microscopy Sciences) in PBS. More than 6 views were randomly selected for each coverslip and images were taken at 10x magnification with a consistent exposure time across all samples. Quantification was performed using ImageJ with the same threshold for each channel for all samples. The percentage of neurons and glia was calculated with positive staining area that above the threshold of each channel and then scaled the total area of the neurons and glia to a hundred percent. The percentage of neurons and glia from each experiment was then pooled to generate the figures and p-value was calculated with student's t test. The quantification based on cell number (DAPI staining) yielded similar results as those quantified by percentage (Supplementary Figs 2B and 4). For the quantification of LIN28A and LIN28B, images were taken at 20x magnification with the consistent exposure time across all samples. Relative intensity was calculated by the ratio of the positive areas of LIN28A/B to the positive areas of total NPCs (measured by NESTIN). The same threshold for each channel was used across all samples. Relative intensity of nuclear HIF1α was quantified by the ratio of HIF1α-positive region within DAPI-positive region of each cell to the total DAPI area. Statistical analysis was done using a two-tailed, unpaired, student's t-test. Further details for each analysis are included in the figure legends accordingly.

Embryoid Body Formation

Embryoid Bodies (EBs) were generated as described (Chan et al., 2012). Briefly, embryonic stem cell colonies were dissociated from the plate mechanically using StemPro EZPassage Tool and cultured in ultra-low attachment plates (Corning) containing DMEM/F12 supplemented with

20% knockout serum replacement medium (Invitrogen), L-glutamine (Gibco), nonessential amino acids (Gibco), and penicillin–streptomycin.

Generation of HIF deficient ES line

HIF1β, HIF1α, *HIF2α*, or scramble control shRNA *pLKO* lentiviral vector were purchased from Sigma. Lentivirus-infected hESCs or hiPSCs were selected by puromycin as described before (Sherman et al., 2010).

Luciferase Reporter assay

A *LIN28B* promoter driven luciferase reporter was kindly provided by Dr. Joshua T. Mendell (Johns Hopkins University School of Medicine, Baltimore, MD) (Chang et al., 2009). Mutations in a *HIF/MYC* binding site were generated with a QuikChange II XL Site-Directed Mutagenesis Kit (Stratagene) and validated by sequencing. The mutant or the wild type *LIN28B* promoter reporter was co-transfected with control or *c-MYC* plasmid (Addgene #13375) using lipofectamine 2000 (Life Technologies). Cells were lysed 48h post-transfection and subjected to a Dual-Glo luciferase assay as described by the manufacturer (Promega). In DFX experiments, NPCs were transfected with the mutant or the wild type *LIN28B* promoter luciferase reporter and then treated with DFX for 24h before lysed for a Dual-Glo luciferase assay. For *let-7* luciferase assay, NPCs cultured in 20% or 2% O_2 were transfected with the *psiCHECK2-let7* luciferase reporter (Addgene #20932)(Iwasaki et al., 2009) or the *psiCHECK2* control reporter (Promega), lysed 72h post-transfection, and subjected to a Dual-Glo luciferase assay. Luciferase assays were carried out in a GloMax 96 microplate luminometer (Promega).

Let-7 antagomir and siRNA transfection

For the *let-7* antagomir experiment, NPCs were treated with or without 100 μM DFX for 5 days before transfection. Cells was then transfected with Dharmacon miRIDIAN human *let-7b* and *let-7g* hairpin inhibitor (Thermo Scientific) at a final concentration of 20 nM each, or 40 nM miRIDIAN microRNA Hairpin Inhibitor Negative Control #1 (Thermo Scientific) using Lipofectamine RNAiMAX transfection reagent (Life Technologies) in accordance with the manufacturer's instructions. In the knockdown experiments, NPCs were transfected with unique 27mer siRNA duplexes against human *HIF2α, HIF1β, MYC* and *MYCN* genes and the control duplex (Trilencer, Origene) at a final concentration of 40 nM (for double knockdown group, the final concentration is 20 nM of each siRNA) using Lipofectamine RNAiMAX transfection reagent. After transfection, cells were cultured in NPC medium for 5 days before growth factor withdrawal.

Gene expression analysis

RNA isolation, reverse transcription, and real-time PCR were performed as described (Lowry et al., 2008); Patterson et al., 2011). Total RNA was extracted using an RNeasy Mini Kit or a miRNeasy mini Kit (Qiagen). cDNA was synthesized using the Superscript III first-strand cDNA synthesis kit (Invitrogen). Real-time PCR was performed using the SYBR green real-time PCR kit (Roche). Primer sequences are available upon request. In real-time PCR experiments, transcript levels were determined in triplicate reactions and normalized to a beta-Actin control. Mature *let-7* microRNAs were measured with miScript Primer Assays, miScript Reverse

Transcription Kit and miScript SYBR Green PCR kit (Qiagen) according to manufacturer's instruction and normalized with the small RNA U6 as an internal control.

Microarray profiling

Microarray profiling was performed with Affymetrix Human HG-U133 2.0 Plus arrays as described(Lowry et al., 2008). Data were normalized using the Robust Multichip Algorithm in Genespring (Agilent Technology). Probe sets expressed at a raw value of less than 50 in all samples were eliminated from further analysis. Gene expression differences were judged to be significant when a student's t-test p-value was smaller than 0.05 and the fold change compared to a control was at least 1.54. Gene Set Enrichment Analysis (GSEA) was performed using the same criteria. Heat maps were generated using normalized expression data from the GSEA motif list, clustered using Cluster3.0 software, and rendered by Java TreeView. The GEO accession number is GSE61842.

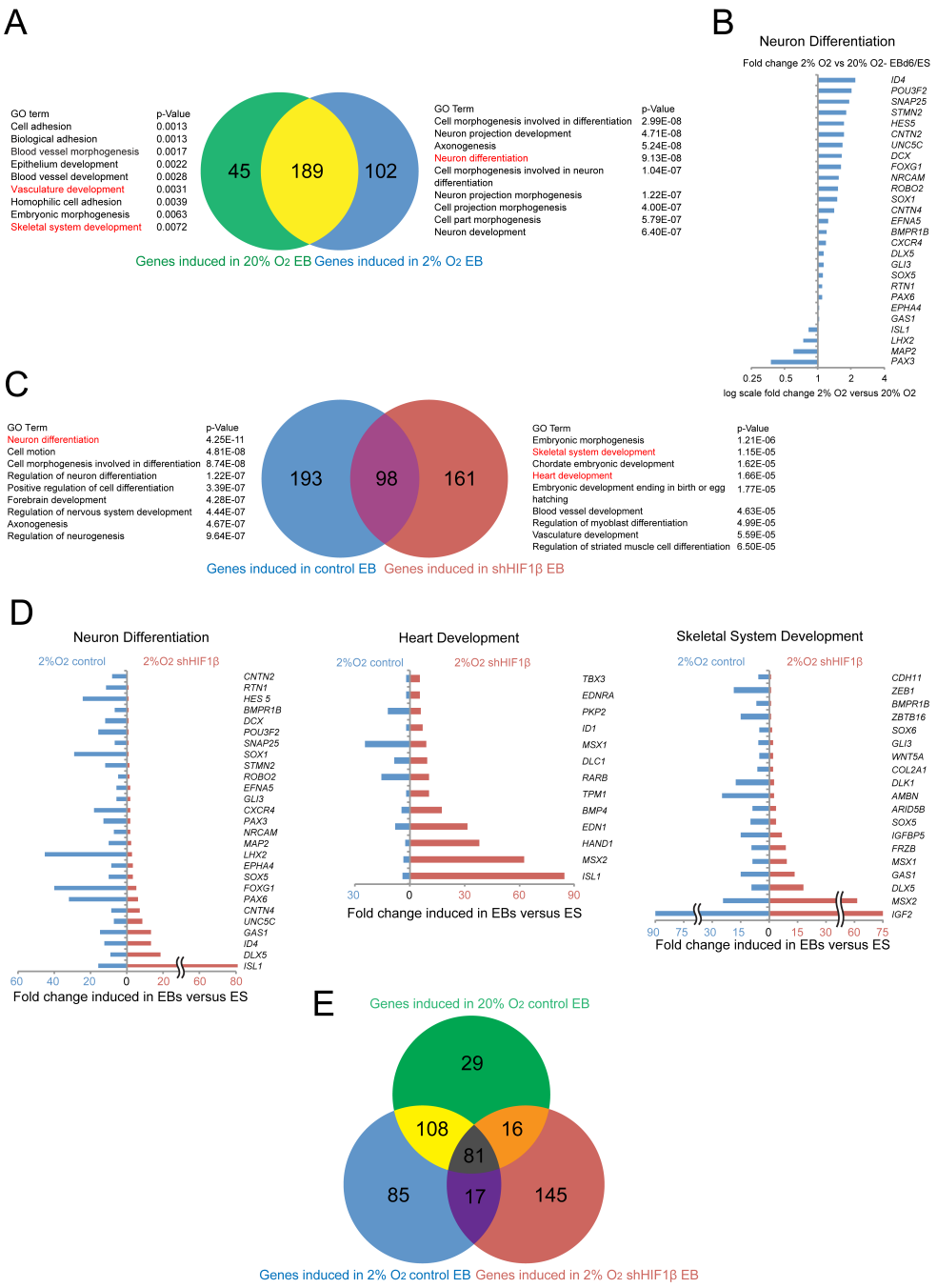


Figure 2-1. Germ layer formation is regulated by the oxygen sensing pathway

A, Embryoid bodies cultured in physiological (2% O_2) or atmospheric oxygen (20% O_2) concentrations display markedly different gene expression profiles, with the Venn diagram outlining the number of genes different. Gene Ontology (GO) analysis suggested that acquisition of all three germ layers were affected by oxygen concentration. All genes in the Venn diagram

were induced over 5 fold in EBs relative to undifferentiated PSCs. **B**, Genes involved in neural differentiation is more dramatically induced in EBs grown in physiological oxygen concentration than EBs grown in atmospheric oxygen concentration. All genes listed here were induced over 5 fold in EBs relative to undifferentiated PSCs. **C**, hESCs with stable introduction of shRNA against HIF1β were used to make EBs under physiological oxygen concentration. Germ layer formation was measured by gene expression profiling and found to be affected as indicated by the Venn diagram. GO analysis uncovered neuron, heart and skeletal systems profoundly affected. **D**, a list of genes and the relative fold change for each in EBs relative to undifferentiated PSCs in either the presence or absence of normal HIF signaling. **E**, a Venn diagram of genes induced in 20% O_2, 2% O_2 and shHIF1β EBs. See also Figure S2-1.

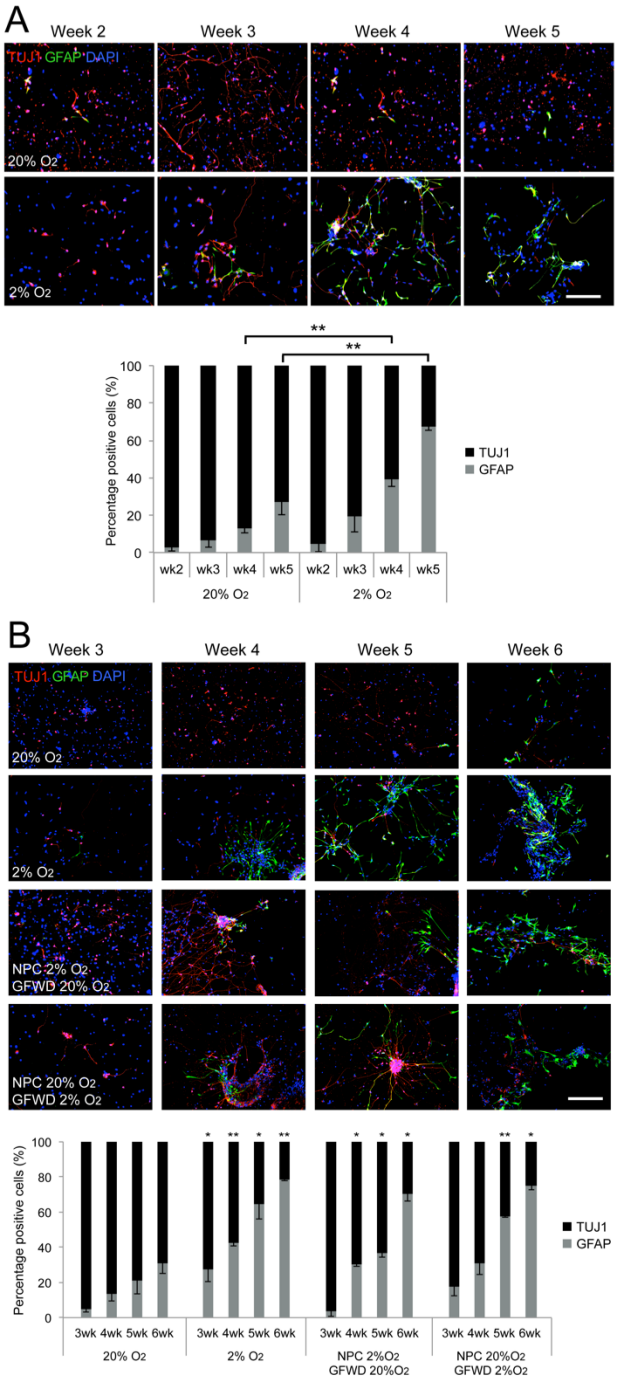


Figure 2-2. Neurogenesis is affected by oxygen tension

A, Top, Directed differentiation of NPCs towards neurons and glia by growth factor withdrawal (GFWD) for 2-5 weeks assays for developmental maturity of progenitors. Culturing NPCs in

either physiological or atmospheric oxygen concentration followed by GFWD for the indicated times generates both neurons and glia, which are assayed by immunostaining for TUJ1 (neurons) or GFAP (glia). Bottom, quantification of immunostaining demonstrates the strong effect of physiological oxygen on gliogenesis. **B**, GFWD assay with NPCs grown in different conditions to assess the permanence of the effect of physiological oxygen on differentiation. NPCs were either grown under physiological or atmospheric oxygen for 5 days and then maintained under such conditions or switched to lower/higher oxygen during GFWD. Quantification shows that even a brief exposure to physiological oxygen drives gliogenesis. (A-B: n=3 independent experiments; Mean ± SEM; * $p<0.05$, ** $p < 0.01$; student's t test compared with 20% O_2 at each time point; scale bars, 200μm). See also Figure S2.

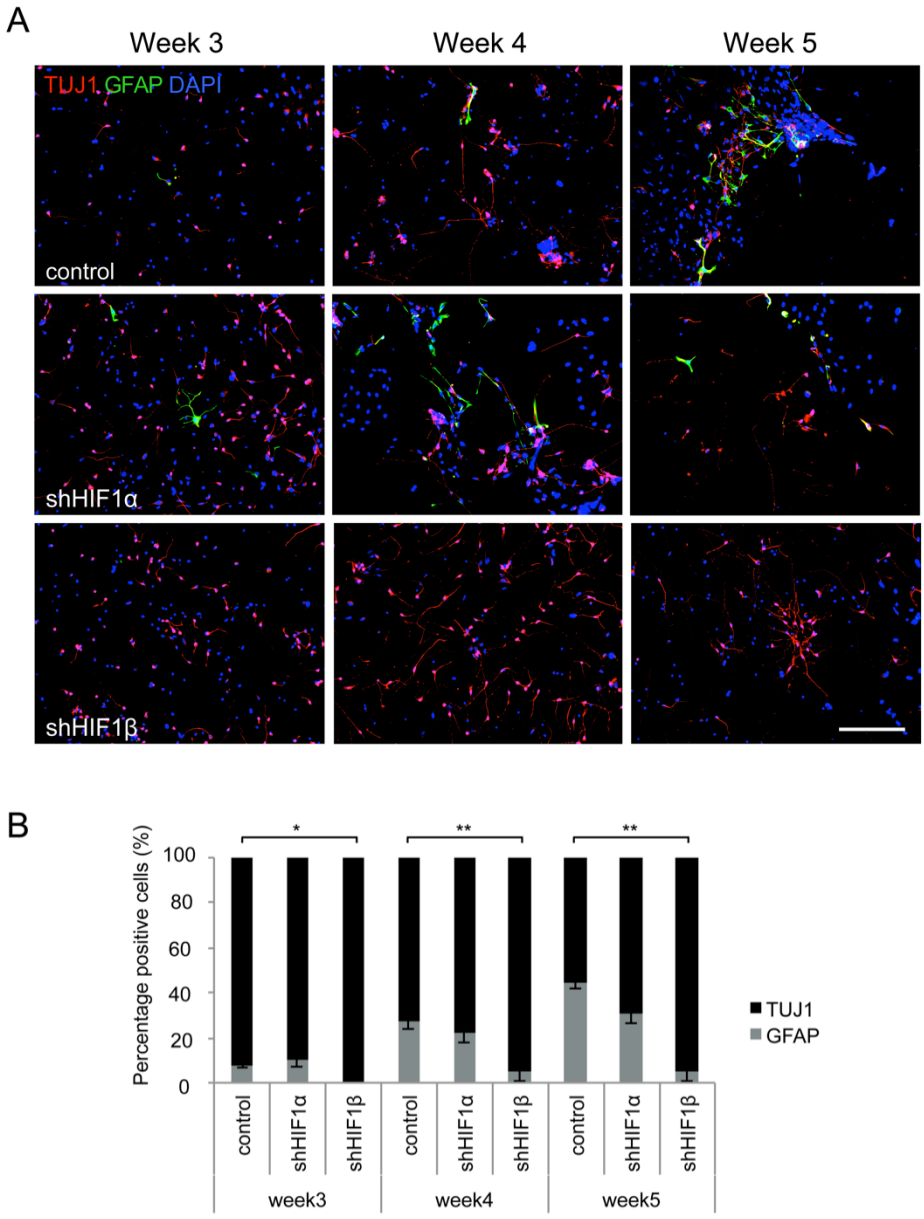


Figure 2-3. The HIF pathway regulates neurogenesis

A, NPCs were generated from hESC lines with stable integration of shRNA against HIF1α, HIF1β, or scramble control. **B**, GFWD assay and quantification of neurons (TUJ1) and glia (GFAP) indicate that HIF1α is required for gliogenesis in physiological oxygen concentration. (n=3 independent experiments; Mean ± SEM; * $p<0.05$, ** $p<0.01$; student's t test compared with control at each time point; scale bars, 200μm).

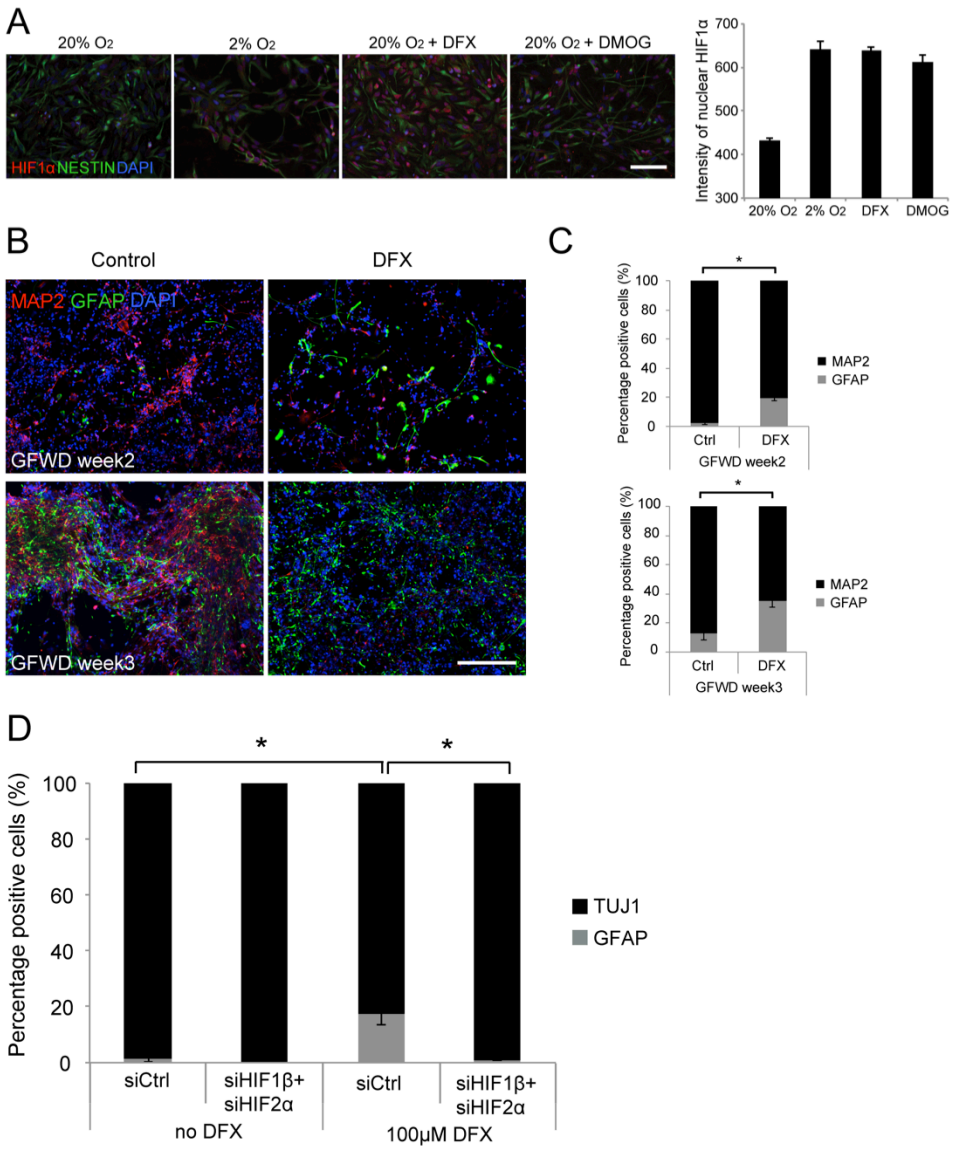


Figure 2-4. Small molecule driven HIF activation can drive gliogenesis

A, Immunostaining for HIF1α proteins in the nucleus showed that lowering oxygen to 2% was sufficient to drive nuclear translocation and stabilization of HIF1α. Using small molecule inhibitors of HIF degradation (DFX and DMOG) also led to HIF1α stabilization and nuclear localization, even in the presence of 20% oxygen. (n>100 cells per treatment; Mean ± SEM; scale bars, 100μm). **B**, In GFWD assays, DFX treatment led to an increase in astrocytes as measured by GFAP at different time points. **C**, A quantification of percentage of neurons (MAP2) and astrocytes (GFAP) at indicated time points. (n=3 independent experiments with two different human ESC-derived NPCs and one human iPSC-derived NPC; Mean ± SEM; * $p<0.05$; student's t test; scale bars, 200μm). **D**, GFWD assay with siRNA against HIF1β and HIF2α

demonstrated that the effect of DFX on gliogenesis strictly depends on the HIF sensing pathway. (n=3 independent experiments; Mean ± SEM; * $p < 0.05$; student's t test;) See also Figure S2-3.

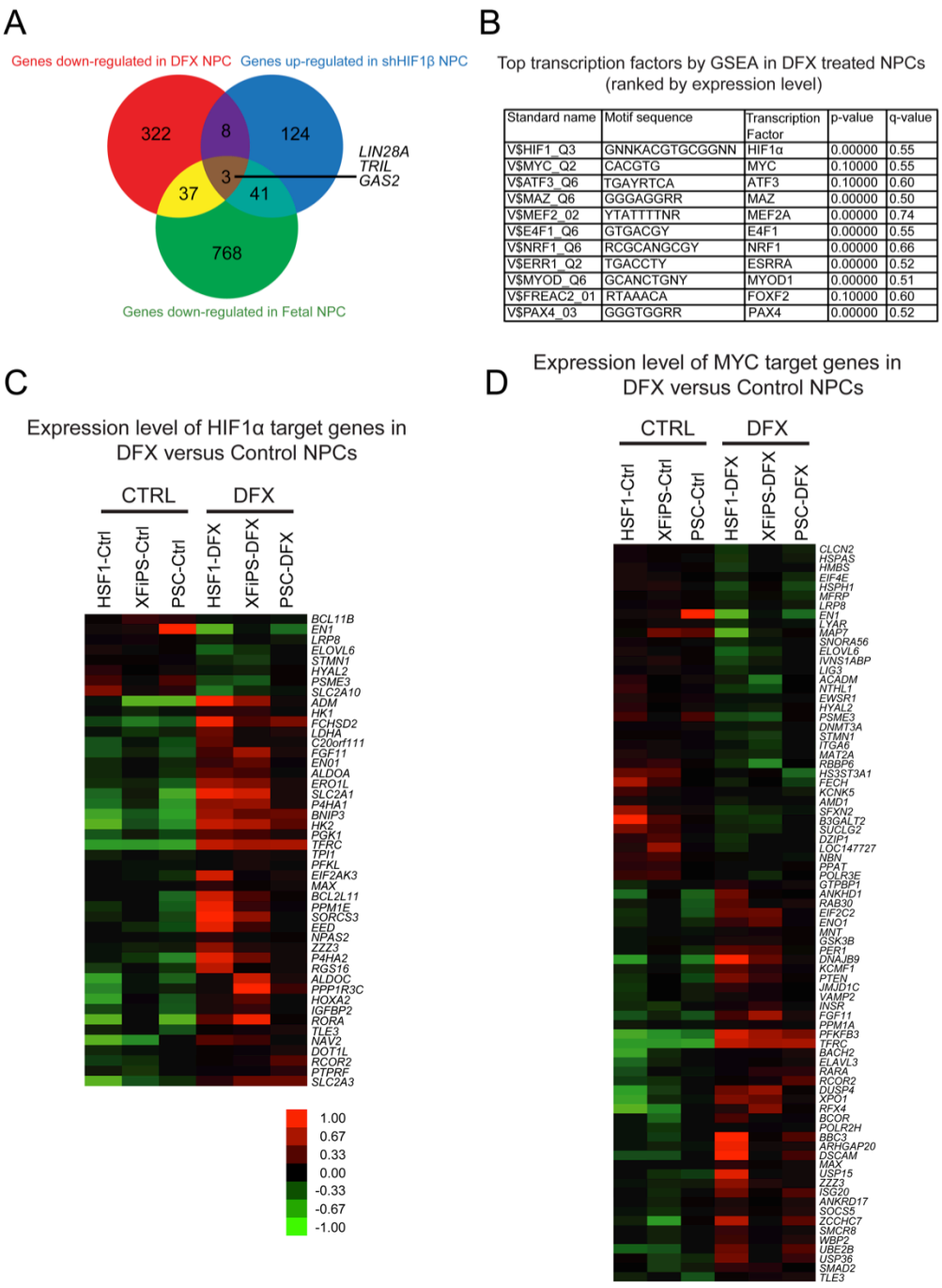


Figure 2-5. Identification of important target genes of the HIF pathway in neurogenesis

A, Gene expression profiling led to the identification of numerous expression changes in response to altered HIF activity. Overlapping these gene expression changes identified 3 genes

in common. **B**, GSEA analysis was performed for the list of expression changes observed upon DFX treatment to identify transcription factors (TF) that could be driving these changes. The list was narrowed by retaining only the TFs that were expressed in NPCs under either condition. Shown are the highest ranked TFs by both p-value and expression level. Note that HIF and MYC were at the top of the list of TFs whose binding sites were enriched in genes that were changed by DFX. **C**, A heat map of established HIF target genes in DFX treated cells versus control. Red indicates induction; green indicates reduction. **D**, A heat map of established MYC target genes in DFX treated cells versus control. See also Table S2-1.

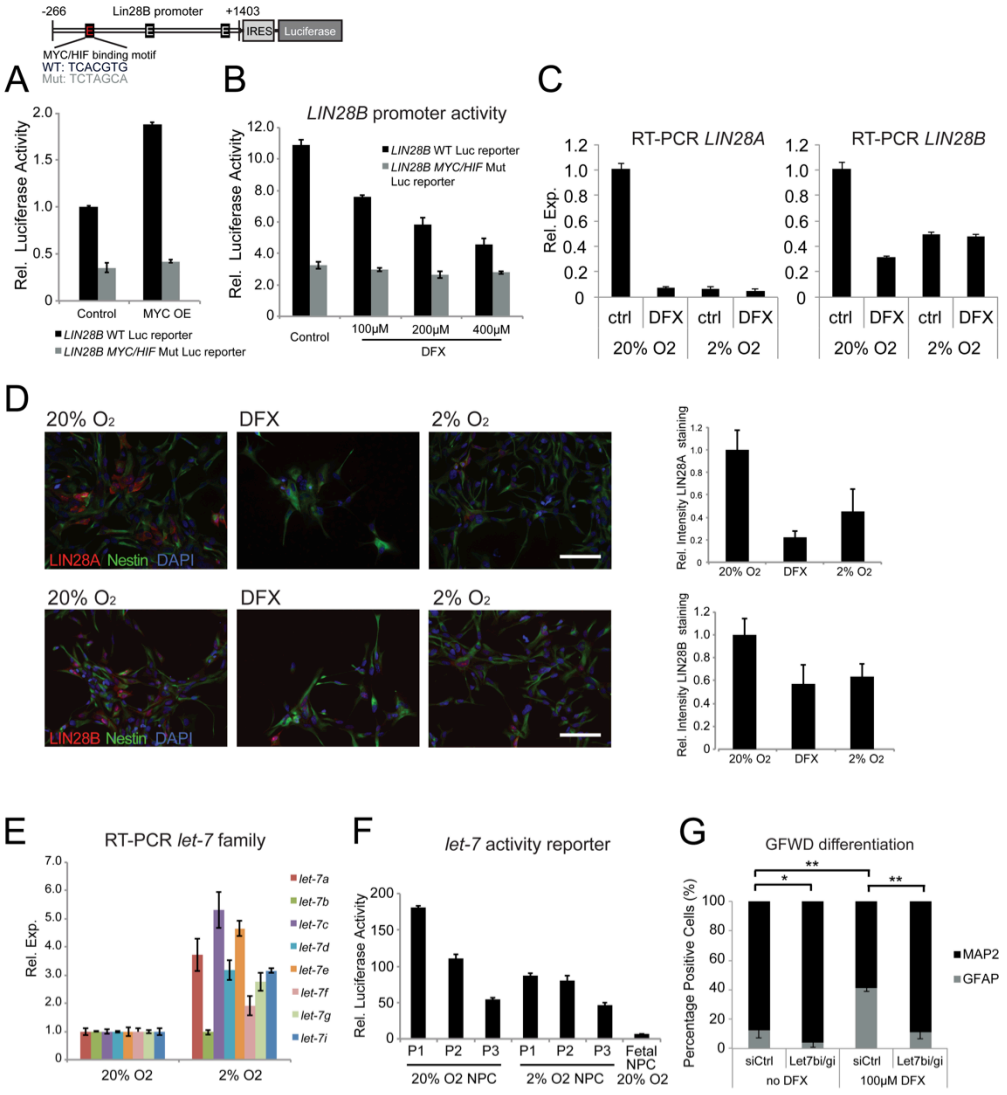


Figure 2-6. LIN28 is regulated jointly by HIF and MYC through a shared binding site

A, Top, a diagram shows the shared binding site of MYC and HIF in Lin28B promoter (MYC binding site "CACGTG", HIF binding site "TCACGT"). Bottom, a luciferase-based reporter for the LIN28B gene showed a higher activity with overexpression of MYC, and a dramatic decrease in activity and insensitivity to MYC when the shared MYC/HIF binding site is mutated. Shown is relative luciferase activity normalized to constitutive reporter with and without activation by overexpression of MYC. (n=2 independent experiments; Mean ± SD). **B**, The LIN28B reporter is silenced by addition of DFX to the culture medium, and this effect is blocked in a reporter lacking a functional MYC/HIF site. (n=3 independent experiments; Mean ± SD) **C**,

Both LIN28A and LIN28B RNA expression were abrogated by either DFX treatment or exposure to physiological oxygen concentration. (n=3 independent experiments; Mean ± SEM) **D**, Immunostaining for LIN28A and LIN28B in the indicated conditions demonstrates downregulation of these proteins in physiological oxygen or with DFX treatment. The effect is quantified (right) by intensity of staining on per cell basis. (n>100 cells per treatment; Mean ± SEM; scale bars, 100μm) **E**, RT-PCR for *let-7* family members shows an increase in physiological oxygen in NPCs. (n=2 independent experiments; Mean ± SEM). **F**, A luciferase reporter with *let-7* binding sites in the 3' UTR shows increased *let-7* activity (represented as decreased luciferase activity) in physiological oxygen, or over passage, which is known to induce *let-7* activity in PSC-NPCs. Fetal tissue derived NPC is known to have high *let-7* activity, serves as a positive control (Patterson et al., 2012) (n=4 biological replicates; Mean ± SD). **G**, The effect of DFX on gliogenesis is completely blocked by coordinated inhibition of *let-7* activity by the addition of *let-7* antagomirs. (n=3 independent experiments; Mean ± SEM; * $p<0.05$, ** $p<0.01$; student's t test). See also Figure S2-4.

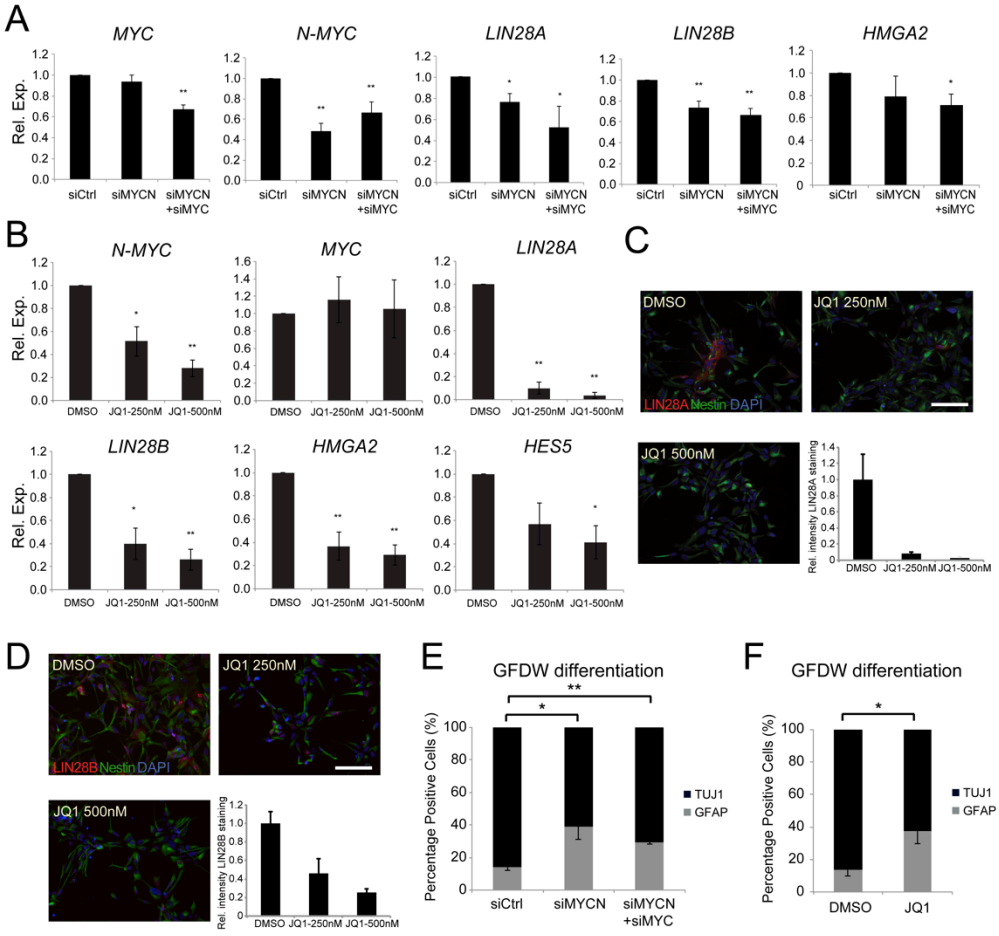


Figure 2-7. MYC inhibition mimics the effect of HIF activation to suppress immaturity markers and promote gliogenesis

A, Expression of *LIN28A, LIN28B* and *HMGA2* after siRNA against *NMYC* and *MYC*. Values shown are relative to housekeeping gene (*beta-Actin*). (n=3 independent experiments; Mean ± SEM; * $p<0.05$, ** $p<0.01$; student's t test compared with siCtrl). **B**, PSC-NPCs were treated with two doses of JQ1, a small molecule inhibitor of *MYC* expression. NPCs treated with JQ1 showed decreased expression of *NMYC, LIN28A, LIN28B*, *HMGA2* and *HES5* by RT-PCR. (n=3 independent experiments; Mean ± SEM; * $p<0.05$, ** $p<0.01$ compared with DMSO control; student's t test). **C and D**, Expression of LIN28B and LIN28A proteins were measured by immunostaining and quantified on per cell basis. (n>600 cells for each treatment; Mean ± SEM; scale bars, 100µm). **E**, After knockdown of NMYC by siRNA, a GFWD assay shows increased gliogenesis from PSC-NPCs. **F**, Treatment of PSC-NPCs with 250 nM JQ1 led to increased

gliogenesis as measured by quantification of GFWD assay. (E-F: n=4 independent experiments with either hESC or hiPSC-derived NPCs; Mean ± SEM; * $p<0.05$, ** $p<0.01$; student's t test)

References

Adelman, D.M., Gertsenstein, M., Nagy, A., Simon, M.C., and Maltepe, E. (2000). Placental cell fates are regulated *in vivo* by HIF-mediated hypoxia responses. Genes Dev *14*, 3191-3203.

Amarilio, R., Viukov, S.V., Sharir, A., Eshkar-Oren, I., Johnson, R.S., and Zelzer, E. (2007). HIF1alpha regulation of Sox9 is necessary to maintain differentiation of hypoxic prechondrogenic cells during early skeletogenesis. Development *134*, 3917-3928.

Balzer, E., Heine, C., Jiang, Q., Lee, V.M., and Moss, E.G. (2010). LIN28 alters cell fate succession and acts independently of the *let-7* microRNA during neurogliogenesis *in vitro*. Development *137*, 891-900.

Chan, D.N., Azghadi, S.F., Feng, J., and Lowry, W.E. (2012). PTK7 marks the first human developmental EMT *in vitro*. PLoS ONE *7*, e50432.

Chang, T.C., Zeitels, L.R., Hwang, H.W., Chivukula, R.R., Wentzel, E.A., Dews, M., Jung, J., Gao, P., Dang, C.V., Beer, M.A.*, et al.* (2009). Lin-28B transactivation is necessary for Myc-mediated *let-7* repression and proliferation. Proceedings of the National Academy of Sciences of the United States of America *106*, 3384-3389.

Cimadamore, F., Amador-Arjona, A., Chen, C., Huang, C.T., and Terskikh, A.V. (2013). SOX2-LIN28/*let-7* pathway regulates proliferation and neurogenesis in neural precursors. Proceedings of the National Academy of Sciences of the United States of America *110*, E3017-3026.

Corn, P.G., Ricci, M.S., Scata, K.A., Arsham, A.M., Simon, M.C., Dicker, D.T., and El-Deiry, W.S. (2005). Mxi1 is induced by hypoxia in a HIF-1-dependent manner and protects cells from c-Myc-induced apoptosis. Cancer Biol Ther *4*, 1285-1294.

Covello, K.L., Kehler, J., Yu, H., Gordan, J.D., Arsham, A.M., Hu, C.J., Labosky, P.A., Simon, M.C., and Keith, B. (2006). HIF-2alpha regulates Oct-4: effects of hypoxia on stem cell function, embryonic development, and tumor growth. Genes Dev *20*, 557-570.

Cowden Dahl, K.D., Fryer, B.H., Mack, F.A., Compernolle, V., Maltepe, E., Adelman, D.M., Carmeliet, P., and Simon, M.C. (2005). Hypoxia-inducible factors 1alpha and 2alpha regulate trophoblast differentiation. Mol Cell Biol *25*, 10479-10491.

Delmore, J.E., Issa, G.C., Lemieux, M.E., Rahl, P.B., Shi, J., Jacobs, H.M., Kastritis, E., Gilpatrick, T., Paranal, R.M., Qi, J.*, et al.* (2011). BET bromodomain inhibition as a therapeutic strategy to target c-Myc. Cell *146*, 904-917.

Denko, N.C. (2008). Hypoxia, HIF1 and glucose metabolism in the solid tumour. Nat Rev Cancer *8*, 705-713.

Dunwoodie, S.L. (2009). The role of hypoxia in development of the Mammalian embryo. Dev Cell *17*, 755-773.

Ezashi, T., Das, P., and Roberts, R.M. (2005). Low O2 tensions and the prevention of differentiation of hES cells. Proc Natl Acad Sci U S A *102*, 4783-4788.

Forristal, C.E., Wright, K.L., Hanley, N.A., Oreffo, R.O., and Houghton, F.D. (2010). Hypoxia inducible factors regulate pluripotency and proliferation in human embryonic stem cells cultured at reduced oxygen tensions. Reproduction *139*, 85-97.

Gordan, J.D., Bertout, J.A., Hu, C.J., Diehl, J.A., and Simon, M.C. (2007). HIF-2alpha promotes hypoxic cell proliferation by enhancing c-myc transcriptional activity. Cancer cell *11*, 335-347.

Iwasaki, S., Kawamata, T., and Tomari, Y. (2009). Drosophila argonaute1 and argonaute2 employ distinct mechanisms for translational repression. Molecular cell *34*, 58-67.

Kawahara, H., Okada, Y., Imai, T., Iwanami, A., Mischel, P.S., and Okano, H. (2011). Musashi1 cooperates in abnormal cell lineage protein 28 (Lin28)-mediated *let-7* family microRNA biogenesis in early neural differentiation. The Journal of biological chemistry *286*, 16121-16130.

Koshiji, M., Kageyama, Y., Pete, E.A., Horikawa, I., Barrett, J.C., and Huang, L.E. (2004). HIF-1alpha induces cell cycle arrest by functionally counteracting Myc. Embo J *23*, 1949-1956.

Kozak, K.R., Abbott, B., and Hankinson, O. (1997). ARNT-deficient mice and placental differentiation. Dev Biol *191*, 297-305.

Krishnan, J., Ahuja, P., Bodenmann, S., Knapik, D., Perriard, E., Krek, W., and Perriard, J.C. (2008). Essential role of developmentally activated hypoxia-inducible factor 1alpha for cardiac morphogenesis and function. Circ Res *103*, 1139-1146.

La Torre, A., Georgi, S., and Reh, T.A. (2013). Conserved microRNA pathway regulates developmental timing of retinal neurogenesis. Proceedings of the National Academy of Sciences of the United States of America *110*, E2362-2370.

Lendahl, U., Lee, K.L., Yang, H., and Poellinger, L. (2009). Generating specificity and diversity in the transcriptional response to hypoxia. Nat Rev Genet *10*, 821-832.

Lengner, C.J., Gimelbrant, A.A., Erwin, J.A., Cheng, A.W., Guenther, M.G., Welstead, G.G., Alagappan, R., Frampton, G.M., Xu, P., Muffat, J.*, et al.* (2010). Derivation of pre-X inactivation human embryonic stem cells under physiological oxygen concentrations. Cell *141*, 872-883.

Licht, A.H., Muller-Holtkamp, F., Flamme, I., and Breier, G. (2006). Inhibition of hypoxia-inducible factor activity in endothelial cells disrupts embryonic cardiovascular development. Blood *107*, 584-590.

Lim, H.J., Han, J., Woo, D.H., Kim, S.E., Kim, S.K., Kang, H.G., and Kim, J.H. (2011). Biochemical and morphological effects of hypoxic environment on human embryonic stem cells in long-term culture and differentiating embryoid bodies. Mol Cells *31*, 123-132.

Lowry, W.E., Richter, L., Yachechko, R., Pyle, A.D., Tchieu, J., Sridharan, R., Clark, A.T., and Plath, K. (2008). Generation of human induced pluripotent stem cells from dermal fibroblasts. Proceedings of the National Academy of Sciences of the United States of America *105*, 2883-2888.

Majmundar, A.J., Wong, W.J., and Simon, M.C. (2010). Hypoxia-inducible factors and the response to hypoxic stress. Mol Cell *40*, 294-309.

Mertz, J.A., Conery, A.R., Bryant, B.M., Sandy, P., Balasubramanian, S., Mele, D.A., Bergeron, L., and Sims, R.J., 3rd (2011). Targeting MYC dependence in cancer by inhibiting BET bromodomains. Proceedings of the National Academy of Sciences of the United States of America *108*, 16669-16674.

Miyata, T., Kawaguchi, D., Kawaguchi, A., and Gotoh, Y. (2010). Mechanisms that regulate the number of neurons during mouse neocortical development. Current opinion in neurobiology *20*, 22-28.

Mohyeldin, A., Garzon-Muvdi, T., and Quinones-Hinojosa, A. (2010). Oxygen in stem cell biology: a critical component of the stem cell niche. Cell Stem Cell *7*, 150-161.

Mutoh, T., Sanosaka, T., Ito, K., and Nakashima, K. (2012). Oxygen levels epigenetically regulate fate switching of neural precursor cells via hypoxia-inducible factor 1alpha-notch signal interaction in the developing brain. Stem Cells *30*, 561-569.

Nagao, M., Campbell, K., Burns, K., Kuan, C.Y., Trumpp, A., and Nakafuku, M. (2008). Coordinated control of self-renewal and differentiation of neural stem cells by Myc and the p19ARF-p53 pathway. The Journal of cell biology *183*, 1243-1257.

Ng, K.M., Lee, Y.K., Chan, Y.C., Lai, W.H., Fung, M.L., Li, R.A., Siu, C.W., and Tse, H.F. (2010). Exogenous expression of HIF-1 alpha promotes cardiac differentiation of embryonic stem cells. J Mol Cell Cardiol *48*, 1129-1137.

Patterson, M., Chan, D.N., Ha, I., Case, D., Cui, Y., Handel, B.V., Mikkola, H.K., and Lowry, W.E. (2012). Defining the nature of human pluripotent stem cell progeny. Cell research *22*, 178-193.

Patterson, M., Gaeta, X., Loo, K., Edwards, M., Smale, S.T., Azghadi, S., Douglass, S., Pellegrini, M., and WE, L. (in press). The LIN28/*let-7*circuit can act through Notch to control developmental progression in the human nervous system. Stem Cell Reports.

Prado-Lopez, S., Conesa, A., Arminan, A., Martinez-Losa, M., Escobedo-Lucea, C., Gandia, C., Tarazona, S., Melguizo, D., Blesa, D., Montaner, D.*, et al.* (2010). Hypoxia promotes efficient differentiation of human embryonic stem cells to functional endothelium. Stem Cells *28*, 407-418.

Provot, S., Zinyk, D., Gunes, Y., Kathri, R., Le, Q., Kronenberg, H.M., Johnson, R.S., Longaker, M.T., Giaccia, A.J., and Schipani, E. (2007). Hif-1alpha regulates differentiation of limb bud mesenchyme and joint development. J Cell Biol *177*, 451-464.

Sanosaka, T., Namihira, M., Asano, H., Kohyama, J., Aisaki, K., Igarashi, K., Kanno, J., and Nakashima, K. (2008). Identification of genes that restrict astrocyte differentiation of midgestational neural precursor cells. Neuroscience *155*, 780-788.

Sherman, M.H., Kuraishy, A.I., Deshpande, C., Hong, J.S., Cacalano, N.A., Gatti, R.A., Manis, J.P., Damore, M.A., Pellegrini, M., and Teitell, M.A. (2010). AID-induced genotoxic stress promotes B cell differentiation in the germinal center via ATM and LKB1 signaling. Mol Cell *39*, 873-885.

Silver, I., and Erecinska, M. (1998). Oxygen and ion concentrations in normoxic and hypoxic brain cells. Adv Exp Med Biol *454*, 7-16.

Simon, M.C., and Keith, B. (2008). The role of oxygen availability in embryonic development and stem cell function. Nat Rev Mol Cell Biol *9*, 285-296.

Thomson, J.A., Itskovitz-Eldor, J., Shapiro, S.S., Waknitz, M.A., Swiergiel, J.J., Marshall, V.S., and Jones, J.M. (1998). Embryonic stem cell lines derived from human blastocysts. Science (New York, NY *282*, 1145-1147.

Tomita, S., Ueno, M., Sakamoto, M., Kitahama, Y., Ueki, M., Maekawa, N., Sakamoto, H., Gassmann, M., Kageyama, R., Ueda, N.*, et al.* (2003). Defective brain development in mice lacking the Hif-1alpha gene in neural cells. Molecular and cellular biology *23*, 6739-6749.

Westfall, S.D., Sachdev, S., Das, P., Hearne, L.B., Hannink, M., Roberts, R.M., and Ezashi, T. (2008). Identification of oxygen-sensitive transcriptional programs in human embryonic stem cells. Stem Cells Dev *17*, 869-881.

Wouters, B.G., and Koritzinsky, M. (2008). Hypoxia signalling through mTOR and the unfolded protein response in cancer. Nat Rev Cancer *8*, 851-864.

Xia, X., Lemieux, M.E., Li, W., Carroll, J.S., Brown, M., Liu, X.S., and Kung, A.L. (2009). Integrative analysis of HIF binding and transactivation reveals its role in maintaining histone methylation homeostasis. Proc Natl Acad Sci U S A *106*, 4260-4265.

Yoon, D., Okhotin, D.V., Kim, B., Okhotina, Y., Okhotin, D.J., Miasnikova, G.Y., Sergueeva, A.I., Polyakova, L.A., Maslow, A., Lee, Y.*, et al.* (2010). Increased size of solid organs in patients with Chuvash polycythemia and in mice with altered expression of HIF-1alpha and HIF-2alpha. J Mol Med (Berl) *88*, 523-530.

Yoshida, Y., Takahashi, K., Okita, K., Ichisaka, T., and Yamanaka, S. (2009). Hypoxia enhances the generation of induced pluripotent stem cells. Cell Stem Cell *5*, 237-241.

Zhang, H., Gao, P., Fukuda, R., Kumar, G., Krishnamachary, B., Zeller, K.I., Dang, C.V., and Semenza, G.L. (2007). HIF-1 inhibits mitochondrial biogenesis and cellular respiration in VHL-deficient renal cell carcinoma by repression of C-MYC activity. Cancer cell *11*, 407-420.

Figure S2-1

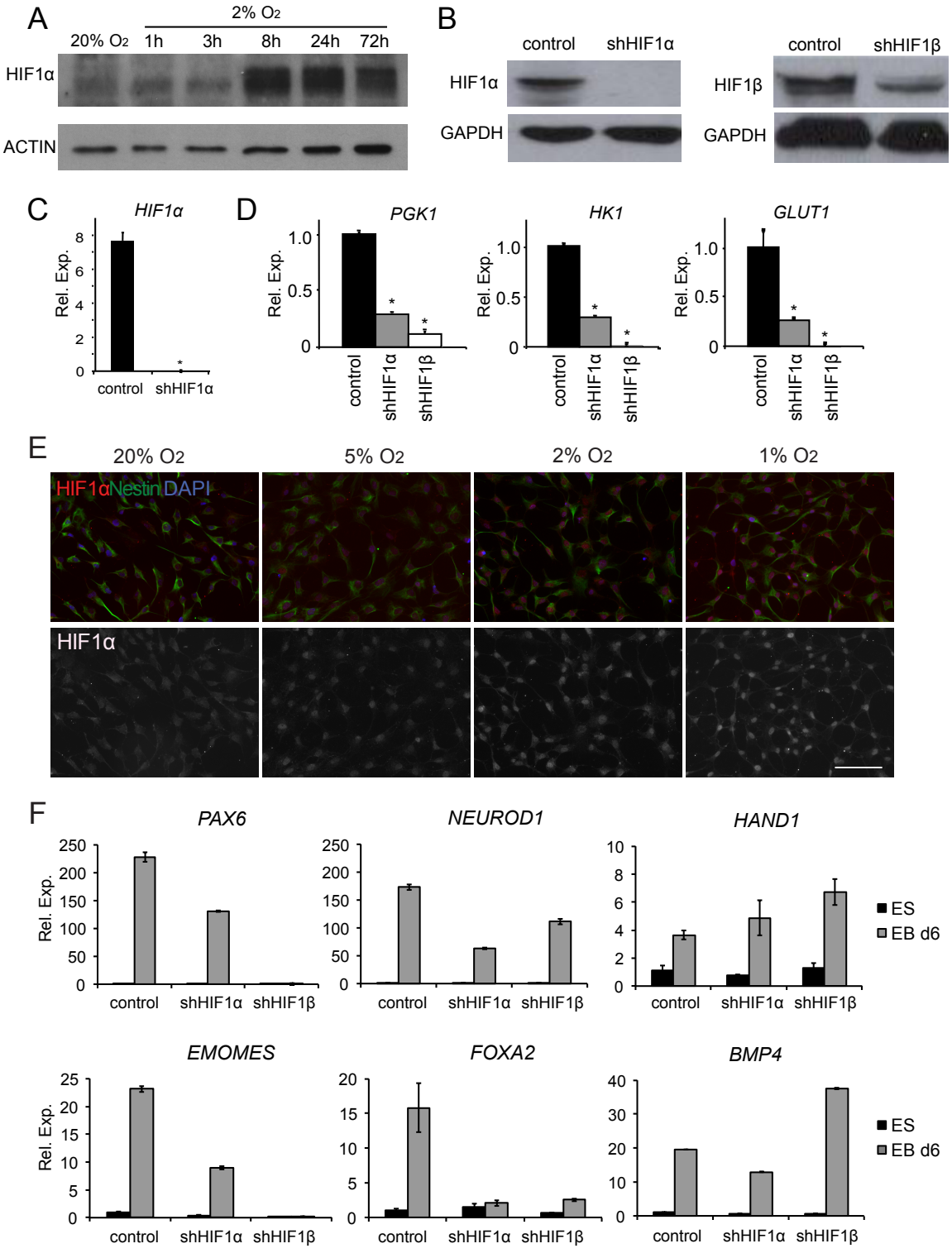

A
2% O2
20% O2
1h
3h
8h
24h
72h
HIF1α
ACTIN
B
control
shHIF1α
HIF1α
GAPDH
control
shHIF1β
HIF1β
GAPDH
C
HIF1α
Rel. Exp.
control
shHIF1α
D
PGK1
HK1
GLUT1
Rel. Exp.
control
shHIF1α
shHIF1β
E
20% O2
5% O2
2% O2
1% O2
HIF1αNestin DAPI
HIF1α
F
PAX6
NEUROD1
HAND1
EMOMES
FOXA2
BMP4
Rel. Exp.
control
shHIF1α
shHIF1β
ES
EB d6

Figure S2-1. Generation of hESC lines with diminished HIF signaling, related to Figure 2-1.

Endogenous HIF in hESCs grown in normoxia is required for maximal induction of developmental genes. **A,** HIF1α protein in 20% O_2 and 2% O_2 quantified by western blot. **B,** Western blot showing shHIF1β and shHIF1α knockdown in HSF1 ES cells in 5% oxygen, day 1. **C**, mRNA expression of HIF1α in control and shHIF1α knockdown hESCs cultured in normoxia. **D,** mRNA expression of HIF1α target genes in hESCs cultured in 20% O_2 with and without HIF knockdown. (A-D: n=3 independent experiments; Mean ± SD; * $p<0.05$; student's t test) **E,** The effect of different oxygen tension on HIF1α nuclear translocation in NPCs. HSF1 hESC-derived NPCs was treated with various oxygen concentrations for 24 hours before fixation. (scale bars, 100 μm) **F,** RT-PCR showed genes representing three germ layers in control and HIF knockdown EBs after being induced to differentiate in 2% O_2 for 6 days. (n=2 independent experiments; Mean ± SEM)

Figure S2-2

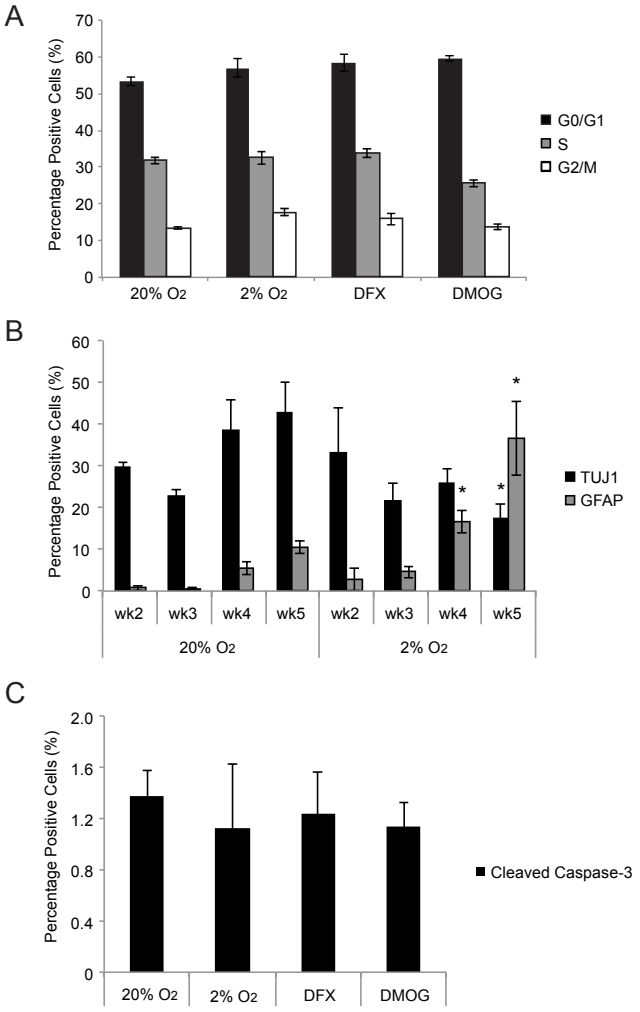


Figure S2-2. The effect of oxygen tension on proliferation and apoptosis, related to Figure 2-2.

A, Cell cycle analysis of XFiPS-NPCs treated in 20% O_2, 2% O_2, 100 μM DFX and 250 μM DMOG, respectively for 4 days. There is no significant difference on each stage of cell cycle among 20% O_2, 2% O_2, or DFX treated NPCs. DMOG treatment increased S-phase compared with 20% O_2. (n=3 biological replicates; Mean ± SEM) **B,** A different way to quantify Figure 2-2A, the directed differentiation of NPCs towards neurons and glia by GFWD for 2-5 weeks in either 2% or 20% O_2. Neurons and glia were assayed by immunostaining for TUJ1 (neurons) and GFAP (glia). The total cell number was quantified by DAPI staining. (n=3 independent experiments; Mean ± SEM; * $p<0.05$; student's t test, compared with 20% O_2 at each time point) **C,** a staining quantification of cleaved Caspase-3 staining on NPCs treated in 20% O_2, 2% O_2,

100 μM DFX or 250 μM DMOG for 4 days. The percentage was normalized with total cell number (DAPI staining). There is no significant difference in cleaved Caspase-3 positive cells between each treatment and 20% O_2 untreated group. (n=3 independent experiments; Mean ± SEM; student's t test)

Figure S2-3

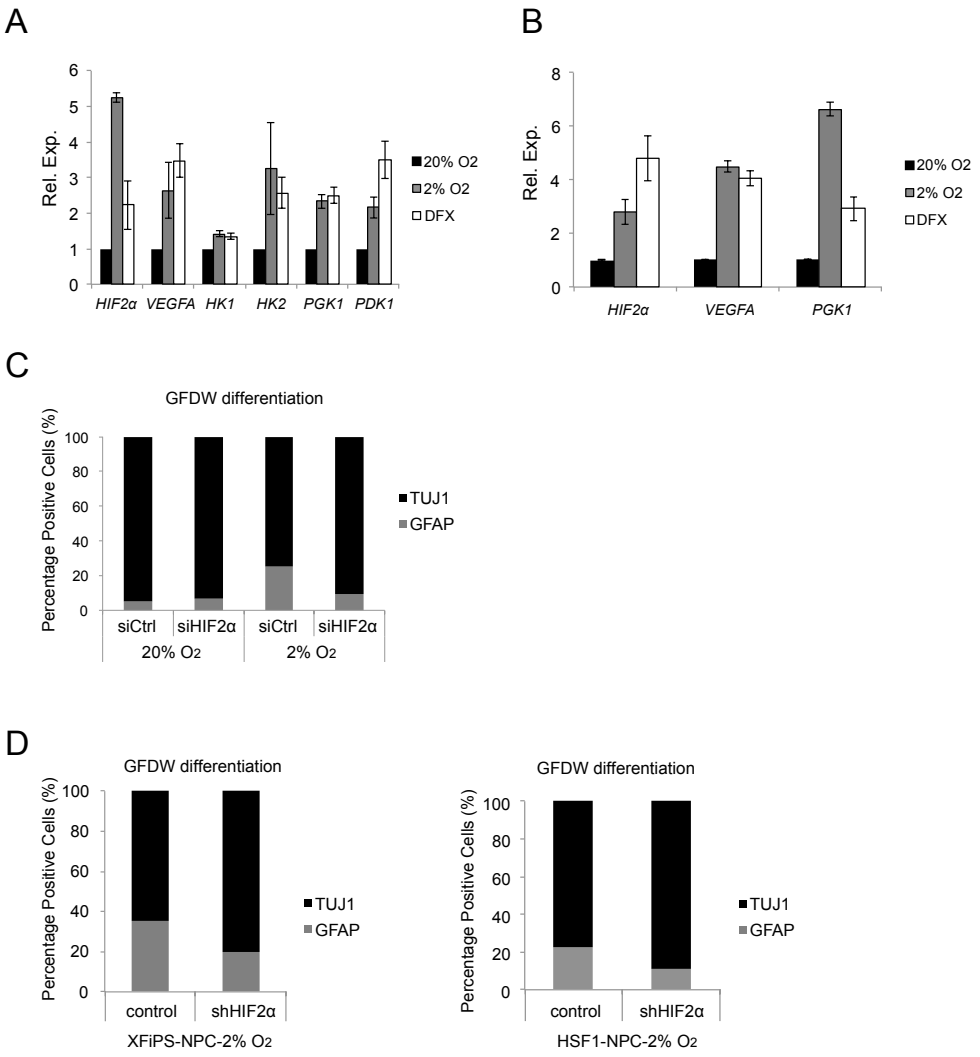


Figure S2-3. HIF2α is induced by low oxygen tension and DFX treatment, related to Figure 4.

A, mRNA expression of HIF1α target genes in NPCs treated with 20% O_2, 2% O_2 and DFX were profiled by microarray. (n=3 biological replicates, Mean ± SEM) **B,** mRNA expression of HIF1α targeted genes in NPCs treated with 20% O_2, 2% O_2 and DFX measured by RT-PCR. (n=3 independent experiments; Mean ± SEM) **C,** A GFWD differentiation assay with siRNA against HIF2α in 20% O_2 and 2% O_2. It demonstrated that the HIF2α promotes gliogenesis only in 2% O_2 when it was highly induced. **D,** NPCs were generated from either hESC or hiPSC lines with a stable knockdown of HIF2α using shRNA. GFWD assay and quantification of neurons (TUJ1) and glia (GFAP) indicate that HIF2α is required for gliogenesis in 2% O_2.

Figure S2-4

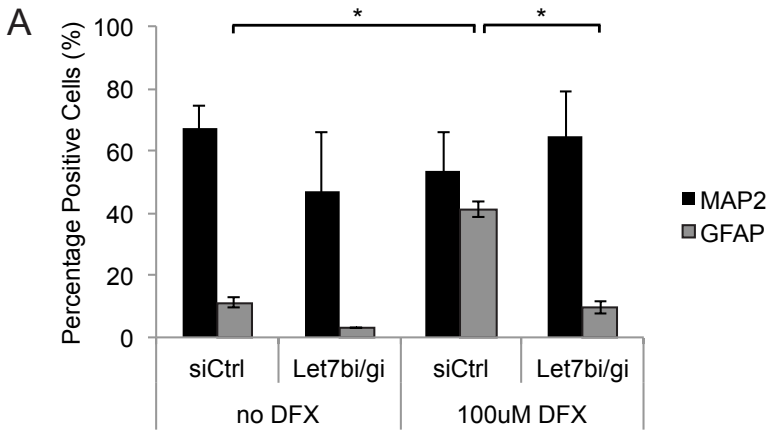


Figure S2-4 The effect of DFX on gliogenesis is completely blocked by coordinated inhibition of *let-7* activity by antagomirs, related to Figure 2-6. This figure is a different way to quantify the 3-week GFWD data in Figure 2-6G. Neurons and glia were assayed by immunostaining for MAP2 (neurons) and GFAP (glia). The relative percentages were normalized with total nuclei (DAPI staining). (n=3 independent experiments; Mean ± SEM; * $p<0.05$; student's t test)

Table S2-1. A complete list of TFs regulating HIF target genes predicted by GSEA, related to Figure 2-5.

Top 20 enriched motifs in DFX treated NPCs				
Standard name	Motif sequence	Transcription Factor	p-value (DFX vs ctrl)	q-value (DFX vs ctrl)
V$NFY_Q6_01	GATTGGY	UNKNOWN	0.00000	0.46
MIR-30A-5P,MIR-30C,MIR-30D,MIR-30B,MIR-30E-5P	TGTTTAC	MIR-30	0.00000	0.47
V$AREB6_01	CAGGTA	TCF8	0.00000	0.48
V$MAZ_Q6	GGGAGGRR	MAZ (MYC-associated zinc finger protein)	0.00000	0.50
	TGCGCANK	UNKNOWN	0.00000	0.50
V$MYOD_Q6	GCANCTGNY	MYOD1	0.00000	0.51
	YGCGYRCGC	UNKNOWN	0.00000	0.51
	RNGTGGGC	UNKNOWN	0.00000	0.52
V$ERR1_Q2	TGACCTY	ESRRA	0.00000	0.52
V$PAX4_03	GGGTGGRR	PAX4	0.00000	0.52
V$E4F1_Q6	GTGACGY	E4F1	0.00000	0.55
V$HIF1_Q3	GNNKACGTGCGGNN	HIF1A	0.00000	0.55
	CTTTAAR	UNKNOWN	0.00000	0.56
V$FOXO4_01	TTGTTT	MLLT7	0.00000	0.60
V$NRF1_Q6	RCGCANGCGY	NRF1	0.00000	0.66

V$HNF3_Q6	TGTTTGY	HNF3	0.00000	0.67
V$MEF2_02	YTATTTTNR	MEF2A	0.00000	0.74
V$MYC_Q2	CACGTG	MYC	0.10000	0.55
V$ATF3_Q6	TGAYRTCA	ATF3	0.10000	0.60
V$FREAC2_01	RTAAACA	FOXF2	0.10000	0.60

Supplemental Experimental Procedures

Cell cycle analysis

XFiPS cell derived NPCs were treated in 20% O_2, 2% O_2, 100 μM DFX and 250 μM DMOG, respectively for 4 days before fixation. Cells were dissociated into single cell with 20% TrypLE (Life Technologies) and fixed with 70% ice-cold ethanol at 4°C for 1 hour. After centrifugation at 200*g* for 10 minutes at 4°C, cells were resuspended in a staining mix containing 0.2 mg/ml RNase A (QIAGEN) and 20 μg/ml propidium iodide (Sigma), and were stained at 37°C for 15 minutes. Cells were then analyzed on a BD LSR cytofluorimeter using FACSDiva Software (BD). A total of 10,000 events per sample were collected. Cell cycle analysis was performed using FlowJo software (TreeStar).

CHAPTER 3

Molecular traces of a low oxygen state in human neural progenitors

ABSTRACT

Oxygen tension clearly plays an important role in a variety of developmental settings. Our own work has shown that lowered oxygen tension in human neural progenitors leads to irreversible changes in the differentiation potential towards the glial lineage. The molecular basis for the permanence of this effect is unknown. Through an integrative analysis of the molecular events induced by low oxygen tension, we are able to distinguish acute versus chronic changes which are dependent specifically on activation of Hypoxia Induced Factor (HIF) signaling. Taking advantage of histone mass spectrometry, RNA-seq, ChIP-seq, and metabolomics, we uncovered evidence of a coherent response of the cell at the transcriptional, epigenetic and metabolic levels that correlates with a persistent cell fate decision in human neural progenitors. Furthermore, we found that even transient activation of the HIF pathway led to long-term changes at the transcriptional and epigenetic level. We propose that this form of molecular memory underlies long term changes in differentiation potential of progenitors in the nervous system.

INTRODUCTION

Whether *in vivo* or *in vitro*, all cells respond to the relative level of oxygen in their immediate environment. During development, the environment changes in innumerable ways, but the role of oxygenation of tissue is clearly critical. Vascularization brings increased oxygen tension to developing tissues, and as a result, cell fate decisions are altered. Our previous data showed that an acute treatment of low oxygen tension can have long lasting effects on the differentiation potential of human neural progenitors (Xie et al., 2014). Just a brief treatment of three days left these progenitors permanently more gliogenic in an unbiased differentiation assay. This is developmentally relevant, as these progenitors are known to first undergo a wave of

neurogenesis to generate neurons, and then proceed to a later stage of development where they make glia. Recent evidence from murine models has shown that a common progenitor/stem cell *in vivo* appears to evolved across development as opposed to the idea that there are distinct classes of progenitors giving rise to neurons versus glia (Alvarez-Buylla et al., 2001; Rowitch and Kriegstein, 2010). In the adult brain, radial glia cells (RGCs) have been widely accepted as a common progenitor that gives rise to both neuronal and glial lineages, through direct conversion or intermediate progenitors (Paridaen and Huttner, 2014; Rowitch and Kriegstein, 2010). During mammalian neocortical development, neural progenitors first undergo symmetric divisions to expand the progenitor pool. Those actively dividing progenitors are called neuroepithelial cells (NECs), because they have adherens junctions (AJs) and tight junctions (TJs) which commonly mediate cell-cell adhesion in epithelial cells. Single-cell RNA-sequencing reveals that the NECs express high level of *VIM*, *SOX2* and *PAX6*, as well as proliferative markers, such as *CDK1, CCND2* and *ASPM* (Pollen et al., 2014). As NECs turn into RGCs, they lose tight junctions but maintain adherens junctions and initiate the expression of astroglial markers such as GLAST and FABP7 (BLBP). However, the mechanisms underlying NEC to RGC transition are poorly understood (Paridaen and Huttner, 2014). At the onset of neurogenesis, RGCs divide mainly asymmetrically, giving rise to one RGC daughter cell and one differentiating daughter cell. This process involves cell cycle exit from the progenitor state into the post-mitotic neuron (Paridaen and Huttner, 2014). Gliogenesis generally follows neurogenesis in the developing brain (Miller and Gauthier, 2007). Astrocytes arise from various sources in the developing central nervous system. They can be produced 1) directly from RGCs within ventricular zone, 2) by direct transformation of RGCs at the end of neurogenesis, 3) from an astrocyte-restricted progenitor population, or 4) from proliferation of newly born astrocytes (Schitine et al., 2015; Sloan and

Barres, 2014). However, neurogenesis and gliogenesis partially overlap and the precise temporal relationship at the individual progenitor level remains largely unknown. To date, the astrocyte-restricted progenitors have not been well identified and characterized. Therefore, the identification of progenitors *in vitro* that could be coaxed to accelerate their developmental decision timing could be relevant to *in vivo* development as well.

Our own work left much of the molecular basis for these effects unknown. We identified that LIN28, a regulator of *let-7* family of miRNAs, is a target of hypoxia/HIF signaling. However, many questions remained as to how transient activation of HIF could initiate permanent effects downstream. The HIF signaling pathway is known to have pleiotropic effects on the cell due to the ability of the HIF1α and HIF1β to cooperatively bind to numerous target genes to drive important transcriptional changes related to cell cycle, metabolism, etc. Activity of HIF1α is mostly regulated by the active proteolysis of this protein at atmospheric oxygen concentrations by iron-sensitive PHD enzymes. So despite the fact that HIF is one of the more highly transcribed genes in the cell, protein only accumulates in the nucleus if the PHD proteins are inhibited. Therefore, as soon as oxygen concentrations rise, HIF protein and the pathways it promotes are silenced.

Activation of the HIF pathway is known to induce changes in transcription, metabolism, and epigenetic regulation, so here we measured all these to understand the effect of this pathway both acutely and chronically in our model of human neural development. We describe profound molecular changes that occur quickly in response to this pathway, and integrate these data to

paint a complete picture of how progenitors sense their environment and make a coherent response.

RESULTS

To determine how cells respond both acutely and chronically to altered oxygen tension, we take advantage of a developmental model of the human nervous system. Human neural progenitors made from induced pluripotent stem cells or embryonic stem cells will make neurons and glia once mitogenic factors (EGF/FGF) are removed from the culture. Importantly, the progeny of pluripotent stem cells represent very early stage cells that would only be found in the first half of the first trimester of gestation (Patterson et al., 2011; Yang et al., 2008). As such, human neural progenitors made from pluripotent stem cells are universally known to be more neurogenic than gliogenic, producing far more neurons than astrocytes or oligodendrocytes. These progenitors have a very low gliogenic capability early in differentiation, but can be pushed towards gliogenic lineages by extending the culture, or experimentally promoting maturation (Patterson et al., 2014; 2011; Xie et al., 2014).

Evidence of this neurogenic bias is highlighted in Fig 3-1A, where in 20% oxygen, these progenitors produce roughly 3 times the number of neurons as astrocytes. However, when the same progenitors are cultured in 2% oxygen, this bias is altered such that these cells then made equal numbers of neurons and astrocytes (Fig 3-1A). Importantly, and consistent with previous results, we found that growing neural progenitors in 2% oxygen and then switching them to 20% oxygen for differentiation still left them more gliogenic (Fig 3-1A). The same is true if the progenitors were grown in 20% oxygen but treated with DFX, an iron-chelating agent that blocks

degradation of HIF by the PHD pathway (Fig 3-1B), or with DMOG, another compound able to stabilize HIF protein even in atmospheric oxygen (not shown).

To identify the transcriptional response specifically to HIF activation, we treated cells with low oxygen, DFX, or DMOG; then looked at the gene expression changes that occurred across all three manipulations. We hypothesized that this approach would minimize the contribution of off-target effects induced by each of the three manipulations, and allow us to focus on just those changes caused by regulation of HIF activity. After three days of these treatments, RNA was collected and processed for RNA-seq. Across the three treatments, 2076 differentially expressed genes were identified (Fig 3-2A). Gene ontology analysis on the upregulated genes showed a strong bias towards genes involved in glycolysis (Fig 3-2B). These results are consistent with significant literature demonstrating that activation of HIF can promote glycolysis, but this has not yet been shown in human neural progenitor cells. Ontological analysis of the down-regulated genes demonstrated a clear suppression of genes important for mitochondrial activity, oxidative phosphorylation, as well as the cell cycle (Fig 3-2C). These results are also consistent with the notion that HIF activation induces glycolysis, but suppresses oxidative phosphorylation and mitochondrial respiration. The fact that cell cycle genes were suppressed is consistent with our observation that extended treatment (beyond 3 days) with HIF stabilizers or with lowered oxygen tension led to slower growth of neural progenitors, but is in conflict with previous data on a role for proliferation by hypoxia in murine neural progenitors (Studer et al., 2000).

A closer look at the transcriptional changes induced by HIF signaling pointed towards a very specific cell fate transition taking place in these cultures with a correlation to human

development. Neural progenitors made from pluripotent stem cells are known to represent very early stage cells that would be the equivalent to actively dividing neuroepithelial cells, as identified by high levels of NEC marker *VIM*, *SOX2* and *NESTIN*, as well as AJs and TJs that mediate cell-cell adhesion. After HIF activation, these progenitors induce the expression of a variety of genes consistent with a transition to radial glial progenitor. *NOTCH1* was significantly upregulated in all three conditions upon HIF activation. Activated Notch1 can promote radial glial fate in mouse forebrain before the onset of neurogenesis (Gaiano et al., 2000). FABP7 (also called BLBP), a marker for RGCs, was also induced by HIF activation, and remained upregulated after treatment withdrawal. Meanwhile, ontological analysis of down-regulated genes identified categories such as mitotic cell cycle and M phase. This observation correlates with the fact that RGCs switch from symmetric to asymmetric division, giving rise to one RGC daughter cell and one differentiating cell. Among the upregulated GO categories, neuronal projection development and axonogenesis are indications of newly born neurons (Fig 3-2B).

One possibility is that astrocyte-restricted progenitors were generated upon HIF activation. In fact, a number of transcription factors that activate astrogliogenesis were induced upon HIF activation, such as NFIX (Wilczynska et al., 2009) and SOX9 (Kang et al., 2012). In addition, CD44 was highly induced in all three HIF activation conditions. Previous studies showed that CD44 expression identifies astrocyte-restricted precursor cells (Liu et al., 2004; Shaltouki et al., 2013). This data is consistent with the observation that HIF activated progenitors are more gliogenic, and suggest that HIF can promote the cell fate transition toward radial glial progenitors.

To uncover transcriptional changes that persist after HIF induction has stopped we also profiled cells after a pulse-chase treatment (3-day treatment, 3-day return to baseline). Again, looking at genes whose pattern changes consistently across all three types of treatment, but this time after a chase of three days, we identified only 27 genes that remained upregulated, and 46 genes remained downregulated ($p<0.05$). Ontological analysis suggested an enrichment of negative regulation of cell proliferation, which would be consistent with down regulation of cell cycle at day3 (Fig 3-2D). Genes that remained downregulated were enriched in categories such as regulation of cell adhesion, extracellular region, and actin binding (Fig 3-2E), suggestive of a NEC to RGC transition. Importantly, these data pointed to chronic transcriptional changes that could be evidence of molecular memory.

To determine whether the ontological results were indicative of physiological changes in these progenitors, we performed metabolomics analysis with labeled glucose to measure general metabolic pathway activity as well as glycolytic flux. Cells were treated with each of the HIF stabilizing protocols, and then labeled with U13C-Glucose. Metabolites from isolated cells were identified by tandem mass spectrometry. These analyses pointed strongly to a dramatic decrease in oxidative phosphorylation as indicated by significant decrease of labeled glucose in metabolites within the TCA cycle (Fig 3-3A) and metabolites directly converted from the TCA cycle (Fig 3-3B). Increase in glucose flux and utilization of glycolysis upon induction of HIF signaling was indicated by an increased relative amount of labeled lactate in all treated groups (Fig 3-3C). These results suggest that glucose metabolism is consistent with transcriptional changes upon HIF activation.

The idea of epigenetic memory stems from experiments that showed persistent phenotypes following manipulations that affected epigenetic regulation, but left genetic elements unaffected. The study of epigenetic memory is hampered by the fact that there are a large number of histone modifications that make up the histone code, and until recently there was no method to survey a large number of them as one can with RNA transcripts. We applied a broad approach to identify epigenetic modifications that change in abundance across the genome in response to activation of HIF signaling. Through isolation of histones and mass spectrometry, the relative abundance of theoretically any covalent modification on histone can be assessed (Evertts et al., 2010; Sridharan et al., 2013; Zee et al., 2010). We isolated histones from cells treated with low oxygen, DFX or DMOG, and performed mass spectrometry to define the relative levels of individual histone post-translational modifications across H3 and H4, H2B and H2A. Again looking for changes across all three treatments, we uncovered just two significant alterations of histone modifications out of hundreds possible.

H3K9Me3 and H3K9Me2 were strongly increased in treated cells (Fig 3-4A). As a result, relative levels of H3K9Me1 or unmethylated H3K9 were decreased, demonstrating that histone 3 lysine 9 was actively methylated upon HIF activation. This data is consistent with several studies showing that H9K9Me2 can be induced by hypoxia genome-wide (Chen et al., 2006; Johnson et al., 2008) or at specific promoters (Lee et al., 2009; Lu et al., 2011; Wang et al., 2011). H3K9Me3 is known to be associated with transcriptional repression in many contexts. However, previous studies suggested that HIF signaling induces the expression of Jumonji C domain-containing histone demethylases, thus resulting in an decrease of H3K9Me2 and H3K9Me3 (Beyer et al., 2008; Lee et al., 2013).

In addition, H3K27 acetylation was suppressed in terms of absolute abundance (Fig 3-4B). H3K27Ac is associated with active transcription either at the start site or as a mark of enhancers. Therefore, the loss of this mark would be suggestive of loci that downregulate transcription. We validated these findings by western blot with both a pulse and pulse-chase of treatment. Interestingly, the pulse-chase data suggest that these marks could change again in response to loss of HIF signaling to produce an altered histone code (Fig 3-4C).

The mass spectrometry approach uncovered differences in abundance of these histone marks but was not able to identify how the patterns of these marks are altered in terms of location throughout the genome. To understand how the distribution of these marks changes in response to HIF activation, we performed ChIP-seq with both marks in cells again treated with all three HIF activating conditions. To validate the quality of our ChIP-seq approach, we first looked at loci for genes whose expression was strongly changed in response to hypoxia/DFX/DMOG treatment for the relative abundance of H3K27ac. In upregulated genes, such as *PGK1*, there was a strong increase in H3K27Ac, while the converse was true for downregulated genes, like *IGFBP7* (Fig 3-5A). When comparing the expression level of all the genes associated with H3K27Ac marked regions, gene expression level in DMOG group was significantly higher than that in control (Fig 3-5C). This is consistent with what is known about how this mark correlates with active gene expression. To identify more broadly the loci differentially marked by H3K27Ac in response to HIF activation, we analyzed the differential peak fold change distribution after both a pulse and chase of HIF activation. This analysis pointed towards lower K27Ac peaks in HIF activation groups compared with control at day 4 of treatment, and that

both 2% oxygen and DMOG treatments showed persistent changes even after the chase (Fig 3-5B).

In general, the DMOG treatment immunoprecipitation appeared to produce cleaner data. Therefore, much of the following analyses were confined to these samples. By categorizing loci into gene ontological categories, it became clear that treatment with DMOG led to strong increases of H3K27Ac at loci related to hypoxia and glycolysis as expected (Fig 3-5E). In 20% O_2, H3K27Ac marked loci enriched for actin binding and beta-catenin binding (Fig 3-5D), which is consistent with the notion that neural progenitors in 20% O_2 were mainly NECs expressing high level of adherens junctions associated proteins, such as catenins and actin. The disappearance of H3K27Ac on those genes after DMOG treatment was also consistent with down-regulated GO categories in Fig 3-2E, suggesting the cell fate transition from NECs to RGCs and differentiated daughter cells upon HIF activation is also regulated at the epigenetic level. Average profiling using GO categories such as hypoxia and glycolysis showed a clear increase on K27Ac mapped reads in the DMOG treated group, whereas categories such as DNA repair and protein secretion showed no difference between DMOG and control (Fig 3-5F). When looking specifically at loci for genes whose expression remained induced after pulse-chase treatment with DMOG, there was enrichment of the H3K27Ac mark, while loci for downregulated genes were unaffected (Fig 3-5G). This represents evidence for epigenetic memory at loci activated by HIF signaling.

H3K27Ac not only marks sites of active transcription, but also enhancers. Clusters of enhancers, known as super-enhancers, activation of which have been shown to serve as faithful hallmarks of

cell fates (Hnisz et al., 2013; Whyte et al., 2013). An analysis for clustered H3K27Ac sites, or super-enhancers uncovered 1056 activated super-enhancers in 20% oxygen, and just 616 in DMOG (Fig 3-6A). This suggests a large shift in super-enhancer activity between these two conditions. Ontological analysis of genes associated with the active super-enhancers in DMOG treated cells uncovered a strong bias towards metabolic genes, and glycolysis in particular (Fig 3-6B). This result suggests that HIF activation engages super-enhancers at genes important for glycolysis, and links this pathway to both transcriptional and epigenetic regulation.

The mass spectrometry analysis on histones pointed to significant decreases in overall H3K27ac, so we looked into which genomic features accounted for the general drop in this mark. The fact that 20% O_2 showed more engaged super-enhancers was consistent with histone mass spectrometry data showing more H3K27Ac in 20% O_2 group. Although fewer super-enhancers were detected in the DMOG group, those super-enhancers were highly enriched in genes involved glycolysis. However, genes associated with super-enhancers in 20% O_2 did not have a strong enrichment in any GO categories.

When performing similar analyses with data from the H3K9Me3 ChIP-seq, we found first that after a pulse of treatment, H3K9Me3 was significantly higher across all genes, particularly in regions upstream of the TSS (Fig 3-7A). On the other hand, after the chase period, no evidence for an increase persisted, suggesting a lack of memory overall for this mark (Fig 3-7A).

4 days after treatment with DMOG, loci related to hypoxia and glycolysis showed increased levels of this mark, particularly upstream of the TSS (Fig 3-7B). This was surprising considering

the well-established correlation of this mark with epigenetic silencing. One explanation for this observation could be that genes that are dynamically regulated could potentially acquire marks associated with both induction and suppression of expression to allow for a quicker suppression if the stimulatory signal is lost, such as the pulse-chase scenario used here. To test this hypothesis, we looked at genes whose expression did not persist after the chase, namely, were silenced as soon as the HIF signal disappeared. In fact, we did not see particular enrichment differences between acutely or chronically affected genes (Fig 3-7C).

DISCUSSION

Taken together all these data provide an integrated view of both the acute and chronic response of HIF activation in human neural progenitors. HIF activation leads to profound transcriptional, epigenetic and metabolic changes in the cell, and as a result, these cells adopt a phenotype more akin to radial glial progenitors than neuroepithelial progenitors. In fact, these molecular responses are known to be integrated on several levels. First, stabilization of HIF due to suppression of degradation of this protein leads to its accumulation in the nucleus (Xie et al 2014). Upon binding of HIF and induction of target genes such as those described in Fig 3-2, a variety of epigenetic changes can be detected, including acetylation of histone 3 at lysine 27. As a result, super-enhancers of genes known to be critical for the response to hypoxia and induction of glycolysis become activated.

There are two possible interpretations for the observed increased astrogliogenesis after HIF activation. One possibility is that HIF activation facilitates the overall differentiation process of neural progenitors. Gene ontology analyses from Fig 3-2 and Fig 3-5 suggest that HIF signaling

promotes NEC to RGC transition, and asymmetric division of RGCs can generate differentiated daughter cells. Because neurogenesis precedes gliogenesis in development, we observed mostly neurons in the first two weeks of GFWD differentiation. Assuming the initial RGC pool is homogeneous and each RGC starts gliogenesis after several rounds of asymmetric division, early initiation of asymmetric division by HIF should result in an early onset of astrogliogenesis. Moreover, transcription factors that activate astrogliogenesis were induced upon HIF activation, such as NFIX (Wilczynska et al., 2009) and SOX9 (Kang et al., 2012). Those transcription factors may advance the generation of astrocytes from the neurogenic RGCs.

Another interpretation is based on the assumption that the initial RGC pool is heterogeneous, consisting of neuronal progenitors and astrocyte-restricted progenitors, while HIF activation could promote the generation of astrocyte-restricted progenitors. CD44 was identified as a marker for astrocyte-restricted precursor cells in several studies (Liu et al., 2004; Shaltouki et al., 2013). Indeed, we did see an increase of CD44 expression in all groups upon HIF activation. Because CD44 is also observed in neural stem cells, oligodendrocyte precursor cells, and certain types of neurons (Naruse et al., 2013), further studies are needed to characterize those CD44 positive cells and identify whether they contribute to astrogliogenesis. The real mechanism underlining HIF mediated astrogliogenesis is probably much more completed, and possibly a combination of both these scenarios.

While we still do not have a complete understanding of how transient HIF activation leads to a seemingly permanent cell fate transition, our data provide extensive evidence that this is correlated with persistent expression of a small number of genes important for radial glial

progenitors. In addition, at these same genes, the H3K27Ac mark appears to be persistent even after the chase, while the same was not true for downregulated genes. On the other hand, we were unable to detect persistent changes in H3K9Me3 after a pulse chase experiment in either all genes, or even in differentially expressed genes.

There are also several important limitations to the conclusions we can draw from this work. H3K9Me3 ChIP-seq was less informative than H3K27Ac ChIP-seq, for the following reasons: 1) unlike active marks, the relationship between one repressive mark (K9Me3) and gene expression is not very clear. Thus, it is difficult to draw connection between ChIP-seq associated genes and RNA-seq data. 2) The antibody for H3K9Me3 ChIP is not very efficient, resulting in a high background and a low signal-to-noise ratio, and making it harder to define peak regions. In fact, H3K9Me2 was more significantly induced by HIF activation in histone mass spectrometry than H3K9Me3. Both H3K9Me3 and H3K9Me2 contribute to short-term repression of differentiation genes in ESCs. However, due to the notoriously lack of specificity of the H3K9Me2 antibody, we did not perform H3K9Me2 ChIP. 3) Because H3K9Me3 bound regions possess a unique "plateau-like" pattern, which is different from traditional ChIP peak, there are technical difficulties associated with peak-calling algorithms. 4) Most studies compare epigenetic status between very different cell types, such as ESCs versus NPCs, because their transcriptional and epigenetic landscapes are dramatically different, and thus easy to draw a conclusion. We tried to compare differentially marked regions for the same cell type with or without treatment. Due to the small underlying differences, the resolution of H3K9Me3 ChIP might not be able to detect the differentially marked peaks. 5) Furthermore, because each ChIP-seq is normalized by library size, it would have been helpful to add internal spike-in controls in each ChIP-seq in order to

compare ChIP-seq data between samples. To summarize, RNA-seq is the most informative analysis, which detects most transcribed genes with fold change information. Active histone marks, such as H3K27Ac, successfully captured the actively transcribed genes and super-enhancers, but could not detect genes expressed at low levels. Repressive histone marks, such as H3K9Me3 were the least informative among the three, because of above-mentioned limitations.

In total, these results suggest that differentiation of human neural progenitors grown in atmospheric oxygen concentrations remain relatively immature because they have not been generated in physiological conditions that appropriately tune the transcriptome, epigenome, and metabolome. This work represents the most comprehensive molecular analysis of the effect of HIF activation on human neural progenitors, and provides important insights into how cells respond to oxygen levels both acutely and chronically. Furthermore, this work extends our previous efforts to understand how cell fate transitions are controlled in these clinically relevant cells.

MATERIALS AND METHODS

Cell Culture

hESCs and hiPSCs were cultured as described previously (Xie et al., 2014) in accordance with UCLA Embryonic Stem Cell Research Oversight committee. Briefly, feeder-free hESC or hiPSC lines were maintained with mTeSR1 (Stem Cell Technologies) and passaged mechanically. Neural rosette derivation, NPC purification, and differentiation into neurons and glia were performed as described (Patterson et al., 2011). Rosettes were generated by growing PSCs for at least 7 days in Dulbecco's modified Eagle's medium (DMEM)/F12 with N2 and B27 supplements (Invitrogen), 20 ng/ml basic fibroblast growth factor (FGF) (R&D Systems), 1 mM retinoic acid (RA) (Sigma), and 1 mM Sonic Hedgehog Agonist (Calbiochem). NPCs were expanded in NPC medium containing DMEM/F12, N2 and B27, 20 ng/ml basic FGF, and 50 ng/ml EGF (GIBCO) once the rosettes were picked. DFX (Sigma) (100 to 200 mM) and DMOG (Sigma) (250 mM) were added at the NPC stage for 3 to 5 days. Upon differentiation, EGF and FGF were withdrawn from NPC medium for 2 to 6 weeks, called growth factor withdrawal assay (GFWD). Physiological oxygen tension growth was established in 2% O_2, 5% CO_2, and 92% N_2. Atmospheric oxygen tension growth was established in 20% O_2, 5% CO_2, and 75% N_2.

Metabolite Extraction

Cells were incubated in NPC medium containing 17.5 mM U-13C labeled glucose (Cambridge Isotope Labratories) and treated with 20% O_2, 2% O_2, 100 uM DFX, or 250uM DMOG for 24 hours. The following day, cells were rinsed with 150 mM cold ammonium acetate (pH=7.3) and scraped off with 400 µl cold 100% methanol. Shake the plate for 1 minutes, and then add 400 µl

cold H2O. Transfer the cell suspension into Eppendorf tube and add 400 µl cold chloroform. An internal standard of 5 nmol norvaline was added to each sample. Cell suspension was centrifuged at top speed and the aqueous layer was transferred to a glass vial. The metabolites were dried in evaporator (EZ-2Elite, Genevac) and submitted for mass spectrometry analysis.

Immunofluorescent Staining and Quantification

Immunofluorescent staining was performed as described (Xie et al., 2014). Briefly, cells grown on coverslips were fixed at indicated time points with 4% (w/v) paraformaldehyde (Electron Microscopy Sciences) in PBS. Antibodies used include the following: chicken anti-GFAP (Abcam, ab4674), mouse anti-MAP2 (Abcam, ab11267), mouse anti-NESTIN (Neuromics, MO15012. More than six views were randomly selected for each coverslip, and images were taken at 10x magnification with the same exposure time across all samples. Quantification was performed using ImageJ with the same threshold for each channel for all samples. The percentage of neurons or astrocytes was calculated with a positive staining area from each marker and normalized based on cell number (DAPI staining). P-value was calculated with Student's t test.

Histone Extraction and Mass Spectrometry Analysis

Nuclei were isolated and standard acid extraction of histone was performed as described previously (Zee et al., 2012) with modification as described below. Briefly, frozen cell pellets were lysed with 0.3% NP-40, 1 mM dithiothreitol, 10 mM sodium butyrate, 2 mM sodium vanadate, and peotease inhibitor cocktail. The insoluble chromatin pellet was extracted with 0.4N H_2SO_4. Histones were precipitated with final volume of 20% trichloroacetic acid over

night. Histones were washed in acetone with 0.1% HCl using a sealed glass pipette once and washed again with 100% acetone twice. The final histone pellets were air dried and submitted to Benjamin Garcia lab at University of Pennsylvania for quantitative mass spectrometry analysis. The liquid chromatography-mass spectrometry-based proteomics and data analysis was performed as described previously (Garcia et al., 2007; LeRoy et al., 2012; Sridharan et al., 2013).

Western Blot

Western blot analysis was performed using standard procedures as described(Lowry et al., 2005). Antibodies used including: rabbit anti-H3K27Ac (Abcam, Ab4729), mouse anti-β-Actin (Santa Cruz, sc-47778).

Gene Expression Analysis

RNA extraction, reverse transcription and real-time quantitative PCR were performed as described (Xie et al., 2014). Briefly, total RNA was isolated using an RNeasy Mini Kit following protocol described by the manufacturer (QIAGEN). Reverse transcription and real-time PCR were performed using the Superscript III first-strand cDNA synthesis kit (Invitrogen) and the SYBR green real-time PCR kit (Roche), respectively. Transcript levels were determined in triplicate reactions and normalized to housekeeping gene such as beta-actin. Primer sequences are available upon request.

RNA-Sequencing

Total RNA was isolated using an RNeasy Mini Kit (QIAGEN). Library preparation was

performed using TruSeq Standard RNA LT Kit (Illumina) following the standard total RNA sample preparation protocol. The sequencing reactions were run on HiSeq 2000 as single-end 100bp.

RNA-Sequencing Analysis

Tophat was used to align reads to the hg19 genome assembly (Trapnell et al., 2009), using the default settings in Galaxy (http://galaxy.hoffman2.idre.ucla.edu) (Giardine et al., 2005). Multimappers, unmapped reads, and low quality alignments were excluded from analysis. Counts obtained using featureCounts with Gencode annotations were analyzed with the R package edgeR, which uses a negative binomial generalized log-linear model (Robinson et al., 2010). In order to identify genes that were consistently up- or down-regulated across all hypoxia-inducing treatments, the hypoxia-inducing conditions 2% O_2, DFX and DMOG were treated as replicates. This way, genes modulated by only one treatment are penalized by the large variation across the three hypoxia-inducing conditions. An unadjusted p-value threshold of 0.05 was imposed for the likelihood ratio test to select differentially expressed genes. The gene ontology categories were generated with DAVID bioinformatics resources using functional annotation clustering with default settings (Da Wei Huang et al., 2009).

ChIP-Sequencing

ChIP-sequencing was performed as described previously with modifications (Sridharan et al., 2013). Briefly, NPCs were crosslinked by 1% formaldehyde (final concentration) for 10 minutes at room temperature, and quenched with 125mM glycine (final concentration). Cells were re-suspend in sonication buffer containing 50 mM Hepes-KOH (pH=7.9), 140 mM NaCl, 1mM

EDTA (pH=8), 1% Triton X-100, 0.1% sodium Deoxycholate, 1% SDS and protease inhibitor, and sonicated with Misonix sonicator S-4000. Cell extracts were incubated with antibody against H3K27Ac (Abcam, ab4729) or H3K9Me3 (Abcam, ab8898) overnight at 4 °C. Immunoprecipitates were collected with magnetic beads, and washed twice with PBS, low-salt buffer, high-salt buffer and LiCl buffer as described before (Sridharan et al., 2013). Reverse crosslinking was preformed by addition of 1% SDS and proteinase K with gentle shaking overnight at 56°C. DNA was precipitated using phenol-chloroform-isoamyl alcohol mixture (Sigma, P2069) and Phase Lock Gel (5 Prime) according to manufacturer's protocol. ChIP-seq library preparation was performed using Ovation Ultralow System V2 1-16 (NuGEN) following the user's guide. The sequencing was performed on HiSeq 2000 platform with single-end 50bp run.

ChIP-Sequencing Analysis

Reads were trimmed to remove adapters and low-quality ends with cutadapt and sickle. Bowtie2 was used to align reads to the hg38 genome assembly, using the "very-sensitive" settings (Ben Langmead and Salzberg, 2012). Multi-mappers, unmapped reads, and low-quality alignments (MAPQ < 30) were filtered out with samtools (Li, 2009). Duplicates were removed with Picard. H3K27Ac peaks were called with MACS2 in "broad" mode, using a q-value threshold of 0.01. Differential peaks were identified using MAnorm (Shao et al., 2012), double-thresholding on |M| (1) and p-value (0.01).

Heat maps and average profiles of ChIP-seq read pileup signal were generated with ngsplot (Shen et al., 2014). The list of genes belonging to each biological function was obtained from the "hallmark" gene sets of MSigDB (The Broad Institute of Harvard and MIT).

Super-enhancers were identified using the software package ROSE from the Young lab (Lovén et al., 2013; Whyte et al., 2013), with a default stitching distance of 12.5 kb and a TSS exclusion zone of 2 kb.

Functional annotation of peaks and super-enhancers was performed using GREAT (McLean et al., 2010), with default parameters except a distal association extension of 100 kb.

GREAT associations between peaks and genes were also used to select genes whose hypoxia/normoxia Log2 Fold change of transcript expression is displayed in the boxplot. The difference of Log2 Fold changes was tested for significance using a non-parametric Mann-Whitney-Wilcoxon U test.

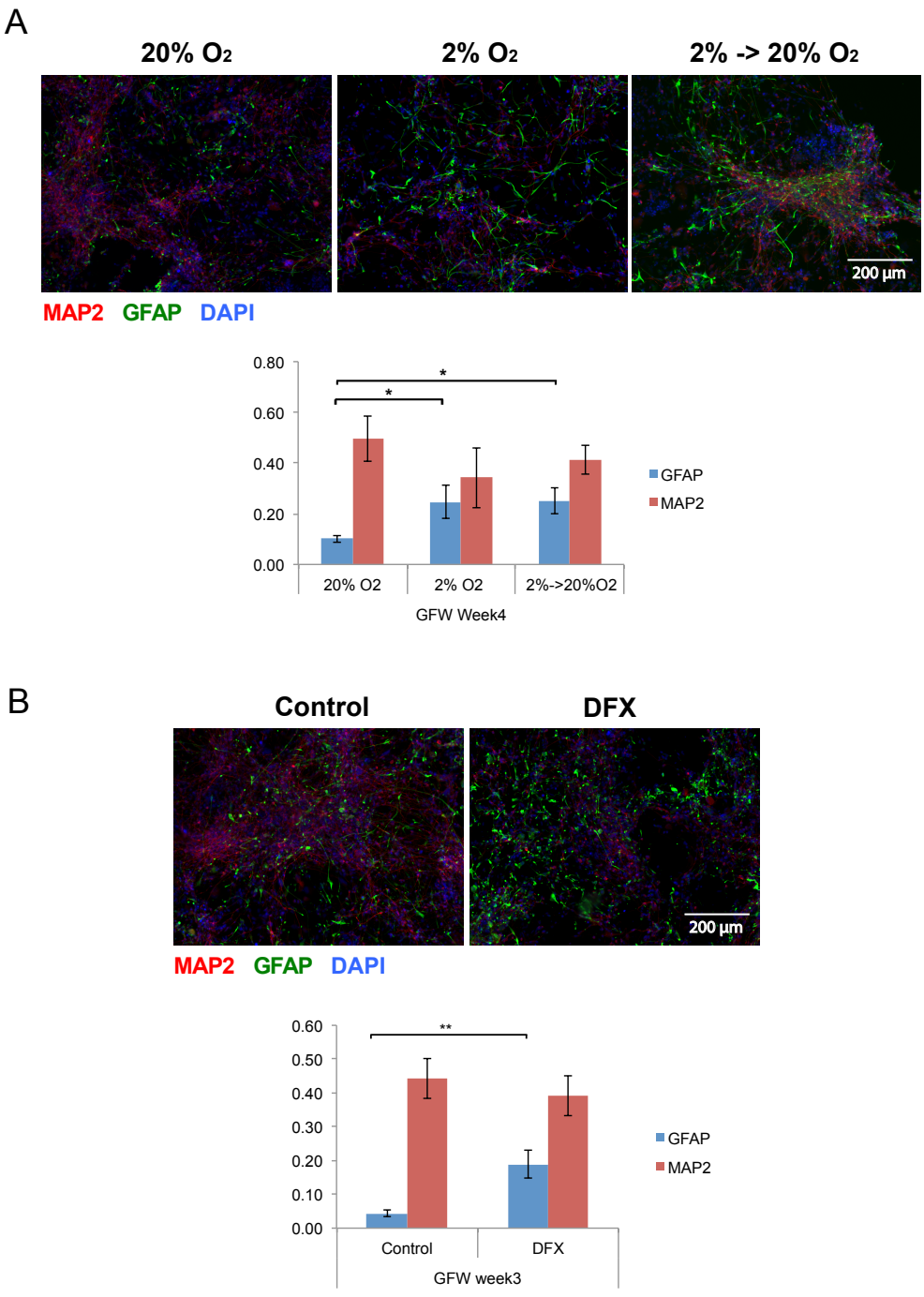
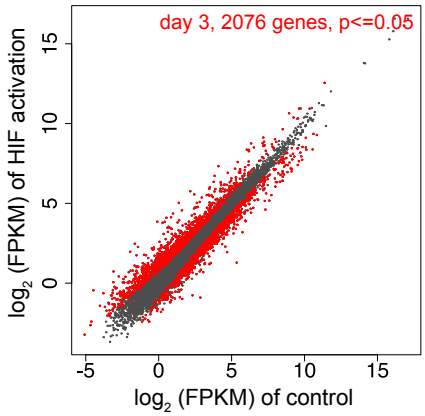


Figure 3-1. Activation of HIF by low oxygen or small molecules at NPC stage promotes generation of astrocyte upon differentiation.

(A) Directed differentiation of NPCs toward neurons and glia by growth factor withdrawal (GFWD) to assay for developmental maturity of progenitors. Top, culturing and differentiating NPCs in atmospheric oxygen tension (20% O_2), prolonged physiological oxygen tension (2% O_2), or a temporal exposure to physiological oxygen tension (2% O_2) in NPC stage and followed by differentiation at 20% O_2 generates both neurons and glia, which are assayed by immunostaining for MAP2 (neurons) or GFAP (astrocytes). Bottom, quantification of immunostaining demonstrates the strong effect of prolonged and temporal physiological oxygen on promoting astrogliogenesis.

(B) Top, DFX treatment at NPC stage led to an increase in astrocytes after 3 weeks of differentiation. Bottom, a quantification of immunostaining suggested an induction of astrocyte (GFAP) percentage upon differentiation. (n = 3 independent experiments with hESC or hiPSC-derived NPCs; mean ± SEM; * $p < 0.05$, ** $p < 0.01$; Student's t test; scale bars, 200 μm)

A



B

Top GO categories for up-regulated genes at day3

Term	p-Value
SP_PIR_KEYWORDS_glycolysis	2.90E-08
GO:0006007~glucose catabolic process	5.03E-07
GO:0031175~neuron projection development	1.04E-06
SP_PIR_KEYWORDS_kinase	1.62E-06
GO:0031344~regulation of cell projection organization	1.91E-06
IPR002165:Plexin	4.45E-06
domain:Fibronectin type-III 3	6.00E-06
GO:0010975~regulation of neuron projection development	6.47E-06
GO:0048666~neuron development	7.78E-06
GO:0006006~glucose metabolic process	1.57E-05
GO:0043005~neuron projection	1.84E-05
GO:0007409~axonogenesis	3.25E-05
GO:0007155~cell adhesion	8.63E-05
GO:0045597~positive regulation of cell differentiation	9.51E-05

C

Top GO categories for down-regulated genes at day3

Term	p-Value
SP_PIR_KEYWORDS_mitochondrion	2.22E-19
GO:0000278~mitotic cell cycle	2.56E-18
GO:0007049~cell cycle	4.30E-15
GO:0031497~chromatin assembly	5.61E-14
GO:0006323~DNA packaging	6.28E-12
GO:0000279~M phase	1.33E-10
IPR007125:Histone core	2.17E-10
GO:0051438~regulation of ubiquitin-protein ligase activity	3.66E-10
SP_PIR_KEYWORDS_cell division	2.18E-09
SP_PIR_KEYWORDS_respiratory chain	5.99E-09
SP_PIR_KEYWORDS_kinetochore	9.63E-09
hsa00190:Oxidative phosphorylation	3.40E-07
GO:0006261~DNA-dependent DNA replication	1.15E-06
GO:0005819~spindle	3.21E-05

D

Top GO categories for remain up-regulated genes at day6

Term	p-Value
SP_PIR_KEYWORDS_signal	5.22E-03
UP_SEQ_FEATURE_signal peptide	5.47E-03
GO:0005578~proteinaceous extracellular matrix	1.12E-02
GO:0008285~negative regulation of cell proliferation	1.14E-02
GO:0031012~extracellular matrix	1.37E-02
GO:0048662~negative regulation of smooth muscle cell proliferation	1.85E-02
SP_PIR_KEYWORDS_glycoprotein	3.69E-02
SP_PIR_KEYWORDS_extracellular matrix	3.88E-02

E

Top GO categories for remain down-regulated genes at day6

Term	p-Value
GO:0030155~regulation of cell adhesion	1.87E-05
GO:0003779~actin binding	8.23E-04
GO:0044421~extracellular region part	1.02E-03
SP_PIR_KEYWORDS_actin-binding	1.69E-03
SP_PIR_KEYWORDS_Secreted	1.94E-03
GO:0030510~regulation of BMP signaling pathway	2.41E-03
GO:0005576~extracellular region	3.12E-03
SP_PIR_KEYWORDS_actin binding	3.13E-03
IPR001478:PDZ/DHR/GLGF	4.36E-03
GO:0008092~cytoskeletal protein binding	5.51E-03
SMART_SM00228:PDZ	6.81E-03
GO:0045785~positive regulation of cell adhesion	9.35E-03

Figure 3-2. RNA-sequencing data on differentially expressed genes between control and HIF activation groups

(A) Scatter plot marking in red the differentially expressed genes from RNA-seq data between

control and three HIF activation conditions. HIF activation group is pooled from RNA-sequencing data using all three treatments: 2% O_2, DFX, and DMOG. ($p < 0.05$, likelihood ratio test)

(B-C) Gene Ontology analysis showed that significantly up-regulated genes by HIF activation are highly enriched in neuron differentiation, regulation of neuron projection, axonogenesis, and glycolysis categories (B), whereas down-regulated genes are enriched in GO categories such as cell cycle, mitochondrion, and DNA replication (C).

(D-E) Gene Ontology categories from genes remain significantly up-regulated (D) or down-regulated (E) after treatment withdrawal. 2% O_2, DFX and DMOG conditions were treated as replicates to calculate significance. ($p < 0.05$, likelihood ratio test)

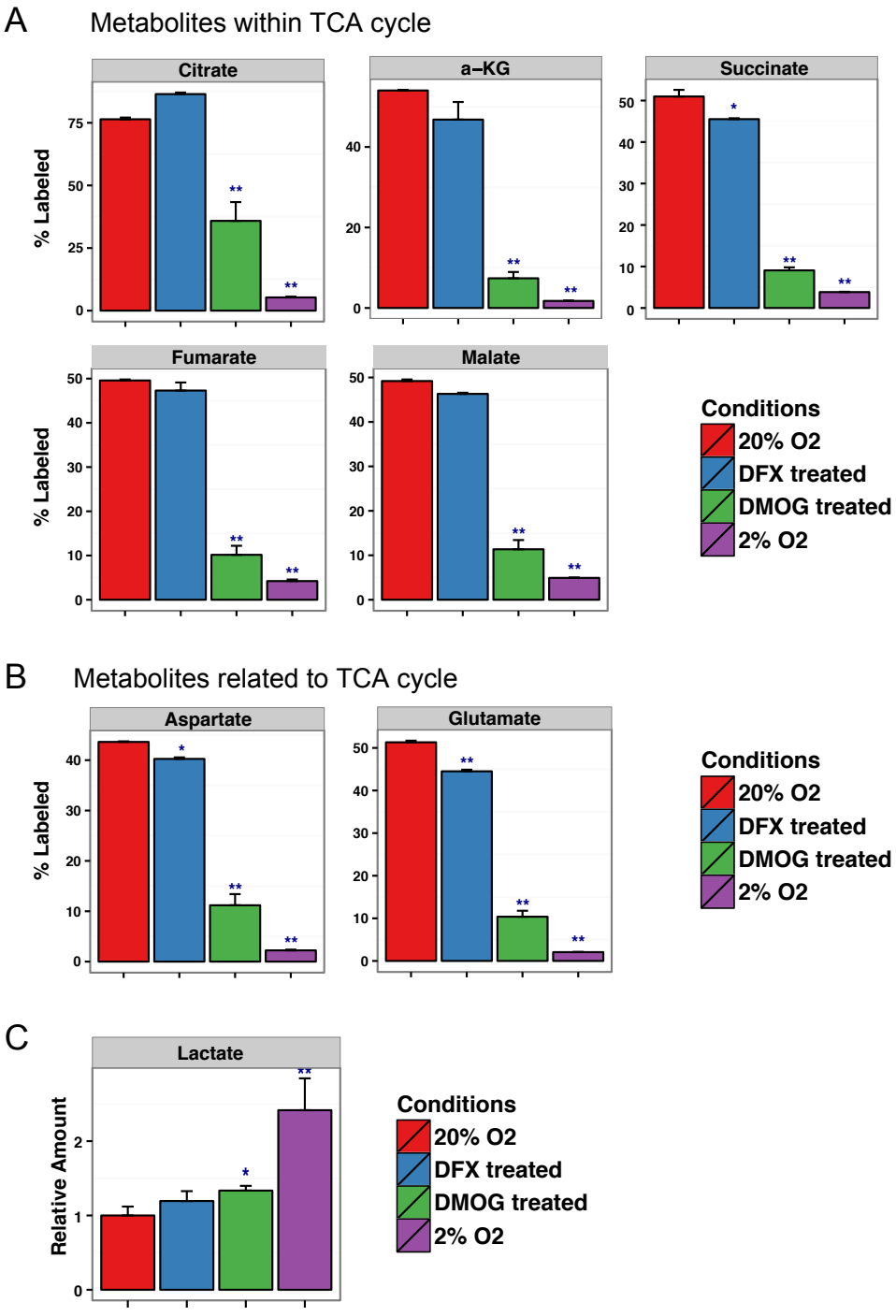


Figure 3-3. Global metabolite analysis suggested increased glycolysis and decreased oxidative phosphorylation upon HIF activation

(A) The percentage of U13C-labeled Glucose in metabolites involved TCA cycle suggested that oxidative phosphorylation in HIF activation groups (2% O_2, DFX or DMOG) are significantly lower compared with untreated control (20% O_2), measured by metabolite mess spectrometry.
(B) The percentage of U13C-labeled Glucose in metabolites related to TCA cycle suggested that oxidative phosphorylation in HIF activation groups (2% O_2, DFX or DMOG) are significantly lower compared with untreated control (20% O_2), measured by metabolite mass spectrometry.
(C) The relative amount of lactate in 2% O_2, DFX or DMOG groups is higher than 20% O_2, suggesting increased glycolysis upon HIF activation (right). (A-C, n = 3 biological replicates; mean ± SD; * $p < 0.05$, ** $p < 0.01$; Student's t test compared with 20% O_2 control)

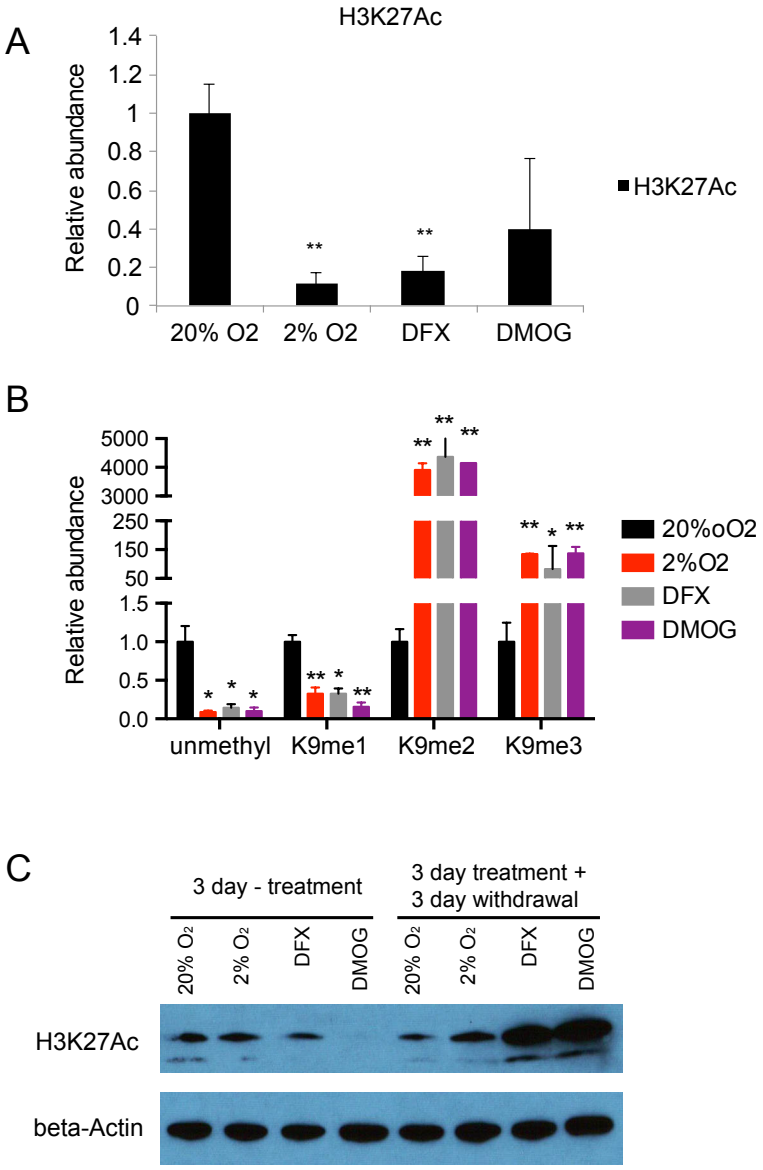


Figure 3-4. Histone mass spectrometry revealed a global change of H3K27Ac and H3K9Me2/3 upon HIF activation

(A) Global H3K27 acetylation was significantly decreased in 2% O_2, DFX and DMOG group compared with untreated control, measured by histone mass spectrometry.

(B) Global H3K9Me2 and H3K9Me3 were significantly increased, whereas H3K9 unmethyl and mono methyl were decreased in all three HIF activation conditions.

(A-B, n = 3 biological replicates, mean ± SEM; * $p < 0.05$, ** $p < 0.01$; Student's t test compared with 20% O_2 control)

(C) Western blot of H3K27 acetylation expression in hiPSC-derived NPCs in pulse (3 day treatment) and chase (3 day treatment + 3 day withdrawal) experiments under different treatments. Actin was used as loading control.

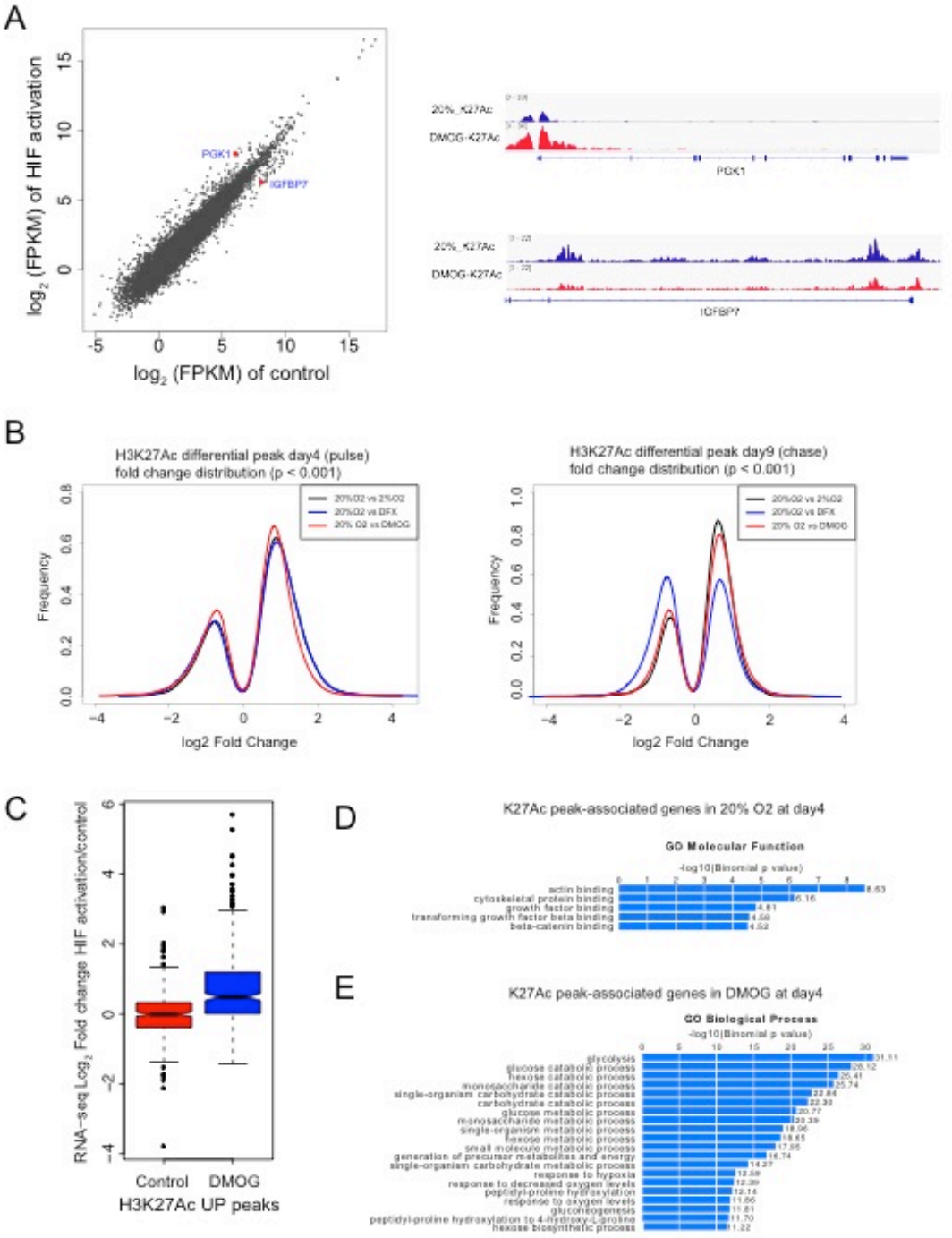


Figure 3-5. ChIP-sequencing data suggested H3K27Ac is highly involved in regulating gene expression upon HIF activation in NPCs.

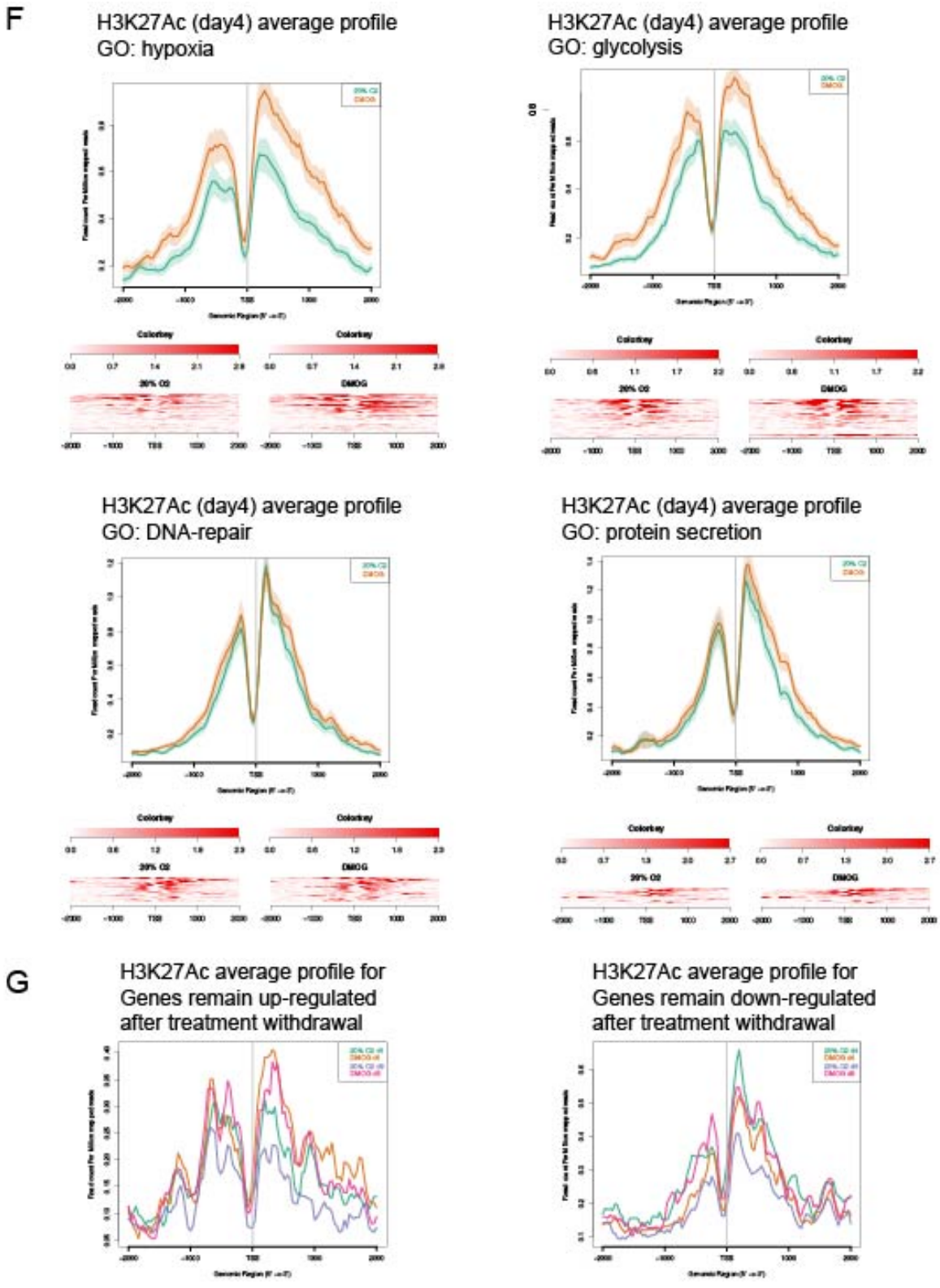


Figure 3-5. ChIP-sequencing data suggested H3K27Ac is highly involved in regulating gene expression upon HIF activation in NPCs.

(A) Left: Scatter plot marking in red the selected genes that are differentially expressed between control and HIF activation groups using RNA-seq data ($p<0.05$, likelihood ratio test). Right: Genomic tracks display H3K27Ac ChIP-seq data on selected up-regulated gene (PGK1) and down-regulated gene (IGFBP7).

(B) Distribution of fold change on H3K27Ac peak height associated with differential peaks between control and HIF activation groups. The left panel is from H3K27Ac ChIP-seq after 4 days of 2% O_2, DFX, or DMIG treatments (pulse); the right panel is 4 days of treatments plus 5 days treatment withdrawal. $\log_2$ (fold change) >1 represents that the height of the peaks in 20% O_2 is more than 2 fold higher than the treatment group (such as 2% O_2). Higher frequency suggested that the number of higher H3K27Ac peaks in control group is more than that of the HIF activation groups.

(C) Box-plot presentation of changes in transcription levels upon HIF activation for the closest differentially expressed genes marked by H3K27Ac (within 100 kb). This figure demonstrated that those genes marked by H3K27Ac upon HIF activation are significantly upregulated in transcription level. ($p < 2.2E-16$, non-parametric Mann-Whitney-Wilcoxon U test)

(D-E) Gene ontology analysis for genes marked by H3K27Ac (within 100 kb) in 20% O_2 control and DMOG treated group. ($q < 0.01$)

(F) Top: average profile of H3K27Ac mapped reads on genes from selected GO categories. Bottom: heat map of H3K27Ac marked region of selected genes close to transcription start site.

(G) Average profiles of H3K27Ac loci (TSS ± 2000bp) on selected genes that remain upregulated (left) or downregulated (right) after DMOG treatment withdrawal.

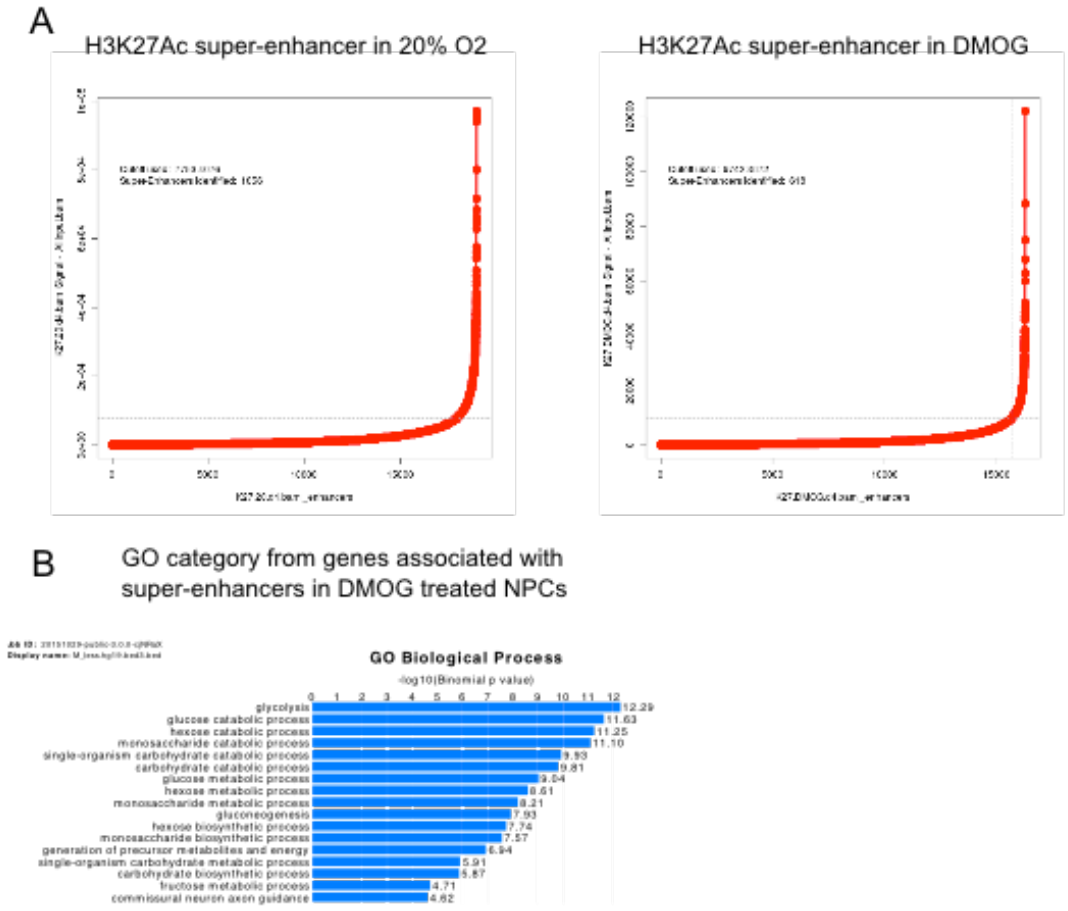


Figure 3-6. H3K27Ac super-enhancer analysis suggested epigenetic regulation of glycolysis related genes upon HIF activation.

(A) Super-enhancers identified in 20% O_2 control (left) and DMOG treated group (right).

(B) Gene ontology categories of super-enhancers associated genes in DMOG treated NPCs.

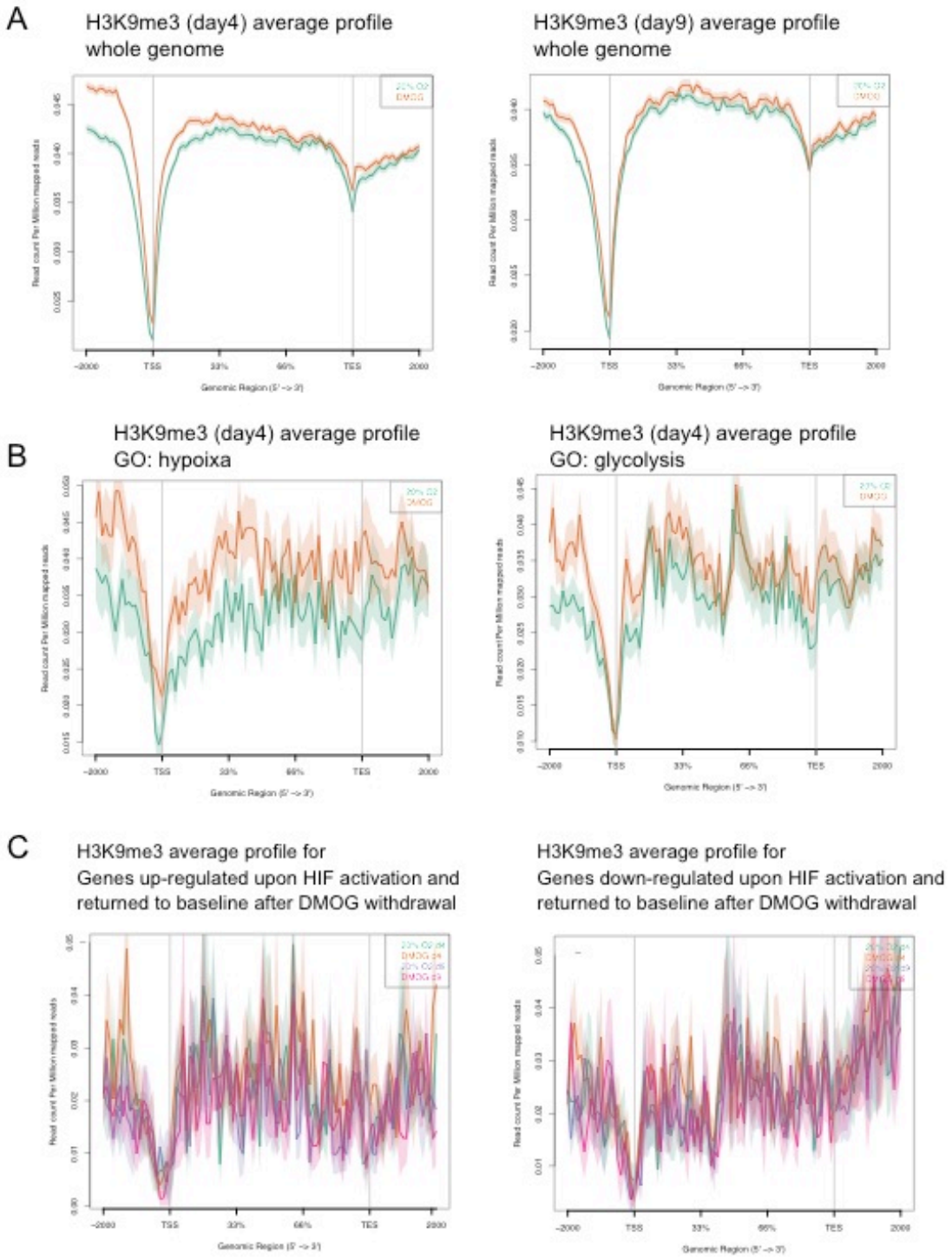


Figure 3-7. There is no clear relationship between distribution of H3K9Me3 loci and HIF regulated transcription changes.

(A) Average profile of H3K9Me3 close to transcription start site (TSS) and gene body. Left, NPCs with or without DMOG treatment for 4 days; right, control and NPCs treated with DMOG for 4 days followed by DMOG withdrawal for 5 days.

(B) Average profile of H3K9Me3 (TSS and TES ± 2000bp) on genes from selected GO categories using NPCs were treated with or without DMOG for 4 days.

(C) Average profile of H3K9Me3 (TSS and TES ± 2000bp) on selected genes that were upregulated (left) or downregulated (right) upon DMOG treatment but went back to baseline level after DMOG withdrawal.

References

Alvarez-Buylla, A., García-Verdugo, J.M., and Tramontin, A.D. (2001). A unified hypothesis on the lineage of neural stem cells. Nat Rev Neurosci *2*, 287–293.

Ben Langmead, and Salzberg, S.L. (2012). Fast gapped-read alignment with Bowtie 2. Nature Methods *9*, 357–359.

Beyer, S., Kristensen, M.M., Jensen, K.S., Johansen, J.V., and Staller, P. (2008). The histone demethylases JMJD1A and JMJD2B are transcriptional targets of hypoxia-inducible factor HIF. The Journal of Biological Chemistry *283*, 36542–36552.

Chen, H., Yan, Y., Davidson, T.L., Shinkai, Y., and Costa, M. (2006). Hypoxic Stress Induces Dimethylated Histone H3 Lysine 9 through Histone Methyltransferase G9a in Mammalian Cells.

Da Wei Huang, Sherman, B.T., and Lempicki, R.A. (2009). Systematic and integrative analysis of large gene lists using DAVID bioinformatics resources. Nat Protoc *4*, 44–57.

Evertts, A.G., Zee, B.M., and Garcia, B.A. (2010). Modern approaches for investigating epigenetic signaling pathways. Journal of Applied Physiology *109*, 927–933.

Gaiano, N., Nye, J.S., and Fishell, G. (2000). Radial Glial Identity Is Promoted by Notch1 Signaling in the Murine Forebrain. Neuron *26*, 395–404.

Garcia, B.A., Mollah, S., Ueberheide, B.M., Busby, S.A., Muratore, T.L., Shabanowitz, J., and Hunt, D.F. (2007). Chemical derivatization of histones for facilitated analysis by mass spectrometry. Nat Protoc *2*, 933–938.

Giardine, B., Riemer, C., Hardison, R.C., Burhans, R., Elnitski, L., Shah, P., Zhang, Y., Blankenberg, D., Albert, I., Taylor, J., et al. (2005). Galaxy: a platform for interactive large-scale genome analysis. Genome Research *15*, 1451–1455.

Hnisz, D., Abraham, B.J., Lee, T.I., Lau, A., Saint-André, V., Sigova, A.A., Hoke, H.A., and Young, R.A. (2013). Super-Enhancers in the Control of Cell Identity and Disease. Cell *155*, 934–947.

Johnson, A.B., Denko, N., and Barton, M.C. (2008). Hypoxia induces a novel signature of chromatin modifications and global repression of transcription. Mutation Research/Fundamental and Molecular Mechanisms of Mutagenesis *640*, 174–179.

Kang, P., Lee, H.K., Glasgow, S.M., Finley, M., Donti, T., Gaber, Z.B., Graham, B.H., Foster, A.E., Novitch, B.G., Gronostajski, R.M., et al. (2012). Sox9 and NFIA Coordinate a Transcriptional Regulatory Cascade during the Initiation of Gliogenesis. Neuron *74*, 79–94.

Lee, H.-Y., Yang, E.G., and Park, H. (2013). Hypoxia enhances the expression of prostate-specific antigen by modifying the quantity and catalytic activity of Jumonji C domain-containing histone demethylases. Carcinogenesis *34*, 2706–2715.

Lee, S.H., Kim, J., Kim, W.H., and Lee, Y.M. (2009). Hypoxic silencing of tumor suppressor RUNX3 by histone modification in gastric cancer cells. Oncogene *28*, 184–194.

LeRoy, G., Chepelev, I., DiMaggio, P.A., and Blanco, M.A. (2012). Proteogenomic characterization and mapping of nucleosomes decoded by Brd and HP1 proteins. Genome ….

Li, H. (2009). Genome Project Data Processing S, Li H, Handsaker B, Wysoker A, Fennell T, Ruan J, Homer N, Marth G, Abecasis G, Durbin R: The Sequence Alignment … (Bioinformatics).

Liu, Y., Han, S.S.W., Wu, Y., Tuohy, T.M.F., Xue, H., Cai, J., Back, S.A., Sherman, L.S., Fischer, I., and Rao, M.S. (2004). CD44 expression identifies astrocyte-restricted precursor cells. Dev. Biol. *276*, 31–46.

Lovén, J., Hoke, H.A., Lin, C.Y., Lau, A., Orlando, D.A., Vakoc, C.R., Bradner, J.E., Lee, T.I., and Young, R.A. (2013). Selective Inhibition of Tumor Oncogenes by Disruption of Super-Enhancers. Cell *153*, 320–334.

Lowry, W.E., Blanpain, C., Nowak, J.A., Guasch, G., Lewis, L., and Fuchs, E. (2005). Defining the impact of beta-catenin/Tcf transactivation on epithelial stem cells. Genes & Development *19*, 1596–1611.

Lu, Y., Chu, A., Turker, M.S., and Glazer, P.M. (2011). Hypoxia-induced epigenetic regulation and silencing of the BRCA1 promoter. Molecular and Cellular Biology *31*, 3339–3350.

McLean, C.Y., Bristor, D., Hiller, M., Clarke, S.L., Schaar, B.T., Lowe, C.B., Wenger, A.M., and Bejerano, G. (2010). GREAT improves functional interpretation of cis-regulatory regions. Nature Biotechnology *28*, 495–501.

Miller, F.D., and Gauthier, A.S. (2007). Timing Is Everything: Making Neurons versus Glia in the Developing Cortex. Neuron *54*, 357–369.

Naruse, M., Shibasaki, K., Yokoyama, S., Kurachi, M., and Ishizaki, Y. (2013). Dynamic Changes of CD44 Expression from Progenitors to Subpopulations of Astrocytes and Neurons in Developing Cerebellum. PLoS ONE *8*, e53109.

Paridaen, J.T., and Huttner, W.B. (2014). Neurogenesis during development of the vertebrate central nervous system. EMBO Reports *15*, e201438447–364.

Patterson, M., Gaeta, X., Loo, K., Edwards, M., Smale, S., Cinkornpumin, J., Xie, Y., Listgarten, J., Azghadi, S., Douglass, S.M., et al. (2014). *let-7* miRNAs Can Act through Notch to Regulate Human Gliogenesis. Stem Cell Reports *3*, 758–773.

Patterson, M., Chan, D.N., Ha, I., Case, D., Cui, Y., Handel, B.V., Mikkola, H.K., and Lowry, W.E. (2011). Defining the nature of human pluripotent stem cell progeny. Cell Res *22*, 178–193.

Pollen, A.A., Nowakowski, T.J., Shuga, J., Wang, X., Leyrat, A.A., Lui, J.H., Li, N., Szpankowski, L., Fowler, B., Chen, P., et al. (2014). Low-coverage single-cell mRNA

sequencing reveals cellular heterogeneity and activated signaling pathways in developing cerebral cortex. Nature Biotechnology *32*, 1053–1058.

Robinson, M.D., McCarthy, D.J., and Smyth, G.K. (2010). edgeR: a Bioconductor package for differential expression analysis of digital gene expression data. Bioinformatics *26*, 139–140.

Rowitch, D.H., and Kriegstein, A.R. (2010). Developmental genetics of vertebrate glial–cell specification. Nature *468*, 214–222.

Schitine, C., Nogaroli, L., Costa, M.R., and Hedin-Pereira, C. (2015). Astrocyte heterogeneity in the brain: from development to disease. Frontiers in Cellular Neuroscience *9*, 76.

Shaltouki, A., Peng, J., Liu, Q., Rao, M.S., and Zeng, X. (2013). Efficient Generation of Astrocytes from Human Pluripotent Stem Cells in Defined Conditions. Stem Cells *31*, 941–952.

Shao, Z., Zhang, Y., Yuan, G.-C., Orkin, S.H., and Waxman, D.J. (2012). MAnorm: a robust model for quantitative comparison of ChIP-Seq data sets. Genome Biology *13*, R16.

Shen, L., Shao, N., Liu, X., and Nestler, E. (2014). ngs.plot: Quick mining and visualization of next-generation sequencing data by integrating genomic databases. BMC Genomics *15*, 284.

Sloan, S.A., and Barres, B.A. (2014). Mechanisms of astrocyte development and their contributions to neurodevelopmental disorders. Current Opinion in Neurobiology *27*, 75–81.

Sridharan, R., Gonzales-Cope, M., Chronis, C., Bonora, G., McKee, R., Huang, C., Patel, S., Lopez, D., Mishra, N., Pellegrini, M., et al. (2013). Proteomic and genomic approaches reveal critical functions of H3K9 methylation and heterochromatin protein-1γ in reprogramming to pluripotency. Nat Cell Biol *15*, 872–882.

Studer, L., Csete, M., Lee, S.H., Kabbani, N., Walikonis, J., Wold, B., and McKay, R. (2000). Enhanced proliferation, survival, and dopaminergic differentiation of CNS precursors in lowered oxygen. J. Neurosci. *20*, 7377–7383.

Trapnell, C., Pachter, L., and Salzberg, S.L. (2009). TopHat: discovering splice junctions with RNA-Seq. Bioinformatics *25*, 1105–1111.

Wang, Z., Yang, D., Zhang, X., Li, T., Li, J., Tang, Y., and Le, W. (2011). Hypoxia-induced down-regulation of neprilysin by histone modification in mouse primary cortical and hippocampal neurons. PLoS ONE *6*, e19229.

Whyte, W.A., Orlando, D.A., Hnisz, D., Abraham, B.J., Lin, C.Y., Kagey, M.H., Rahl, P.B., Lee, T.I., and Young, R.A. (2013). Master Transcription Factors and Mediator Establish Super-Enhancers at Key Cell Identity Genes. Cell *153*, 307–319.

Wilczynska, K.M., Singh, S.K., Adams, B., Bryan, L., Rao, R.R., Valerie, K., Wright, S., Griswold Prenner, I., and Kordula, T. (2009). Nuclear Factor I Isoforms Regulate Gene Expression During the Differentiation of Human Neural Progenitors to Astrocytes. Stem Cells *27*, 1173–1181.

Xie, Y., Zhang, J., Lin, Y., Gaeta, X., Meng, X., Wisidagama, D.R.R., Cinkornpumin, J., Koehler, C.M., Malone, C.S., Teitell, M.A., et al. (2014). Defining the Role of Oxygen Tension in Human Neural Progenitor Fate. Stem Cell Reports *3*, 743–757.

Yang, L., Soonpaa, M.H., Adler, E.D., Roepke, T.K., Kattman, S.J., Kennedy, M., Henckaerts, E., Bonham, K., Abbott, G.W., Linden, R.M., et al. (2008). Human cardiovascular progenitor cells develop from a KDR+ embryonic-stem-cell-derived population. Nature *453*, 524–528.

Zee, B.M., Britton, L.-M.P., Wolle, D., Haberman, D.M., and Garcia, B.A. (2012). Origins and formation of histone methylation across the human cell cycle. Molecular and Cellular Biology *32*, 2503–2514.

Zee, B.M., Levin, R.S., DiMaggio, P.A., and Garcia, B.A. (2010). Global turnover of histone post-translational modifications and variants in human cells. Epigenetics & Chromatin *3*, 1–11.

CHAPTER 4

Conclusions and Perspectives

The concept of physioxia

The purpose of vasculature is to deliver oxygen and nutrients to cells and remove carbon dioxide and other metabolites. The level of oxygen is a key component of physiological state of a tissue or organ, which is dependent on the metabolic requirements and functional status of each organ. In physiological conditions, organ and tissue are characterized by their unique pO_2 level, which is defined as 'physioxia' status (Carreau et al., 2011). For example, the oxygen level in adult brain ranges from 3.1% to 4.4% O_2 (Dings et al., 1998). As researchers attempt to recapitulate tissue-like environments *in vitro*, the concentration of O_2 is an important concern. However, the majority of *in vitro* cell cultures are performed in incubators with 20% O_2, an artificial concentration achieved by balancing 95% air with 5% CO_2. The dissolved oxygen level in the culture medium under these conditions is typically 18% O_2 (Newby et al., 2005), which is much higher than physiological conditions.

The role of physioxia in modeling development *in vitro*

Physiological O_2 tension (less than 5% O_2) has been shown to be important for maintaining the self-renewal and pluripotency of hESCs (Mohyeldin et al., 2010). Low oxygen tension also improves the efficiency of cellular reprograming using OSKM factors (Yoshida et al., 2009). However, the influence of oxygen tension on fidelity of PSC differentiation had not been studied extensively until now. As introduced in chapter 1, embryogenesis before 10 weeks of gestation occurs under a low oxygen level (less than 2.5%) (Genbacev et al., 1997; Simon and Keith, 2008). Thus, we hypothesized that manipulating oxygen tension to a more physiological level *in vitro* would facilitate the transcriptional and functional maturation of human pluripotent stem cell derivatives.

In chapter 2, we characterized the influence of low oxygen in NPC fate determination. We discovered that low oxygen tension promotes astrogliogenesis upon NPC differentiation and determined that hypoxia inducible factors (HIFs) are key transcription factors involved in this process. Activating HIF using small molecules such as DFX facilitated astrogliogenesis, whereas silencing HIF delayed this process. Transcriptional profiling suggested that LIN28 was differentially expressed during this process. We demonstrated that HIF competes with MYC for the same binding sites on the LIN28 promoter. In the presence of HIF activity, LIN28 transcription was significantly decreased by disruption of MYC binding at its promoter. Since LIN28 blocks the maturation of *let-7* family of microRNAs, the expression and activity of mature *let-7* microRNA was higher in NPCs grown in low oxygen tension compared with atmospheric oxygen tension. Inhibition of *let-7* microRNA blocked HIF induced astrogliogenesis, suggesting a functional link between these pathways. Moreover, blocking MYC using small molecules such as JQ1 also resulted in increased astrogliogenesis, which further supported the model that HIF competes with MYC in regulating neural progenitor fate decision. A summary of key points of this model is demonstrated in Figure 4-1.

In chapter 3, we took a more comprehensive approach to characterize the effect of transient low oxygen tension in NPCs at transcriptional, epigenetic and metabolic levels. Using histone mass spectrometry, RNA-seq, metabolomics, and ChIP-seq, we uncovered evidence of a coherent response to HIF activation in cell fate decision making within human neural progenitors. Our PSC-derived NPCs appear to recapitulate the neural epithelial cell (NEC) stage of development, while exposure to HIF activation drove a transition towards the radial glia cell (RGC) stage.

This phenomenon is difficult to model in animal models, and of course otherwise impossible in humans (Paridaen and Huttner, 2014).

Epigenetic analysis suggested that H3K27Ac loci are highly enriched in actin binding and beta-catenin binding in NPCs grown in 20%, providing further evidence for the idea that those cells are mostly NECs which highly express adherens junctions associated proteins. Upon HIF activation, those NECs became RGCs, and presumably underwent asymmetric cell divisions to generate one RGC daughter cell and one terminally differentiated cell. The gene expression profile during this transition was captured by RNA-sequencing, as demonstrated by significantly enriched GO categories, including up-regulated genes in neuron projection development, as well as down-regulated genes in cell adhesion and mitotic cell cycle.

Consistent with the developmental stage that our NPCs undergo NEC-to-RGC transition, RNA-seq data also suggested the initiation of the Cajal-Retzius (CR) cell upon HIF activation. CR cell is one the earliest born neurons in the neocortex (Chowdhury et al., 2010). In mice, CR cell are generated between E10.5 and E12.5 (Bielle et al., 2005), which is equivalent to week 4-6 in human gestation. Thus, the developmental timing of CR cell initiation matches with our PSC-derived NPCs, which we previously showed represent less than 6 weeks of human development (Patterson et al., 2011).

Transcription factor Ebf2 is expressed in the preplate neurons from the earliest stage of their differentiation and regulates the generation of CR neurons in rat (Chuang et al., 2011). The Ebf gene is required to couple neuronal differentiation and cell cycle exit (Garcia-Dominguez et al.,

2003). Transcriptionally, EBF2 was highly expressed in our NPCs, and was induced in all three HIF activation conditions. Its expression level was higher than control even after drug/low oxygen withdrawal. The up-regulation of EBF2 appears to be HIF-dependent in the embryoid body (EB) formation experiment. Upon differentiation, EBF2 was induced over 20-fold in EBs grown in 2% O_2, but is not induced in HIF-deficit EBs or EBs grown in 20% O_2. The most important function of CR cell is to secrete the glycoprotein reelin and express cell adhesion molecules nectins to mediate neuronal migration (Paridaen and Huttner, 2014). In fact, the genes associated with reelin (RELN), reelin receptor (VLDLR), and nectins (CADM3 and PVRL1) were also induced by HIF signaling, which further support the induction of CR cells upon HIF activation.

This phenomenon can be explained developmentally by the CXCL12/CXCR4 axis. CXCL12, a chemokine secreted by leptomeninges, regulates CXCR4-expressing CR cell migration into marginal zone through chemoattraction (Anstötz et al., 2014; Paredes et al., 2006). As a HIF target gene, CXCR4 is induced by hypoxia in monocytes, macrophages and endothelial cells (Schioppa et al., 2003). In our case, CXCR4 expression was significantly induced in NPCs and EBs upon HIF activation. Further studies are required to understand how HIF-mediated CR cell induction is related to cell cycle exit and terminal differentiation. How does HIF regulate EBF2? Is it a direct interaction or through other signaling pathways, such as Notch?

Human PSC-derived NPCs also provide an excellent tool to study the origin of astrocytes, since most of the current knowledge on neocortical development comes from animal models, which may not reflect human development. Several models have been proposed for astrogliogenesis: 1)

RGCs directly transform into astrocytes; 2) RGCs give rise to neuron in the first several rounds of asymmetric divisions, and then start to generate astrocytes; 3) RGCs generate an astrocyte-restricted intermediate progenitor; 4) astrocytes are from proliferation of newborn astrocytes (Schitine et al., 2015; Sloan and Barres, 2014). To date, however, the astrocyte-restricted progenitors have not been well identified or characterized. Although CD44 was identified as a marker for astrocyte-restricted precursor cells in several studies (Liu et al., 2004; Shaltouki et al., 2013), other studies showed that it is also expressed in neural stem cells, oligodendrocyte precursor cells, and certain types of neurons (Naruse et al., 2013). With single cell sequencing and sophisticated cell labeling techniques, we should be able to identify and characterize distinct progenitor populations within the neural progenitor pool upon HIF activation. The advancement of automated imaging and multicolor fluorescent labeling could also enable us to trace specific subtypes of NPC linages *in vitro*, to allow for linage tracing the yet-to-be-identified astrocyte-restricted progenitors.

Modeling early human development *in vitro* has limitations. One disadvantage is that the Petri dish, especially the traditional 2D culture system, is too simple to mimic the complexity of *in vivo* development. *In vivo* nervous system development is not only cell intrinsic, but also tightly regulated by temporal and spatial factors and environmental cues. For example, the laminar position of Cajal-Retzius cells is regulated by cytokines released by leptomeninges. The anterior-posterior or dorsal-ventral patterning of the brain is mediated by gradients of morphogens such as Fgfs, Wnts, Shh, and BMPs. These morphogens will then induce regional specific transcription factors to induce specific subtypes of neurons. Local oxygen tension is influenced by the establishment of the circulatory system. Generation of three-dimensional organoids using

stem-cell-derived cells is a rapid growing field to solve this problem. This technique would enable modeling of development or diseases that involve multiple cell types. Together with tissue-engineering strategies, such as scaffolding polymers, we may be able to generate PSC-derived organoids into functional tissues and organs for regenerative medicine in the future.

Applications of physioxia in cell based therapy and regenerative medicine

Oxygen tension is an important issue during *in vitro* differentiation and expansion of desired cell types for transplantation. Preconditioning of cells with physiological oxygen before transplantation could potentially be beneficial, as demonstrated in the following studies. Transplantation of hypoxia-preconditioned mesenchymal stem cells improved infarcted heart function via increased survival of implanted cells and angiogenesis (Hu et al., 2008). In a cerebral ischemia model, transplantation of hypoxia-preconditioned bone marrow mesenchymal stem cells enhanced angiogenesis and neurogenesis (Wei et al., 2012). Although those studies were performed using mesenchymal stem cells, it is very likely that preconditioning NPCs with low oxygen (or small molecules that activate HIF) could beneficial for cell-based therapy and transplantation.

Preconditioning with low oxygen might increase migration of injected cells through CXCR4-CXCL12 signaling. CXCR4 was highly induced in NPCs upon HIF activation. Its receptor, CXCL12 (also called stromal cell-derived factor-1, SDF-1) is upregulated at the injury site of both stroke (Robin et al., 2006) and traumatic brain injury models (Itoh et al., 2013). CXCR4 expressing NPCs exhibited significantly increased migration when they were overlaid onto stroke brain slices, whereas blocking CXCL4 with neutralizing antibody significantly attenuated

stroke-enhanced NPC migration (Robin et al., 2006). From our RNA-seq data, CXCR4 mRNA was significantly induced in NPCs treated with low oxygen, DFX or DMOG. Thus, it is likely that those NPCs would respond to these chemo-attractive cues and migrate to injury sites where CXCL12 is expressed.

Another advantage of preconditioning could be the induction of growth factors by HIF signaling. For example, HIF targets VEGFA and VEGFB, have been shown to induce neural progenitor cell proliferation and migration (Wittko et al., 2009) and modulate neurogenesis (Calvo et al., 2011). Besides the neuron-related function, VEGF mediated angiogenesis is also helpful for post-stroke recovery (Wei et al., 2012). Members of the TGF beta super family of growth factors, GDF3 and GDF15 were also induced by HIF. GDF-15 is a potent trophic factor for developing and lesioned midbrain dopaminergic neurons *in vitro* and *in vivo*, matching the potency of GDNF (Krieglstein et al., 2002). In summary, induced growth factors could promote the survival and migration of injected NPCs, induce angiogenesis and astrogliogenesis, modulate existing neuronal circuits, and thus contribute to the overall outcome of cell-based therapy.

With this dissertation, we have demonstrated that physiological oxygen tension and HIF signaling play an important role in regulating cell fate decision in human neural progenitors. Our work further suggested that physioxia, or small molecules that activates HIF, can be a simple tool to facilitate cell fate transitions *in vitro* and have the potential to apply to cell-based therapy to treat neurological diseases, such as stroke.

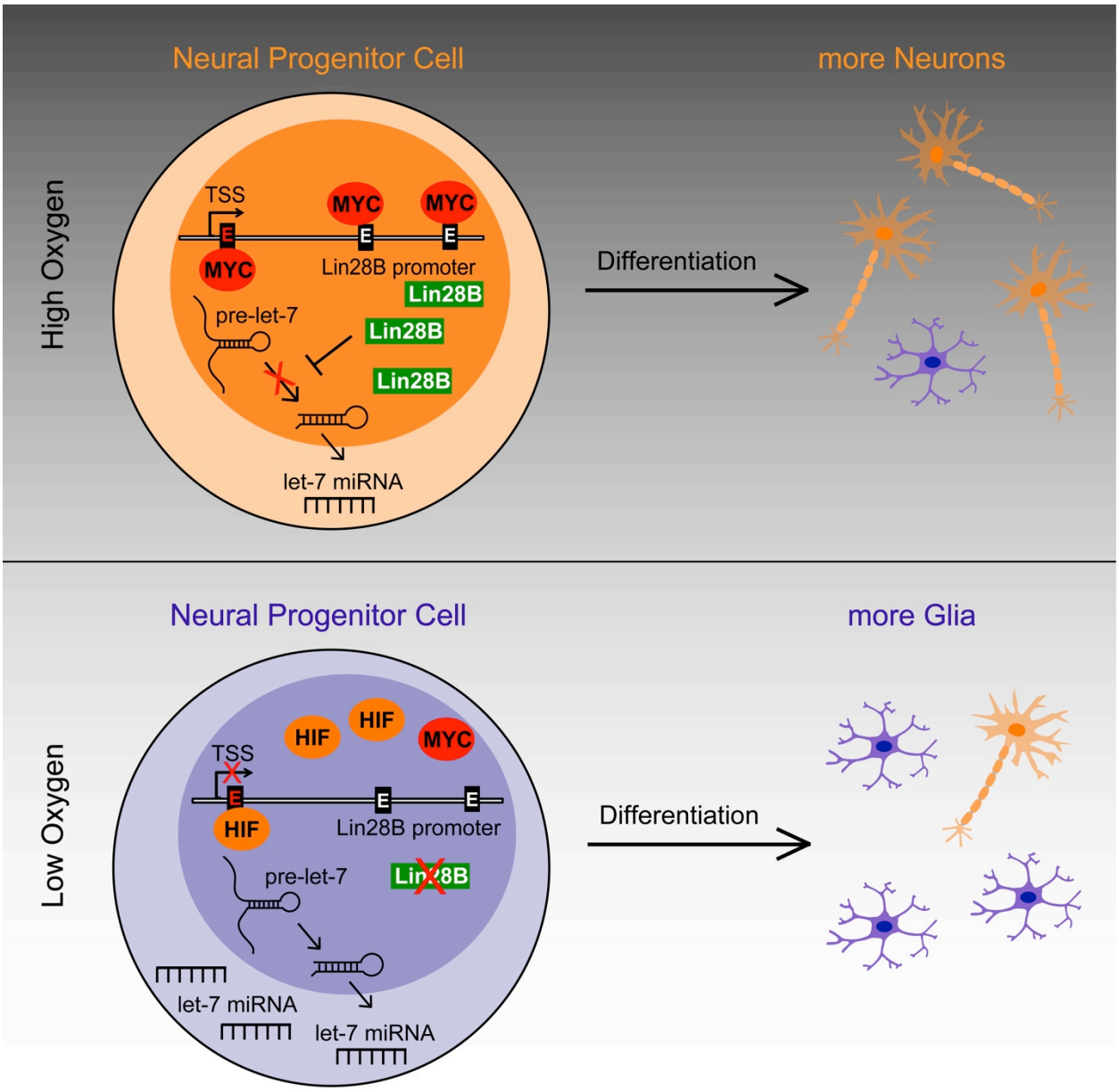


Figure 4-1 A proposed model that NPC differentiation is affected by HIF and MYC through regulating LIN28-*let-7* axis.

Low oxygen tension promotes gliogenesis of human neural progenitors.

HIF activation is required for gliogenic effect of lowered oxygen tension.

HIF acts through MYC to disrupt LIN28/*let-7* in gliogenesis.

Small molecule stimulators of HIF or inhibitors of MYC can drive gliogenesis.

References

Anstötz, M., Cosgrove, K.E., Hack, I., Mugnaini, E., Maccaferri, G., and Lübke, J.H.R. (2014). Morphology, input–output relations and synaptic connectivity of Cajal–Retzius cells in layer 1 of the developing neocortex of CXCR4-EGFP mice. Brain Struct Funct *219*, 2119–2139.

Bielle, F., Griveau, A., Narboux-Nême, N., Vigneau, S., Sigrist, M., Arber, S., Wassef, M., and Pierani, A. (2005). Multiple origins of Cajal-Retzius cells at the borders of the developing pallium. Nat. Neurosci. *8*, 1002–1012.

Calvo, C.-F., Fontaine, R.H., Soueid, J., Tammela, T., Makinen, T., Alfaro-Cervello, C., Bonnaud, F., Miguez, A., Benhaim, L., Xu, Y., et al. (2011). Vascular endothelial growth factor receptor 3 directly regulates murine neurogenesis. Genes & Development *25*, 831–844.

Carreau, A., Hafny Rahbi, B.E., Matejuk, A., Grillon, C., and Kieda, C. (2011). Why is the partial oxygen pressure of human tissues a crucial parameter? Small molecules and hypoxia. Journal of Cellular and Molecular Medicine *15*, 1239–1253.

Chowdhury, T.G., Jimenez, J.C., Bomar, J.M., Cruz-Martin, A., Cantle, J.P., and Portera-Cailliau, C. (2010). Fate of Cajal–Retzius Neurons in the Postnatal Mouse Neocortex. Frontiers in Neuroanatomy *4*, 10.

Chuang, S.-M., Wang, Y., Wang, Q., Liu, K.-M., and Shen, Q. (2011). Ebf2 marks early cortical neurogenesis and regulates the generation of cajal-retzius neurons in the developing cerebral cortex. Dev Neurosci *33*, 479–493.

Dings, J., Meixensberger, J., Jäger, A., and Roosen, K. (1998). Clinical experience with 118 brain tissue oxygen partial pressure catheter probes. Neurosurgery *43*, 1082–1095.

Garcia-Dominguez, M., Poquet, C., Garel, S., and Charnay, P. (2003). Ebf gene function is required for coupling neuronal differentiation and cell cycle exit. Development *130*, 6013–6025.

Genbacev, O., Zhou, Y., Ludlow, J.W., and Fisher, S.J. (1997). Regulation of human placental development by oxygen tension. Science *277*, 1669–1672.

Hu, X., Yu, S.P., Fraser, J.L., Lu, Z., Ogle, M.E., Wang, J.-A., and Wei, L. (2008). Transplantation of hypoxia-preconditioned mesenchymal stem cells improves infarcted heart function via enhanced survival of implanted cells and angiogenesis. The Journal of Thoracic and Cardiovascular Surgery *135*, 799–808.

Itoh, T., Satou, T., Ishida, H., Nishida, S., Tsubaki, M., Hashimoto, S., and Ito, H. (2013). The relationship between SDF-1α/CXCR4 and neural stem cells appearing in damaged area after traumatic brain injury in rats. Neurological Research.

Krieglstein, K., Strelau, J., Schober, A., Sullivan, A., and Unsicker, K. (2002). TGF-β and the regulation of neuron survival and death. Journal of Physiology-Paris *96*, 25–30.

Liu, Y., Han, S.S.W., Wu, Y., Tuohy, T.M.F., Xue, H., Cai, J., Back, S.A., Sherman, L.S., Fischer, I., and Rao, M.S. (2004). CD44 expression identifies astrocyte-restricted precursor cells. Dev. Biol. *276*, 31–46.

Mohyeldin, A., Garzón-Muvdi, T., and Quiñones-Hinojosa, A. (2010). Oxygen in Stem Cell Biology: A Critical Component of the Stem Cell Niche. Cell Stem Cell *7*, 150–161.

Naruse, M., Shibasaki, K., Yokoyama, S., Kurachi, M., and Ishizaki, Y. (2013). Dynamic Changes of CD44 Expression from Progenitors to Subpopulations of Astrocytes and Neurons in Developing Cerebellum. PLoS ONE *8*, e53109.

Newby, D., Marks, L., and Lyall, F. (2005). Dissolved oxygen concentration in culture medium: assumptions and pitfalls. Placenta *26*, 353–357.

Paredes, M.F., Li, G., Berger, O., Baraban, S.C., and Pleasure, S.J. (2006). Stromal-derived factor-1 (CXCL12) regulates laminar position of Cajal-Retzius cells in normal and dysplastic brains. J. Neurosci. *26*, 9404–9412.

Paridaen, J.T., and Huttner, W.B. (2014). Neurogenesis during development of the vertebrate central nervous system. EMBO Reports *15*, e201438447–364.

Patterson, M., Chan, D.N., Ha, I., Case, D., Cui, Y., Handel, B.V., Mikkola, H.K., and Lowry, W.E. (2011). Defining the nature of human pluripotent stem cell progeny. Cell Res *22*, 178–193.

Robin, A.M., Zhang, Z.G., Wang, L., Zhang, R.L., Katakowski, M., Zhang, L., Wang, Y., Zhang, C., and Chopp, M. (2006). Stromal cell-derived factor 1|[alpha]| mediates neural progenitor cell motility after focal cerebral ischemia. Journal of Cerebral Blood Flow & Metabolism *26*, 125–134.

Schioppa, T., Uranchimeg, B., Saccani, A., Biswas, S.K., Doni, A., Rapisarda, A., Bernasconi, S., Saccani, S., Nebuloni, M., Vago, L., et al. (2003). Regulation of the chemokine receptor CXCR4 by hypoxia. J Exp Med *198*, 1391–1402.

Schitine, C., Nogaroli, L., Costa, M.R., and Hedin-Pereira, C. (2015). Astrocyte heterogeneity in the brain: from development to disease. Frontiers in Cellular Neuroscience *9*, 76.

Shaltouki, A., Peng, J., Liu, Q., Rao, M.S., and Zeng, X. (2013). Efficient Generation of Astrocytes from Human Pluripotent Stem Cells in Defined Conditions. Stem Cells *31*, 941–952.

Simon, M.C., and Keith, B. (2008). The role of oxygen availability in embryonic development and stem cell function. Nat Rev Mol Cell Biol *9*, 285–296.

Sloan, S.A., and Barres, B.A. (2014). Mechanisms of astrocyte development and their contributions to neurodevelopmental disorders. Current Opinion in Neurobiology *27*, 75–81.

Wei, L., Fraser, J.L., Lu, Z.-Y., Hu, X., and Yu, S.P. (2012). Transplantation of hypoxia preconditioned bone marrow mesenchymal stem cells enhances angiogenesis and neurogenesis after cerebral ischemia in rats. Neurobiology of Disease *46*, 635–645.

Wittko, I.M., Schänzer, A., Kuzmichev, A., Schneider, F.T., Shibuya, M., Raab, S., and Plate, K.H. (2009). VEGFR-1 regulates adult olfactory bulb neurogenesis and migration of neural progenitors in the rostral migratory stream *in vivo*. J. Neurosci. *29*, 8704–8714.

Yoshida, Y., Takahashi, K., Okita, K., and Ichisaka, T. (2009). Hypoxia enhances the generation of induced pluripotent stem cells. Cell Stem Cell 5, 237–241.